4-23-2008

Provenance Analysis of the Cretaceous Hornbrook Formation of northern California and southern Oregon

Emily J. Beverly
Trinity University

Provenance Analysis of the Cretaceous Hornbrook Formation of northern California and southern Oregon

Emily J. Beverly

A departmental senior thesis submitted to the Department of Geosciences at Trinity University in partial fulfillment of the requirements for graduation with departmental honors.

April 23, 2008

_____
Thesis Advisor

_____
Department Chair

_____
Associate Vice President
for
Academic Affairs

TABLE OF CONTENTS

LIST OF FIGURES

ABSTRACT

The provenance of the Cretaceous Hornbrook Formation, deposited unconformably on the eastern terranes of the Klamath Mountains of northern California and southern Oregon, may prove critical to reconstructing the complex Cretaceous paleogeography of this region. Sandstone petrography from each of the five members of the Hornbrook Formation indicates a variable source region with elements from basement uplift, transitional continent, recycled orogen, and dissected arc sources. A conglomerate clast count from the Klamath River Conglomerate member is broadly consistent with sandstone petrography, but yielded more quartzite and fewer volcanic clasts than the sand-sized fraction. This reflects the different susceptibility to weathering and diagenesis of these rock types. Likewise, Klamath River Conglomerate quartzite clasts contain a Precambrian detrital zircon age distribution very similar to that found in the Antelope Mountain Quartzite within the Yreka subterrane of the eastern Klamath Mountains while all the other Precambrian zircons from the Hornbrook Formation resemble northern Sierra Nevada terranes. This discrepancy suggests that the quartzite was not broken down into sand-sized grains during transport, but rocks from plutonic arc sources were disaggregated. In addition, detrital zircon age spectra from sandstones throughout the strata of the Hornbrook Formation clearly show that the provenance of the Hornbrook Formation changed with time and was not limited to the Klamath Mountains, contrary to past assumptions.

In the Mesozoic detrital zircon age distribution, the reduction in the Early Cretaceous peak and the appearance of a Late Cretaceous peak suggests increasing input from an active magmatic arc other than a Klamath Mountain source. This age signature is supported by the variability of the sandstone petrography, the decreasing volcanic input, and the decreasing

amount of zirconium, which demonstrate either the dissection of a magmatic arc source and/or multiple source regions. Furthermore, the members of the Hornbrook Formation correlate with the combined detrital zircon distributions of the Great Valley Basin more closely than with the combined distributions of the Methow Basin. This data supports past interpretations of the Hornbrook Basin as part of an extensive forearc basin that included the Great Valley Basin and possibly the Ochoco Basin where more research is needed. With the exception of the quartzite clasts in the basal member, Precambrian ages are rare, and Paleozoic ages, common in the Klamath Mountains, occur only in the youngest member of the Hornbrook Formation. Thus, the changing provenance of the Hornbrook Formation likely reflects sediment input from the Klamath Mountains activity and from an adjacent Jurassic-Cretaceous magmatic arc.

INTRODUCTION

The complexity of Cordilleran geology makes it difficult to reconstruct the tectonics and paleogeography of the region through time. Since the Late Devonian, this region has undergone pervasive orogenic deformation, extensive faulting, accretion of terranes, and the formation of magmatic arcs. As a result, many uncertainties still remain in the geology of the Cordillera. Two distinct interpretations have been developed to explain aspects of this complexity and the problems associated with our understanding of the Cretaceous Cordilleran tectonics. Some scientists use paleomagnetic data to suggest that much of the Pacific Northwest and Canadian Cordillera formed much further south relative to its current location and to the North American craton (e.g., Beck et al., 1981; Irving et al., 1985). They hypothesize that the region ("Baja BC") was transported about 3000 km north to its current position on dextral strike-slip faults during and since the Cretaceous (Beck et al., 1981; Irving et al., 1985; Umhoefer, 1987). More recently, some scientists propose that this region was transported north a much shorter distance (~1000 km) than previously suggested (Butler et al., 2001).

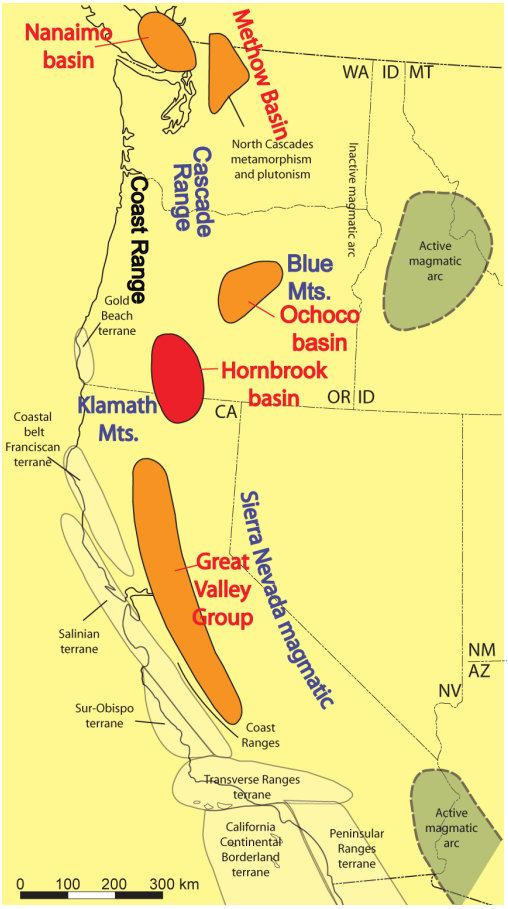

Figure 1: The Hornbrook Basin is show here in red while all other Late Cretaceous basins are shown in orange. The magmatic arcs traditionally associated with these basins are labeled in blue. Map modified from Miller et al. (1992).

A recent reconstruction of the Cretaceous Cordillera by Wyld et al. (2006) uses displacement along known and hypothesized faults as a starting point for Cretaceous paleogeography. While this movement is separate from the transport of the Baja BC terranes, it does not rule out further Baja BC movement. Any fault displacement would affect the numerous Cretaceous forearc basins (Fig. 1), currently separated by considerable a distance. Wyld et al. (2006) suggest that the Cretaceous Hornbrook and Ochoco forearc basins were connected at 100 Ma (Fig. 3) and indicate that the Methow Basin may represent the northward continuation of a Hornbrook-Ochoco Basin (Wyld et al., 2006). In contrast, others suggest that this region formed essentially in situ as a magmatic arc resulting from long-term subduction (e.g., Monger, 1975, 1977; Miller, 1987; Irwin and Wooden, 1999). The reconstruction indicates that an extensive forearc basin formed along the western coast

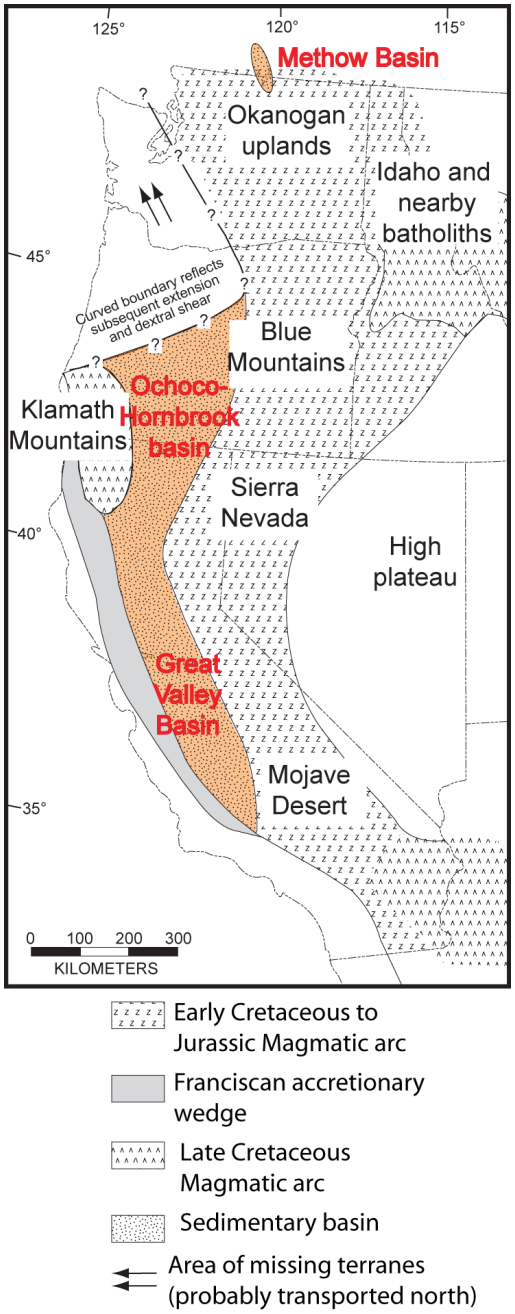

Figure 2: The paleogeographic reconstruction by Miller et al. (1992) combines the Hornbook, Ochoco, and Great Valley Basins into one extensive forearc basin separate from the Methow and other Late Cretaceous basins further north. Modified from Miller et al. (1992).

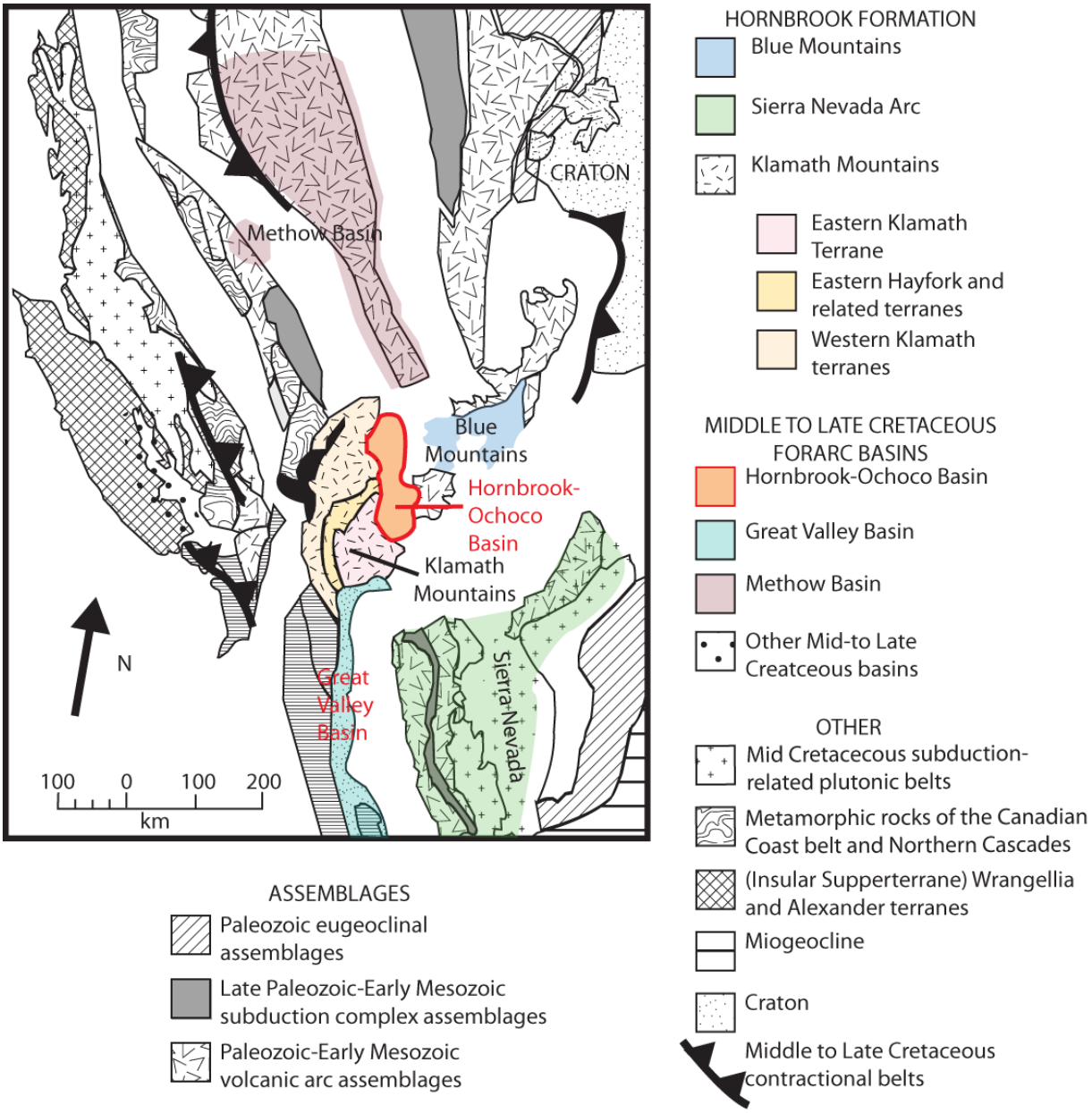

Figure 3: The reconstruction by Wyld et al. (2006) uses known fault displacement before 100 Ma to revaluate Northern Cordilleran geology. The Hornbrook and Ochoco Basins are combined and probably connected to the Methow Basin, which currently is much further north. Wyld et al. (2006) suggest that the Hornbrook-Ochoco Basin was not connected to the Great Valley Basin.

of North America, combining the Hornbrook, Ochoco, and Great Valley Basins and excluding the Methow Basin (Fig. 2; Nilsen, 1984; Kleinhans et al., 1984; Miller et al. 1992).

The relatively unexplored Hornbrook Formation of northern California and southern Oregon was deposited during the Cretaceous Period in a forearc basin near a magmatic arc that formed as a result of subduction (Nilsen, 1984; 1993). In the past Nilsen (1984; 1993) and others concluded that the Hornbrook Formation was solely derived from the Klamath Mountains. This study of the Hornbrook Formation provenance will focus on unresolved issues within this critical region by addressing the following questions:

1. Where was the Hornbrook Basin relative to the North American craton, the magmatic arc, and the surrounding basins during the Cretaceous Period?
2. Were the Great Valley Group of California, the Hornbrook Formation of northern California and southern Oregon, the Ochoco Basin of central Oregon, and the Methow Basin of southern British Columbia and northern Washington (or a subset of these basins) linked within one massive forearc basin, or did they form as separate and discrete basins?
3. Did the provenance and geochemistry of the Hornbrook Formation change over time, indicating an introduction of new source terranes or volcanism in the basin's source region?

Contrary to past assumptions, the petrographic, geochemical, and geochronological data from the Hornbrook Formation clearly show that provenance changed through time and was not limited to the Klamath Mountains. The quartzite clasts from the basal Hornbrook Formation contain a Precambrian detrital zircon age distribution very similar to those found in the eastern Klamath Mountains, while all other Precambrian zircons from sandstones in

Hornbrook Formation correlate more closely with northern Sierra Nevada terranes. With the exception of the quartzite clasts in the basal member, Precambrian ages are rare in the Hornbrook Formation, and Paleozoic ages, common in the Klamath Mountains, occur only in the youngest Hornbrook member. Changes in the Mesozoic age distributions throughout the Hornbrook stratigraphy suggest increasing input from an active magmatic other than a Klamath Mountain source. In addition, the decreasing volcanic input and the decreasing amount of zirconium suggest either the dissection of a magmatic arc source and/or multiple source regions. Finally, zircon age distributions from the Hornbrook Formation correlate with the combined detrital zircon distributions of the Great Valley Basin (Surpless et al., 2002, 2003) more closely than with the combined distributions of the Methow Basin. Taken together, these data support the interpretation by Miller et al. (1992), which connects the Hornbrook and Great Valley Basins, and possibly the Ochoco Basin, into one forearc basin that extended almost the length of the western United States (Fig. 2).

GEOLOGIC SETTING

General History of the North America Cordillera

A summary of the geologic development of the North American Cordillera by Burchfiel et al. (1992) begins with the Late Devonian Antler Orogeny. Allochthonous continental slope and rise rocks were forced east during this orogeny, up onto the continental shelf where they were eroded and deposited in a foreland basin as a result of the continental loading of the Antler allochthon (Burchfiel et al. 1992, and references therein). As the mountains of the Antler Orogeny were dissected, the North American Cordillera again became part of a passive margin during the late Paleozoic (Burchfiel et al., 1992, and references therein). During the Pennsylvanian and Permian Periods, the interior of the

Cordillera was deformed by the uplift of the Ancestral Rockies and by the northward movement of the southwestern region along dextral strike-slip faults, creating a new continental margin (Burchfiel et al., 1992, and references therein). During the Triassic Period, Sonomia was accreted to western North America; however, the Late Triassic and Early Jurassic Periods also mark the beginnings of a magmatic arc (Burchfiel et al., 1992, and references therein) that is a possible source for the Hornbrook Formation.

Terrane Motions and Paleogeography

The highly controversial Baja-British Columbia Hypothesis, originally proposed by Beck (1976), Irving (1985), and Umhoefer (1987), suggests that the Insular superterrane, which includes most of western British Columbia, the Coast belt of British Columbia and northern Washington, have been transported about 3000 km northward to their current positions relative to the craton (Wyld et al., 2006). Paleomagnetic research has determined a range of terrane movement from about 500 km (Vandall, 1993) to 4000 km (Panuska, 1985), creating dissent between the supporters of the "Baja-BC" hypothesis (Beck et al., 1981; Irving et al., 1985; Umhoefer, 1987) and those who support an essentially in situ accretionary belt (e.g., Monger, 1975, 1977; Miller, 1987; Irwin and Wooden, 1999).

The Baja-British Columbia controversy is ongoing, and in recent years new studies support both large-scale (~3000 km) and small-scale (~1000 km) transport. Data presented by Ague and Brandon (1996) and Wynne et al. (1995) suggest that the Coast belt of British Columbia and northern Washington and the Cascade belt of Washington and Oregon have been transported approximately 3000 km to the north. Ague and Brandon (1996) corrected the paleomagnetic data collected from the Mount Stuart Batholith (96-93 Ma) by Beck et al. (1981) using hornblende geobarometry and determined that the batholith had been tilted

about 8° to the southeast, suggesting that the batholith moved 2900 km ± 700 km to the north relative to the North American craton, rather than the original distance of 3500 ± 500 km proposed by Beck et al. (1981). Wynne et al. (1995) analyzed paleomagnetic data from the Upper Cretaceous strata of Mount Tatlow, British Columbia and determined that these strata were displaced approximately 3000 km ± 500 km to the north. This distance conflicts with geologic correlations done by Monger and Price (1996), possibly because authigenic magnetite, usually a secondary alteration, would provide an incorrect paleomagnetic inclination (Butler et al., 2001).

Research by Ward et al. (1997) on the Nanaimo Group also supports the Baja-BC hypothesis. Ward et al. (1997) determined that Nanaimo Group formed at approximately 42° latitude, but this interpretation may be incorrect because the amount of clay within the Nanaimo Group could create an inaccurate and shallower inclination (Butler et al., 2001). Kim and Kodama (1999) determined that Nanaimo Group has typical characteristics of burial compaction, which shallows the inclination. With this error corrected, the Insular superterrane and Coast Belt might have only moved approximately 1500 km (Kim and Kodama, 1999), rather than the 3000 km originally suggested. Butler et al. (2001) reinterpreted the data using the relevant paleomagnetic research and determined that the Insular superterrane and Coast orogen moved approximately 1000 km northward when corrected for tilting, rotational shallowing, and paleomagnetic inclination in sedimentary rocks. Because complex deformation has destroyed or removed the supracrustal rocks of the Cordillera, the Hornbrook Formation becomes an important test of the Baja BC hypothesis (Butler et al., 2001). Approximately 1000 km of displacement would supply a much wider

range of source rock to the Hornbrook Formation and affect previous interpretations of the relationship between the Hornbrook, Ochoco, Methow, and Great Valley Basins.

Recently, Wyld et al. (2006) reconstructed the paleogeography of the Northern Cordillera by restoring Late Cretaceous and Cenozoic contraction and extension, known fault displacements back to 100 Ma, and strike-slip faulting in western California (Fig. 3). While there is a discrepancy about how much movement occurred in the Cordillera, the geologic record of the Northern Cordillera suggests that some terranes, whose movements affect the potential source regions of the Hornbrook Basin, have been transported hundreds of kilometers along now inactive faults (Fig. 3; Wyld et al., 2006). Using the minimum distance the terrane could have been transported to the north since 100 Ma, Wyld et al.'s (2006) reconstruction locates the Insular superterrane about 900 km to the south of its current location with its southern tip just west of the southern Klamath Mountains and brings the Ochoco, Hornbrook, and Methow Basins together (Fig. 3).

Wyld et al. (2006) describe a number of similarities between the Methow, Ochoco, and Hornbrook Basins to further support their reconstruction. All three of these basins were deposited during the late Early Cretaceous and unconformably overlap older terranes (Wyld et al., 2006). Although the Methow Basin is 8 km thick, the majority of the basins are typically 1 to 6 km thick with depositional environments that range from marine to non-marine in both shallowing and deepening progressions (Wyld et al., 2006). The source of sediment within these basins varied over time with both eastern and western sources as the tectonic setting changed (Wyld et al., 2006). Although currently the Hornbrook and Great Valley Basins are located much closer to each other than to the Ochoco or Methow Basins, Wyld et al. (2006) suggest that there are few obvious similarities between the two. The Great

Valley Group lies conformably on oceanic crust rather than as an overlap sequence and it was deposited beginning in the Jurassic unlike the Hornbrook, Ochoco, and Methow Basins (Wyld et al., 2006). The reconstruction done by Wyld et al. (2006) restores the Ochoco and Methow Basins to within 100 km of each other (Fig. 3), making the Methow Basin the logical choice for the northern continuation of the now-truncated Hornbrook-Ochoco Basin (Wyld et al., 2006). Based on this reconstruction, the conventional source regions of the Hornbrook, Methow, and Ochoco Basins need to be reconsidered. Wyld et al. (2006) suggest that the western Idaho shear zone could have provided sediment for the Methow Basin, the northern Cascades for the Hornbrook Basin, and the Klamath Mountains for the Nanaimo Basin, each of which is contrary to past interpretations (Wyld et al., 2006).

In contrast with the model presented by Wyld et al. (2006), Miller et al. (1992) propose a Cretaceous paleogeography that began with subduction in the Early to Middle Jurassic spanning the west coast of North America, creating magmatic arcs and adjacent forearc basins. The model suggests that the Hornbrook, Ochoco, and Great Valley Basins were connected as one large forearc basin along the west coast of the United States, separate from the more northern Methow Basin (Fig. 2). The Hornbrook, Ochoco, Methow, and Great Valley Basins each have a magmatic arc traditionally associated with them due to proximity and analysis of their sedimentary provenance, but debate continues on how this magmatic arc formed (Fig. 2; Burchfiel et al. 1992). The magmatic arc, which includes the Klamath Mountains, Blue Mountains, Sierra Nevada Mountains, and Cascade Volcanoes, occurs throughout the Western Cordillera and contains lithologically analogous components (Rubin et al., 1990, and references therein). For example, each section of the arc consists of a similar basement complex of sedimentary continental slope and rise rocks, Devonian and

Mississippian volcanic flows with coeval intrusive rocks, basinal and epiclastic strata, and similar detrital zircon ages (Rubin et al., 1990, and references therein).

General History of the Hornbrook Formation

The Hornbrook Formation is a Cretaceous overlap assemblage that rests unconformably on Paleozoic, Triassic, and Jurassic terranes of the Klamath Mountains (Fig. 4; Nilsen, 1993). The five members of the Hornbrook Formation are the Klamath River Conglomerate, the Osburger Gulch Sandstone, the Ditch Creek Siltstone, the Rocky Gulch Sandstone, and the Blue Gulch Mudstone (Figs. 5 and 6; Nilsen, 1993). These members of the Hornbrook Formation range in age from possibly Albian at the oldest through Maastrichtian at the youngest (Nilsen, 1993). The Hornbrook Formation was deposited in what began as a nonmarine fluvial system that changed through time with increasing depth into shallow marine, outer shelf, and deep marine environments (Nilsen, 1993).

SOURCE REGIONS FOR THE HORNBROOK FORMATION

The Klamath Mountains

The Klamath Mountains of Northern California and Southern Oregon are composed of several thrust sheets or terranes, which dip slightly to the east along with bedding and foliation (Hacker et al., 1995). These mountains are bounded in the west by the Coast Range thrust fault and the Franciscan Complex and to the east by the Hornbrook Formation (Fig. 4). During the Tertiary Period, these rocks were then buried by volcanic and volcanogenic rocks of the Western Cascade Group (Snoke and Barnes, 2006). To the south, rocks of the Great Valley Group unconformably overlie the Klamath Mountains (Fig. 4; Snoke and Barnes, 2006). The disputed tectonic processes that formed the Klamath Mountains and the associated Hornbrook Basin have sparked two main concepts regarding their formation.

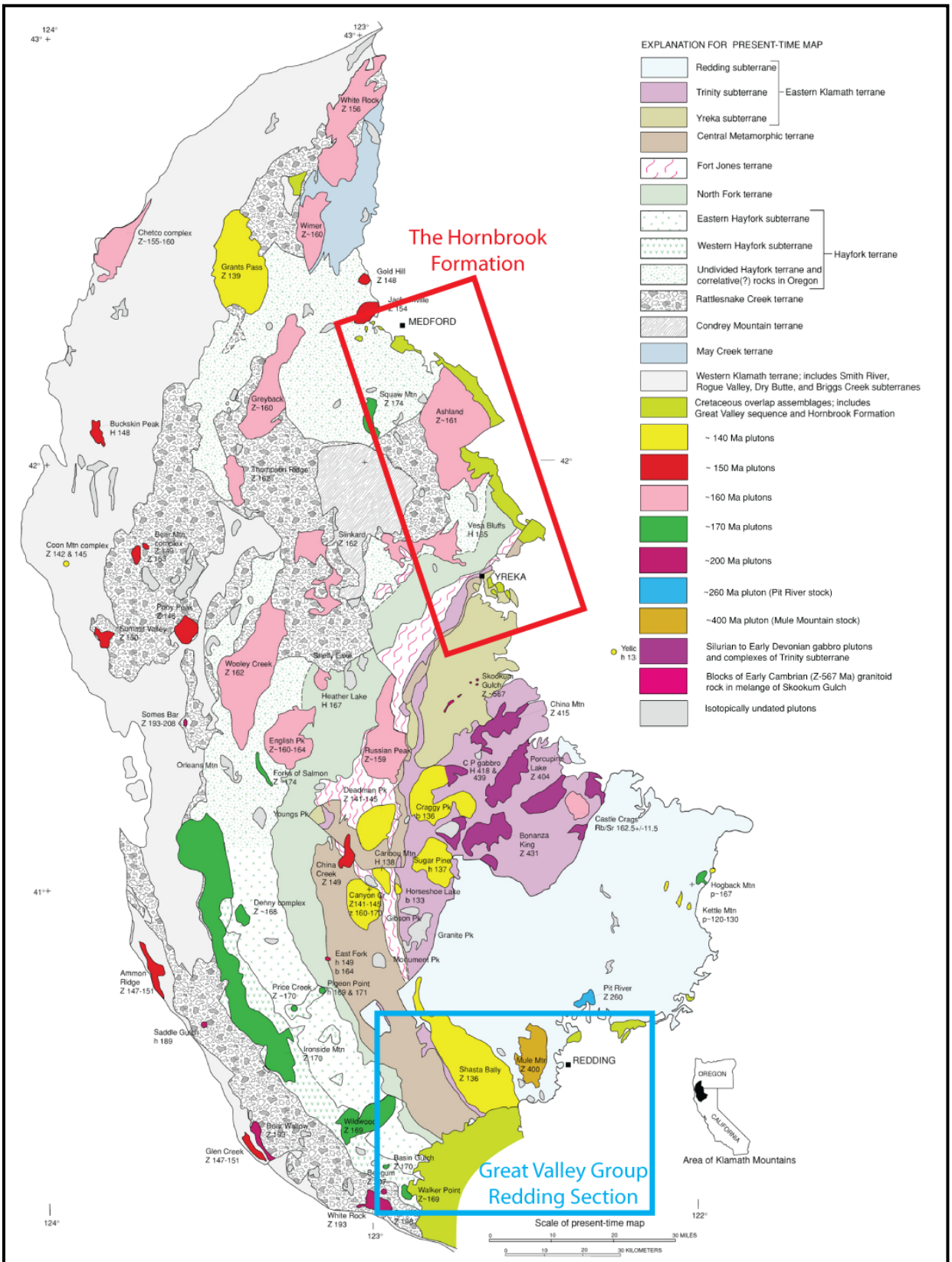

Figure 4: Klamath Mountain accreted terranes, subterranes, and plutons, which suture the terranes together. The Hornbrook Formation rests unconformably on top of the Klamath Mountains. Map modified from Irwin and Wooden (1999).

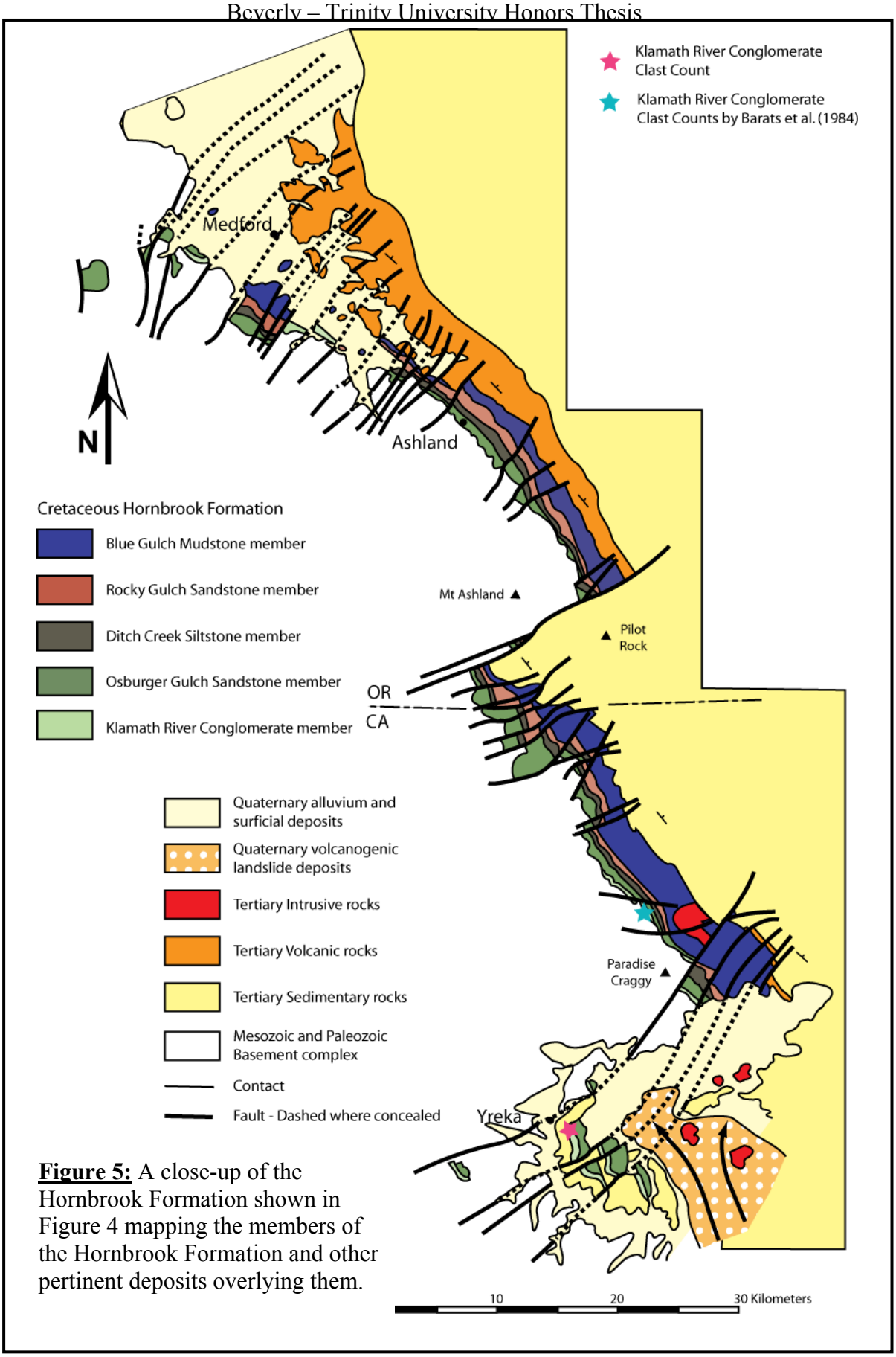

Figure 5: A close-up of the Hornbrook Formation shown in Figure 4 mapping the members of the Hornbrook Formation and other pertinent deposits overlying them.

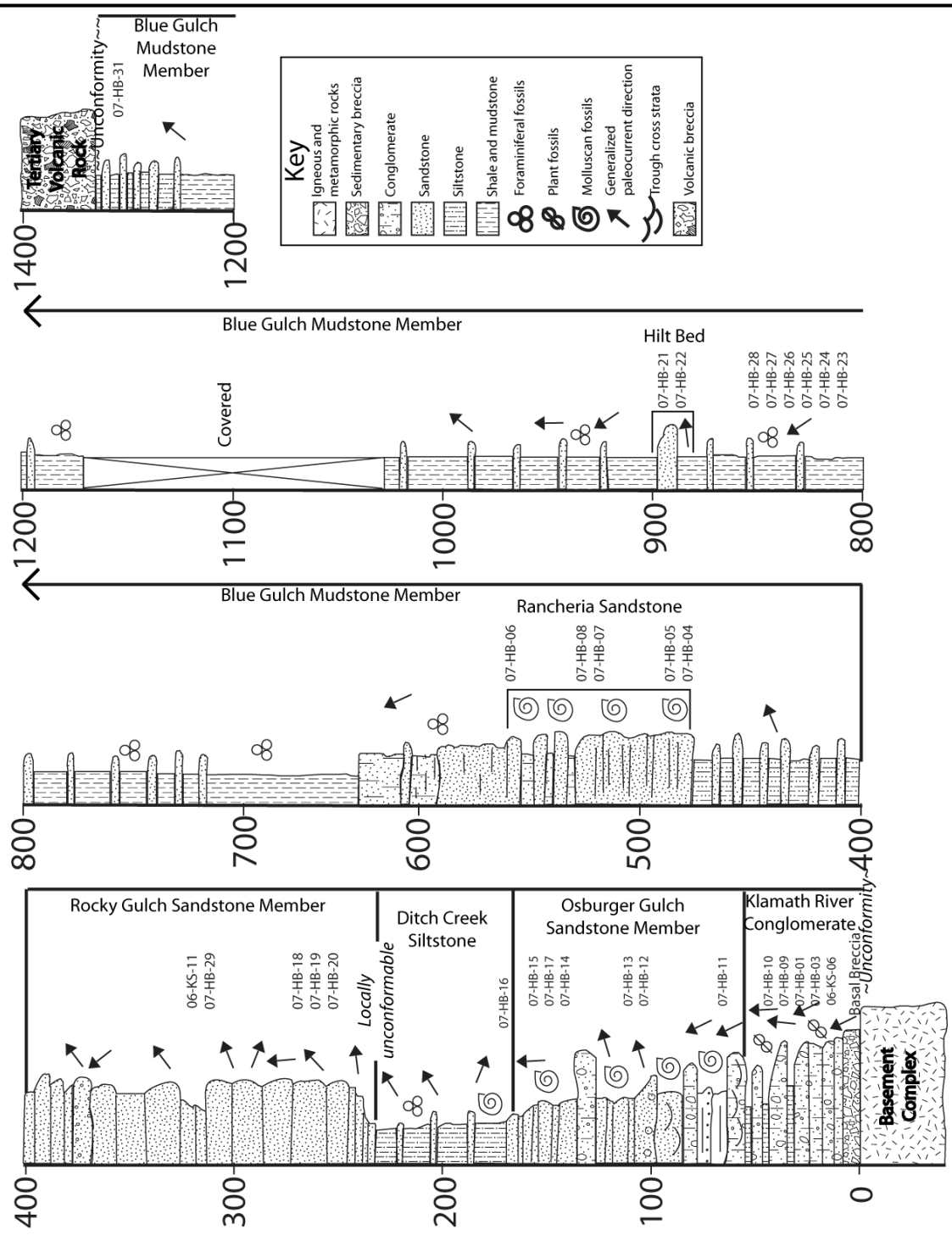

Figure 6: The numbers to the right of the column indicate the approximate location of samples collected from the Hornbrook Formation. See Table 1 for sample descriptions. Note that the type sections used by Nilsen to make the composite stratigraphic column are not necessarily the same outcrop where samples were collected, but they are representative of the Hornbrook Formation. Stratigraphic column and key modified from Nilsen (1992).

Sample #	Rock Member	Location of Outcrop	Location within Outcrop	Rock Type and Purpose
07-HB-31	Blue Gulch Mudstone (Upper)	Dark Hollow Rd. second outcrop in Field Stop 11	Lower section	Sandstone, hand sample
07-HB-22	Hilt Bed (Blue Gulch Mudstone)	Hilt Exit off of I-5 on private road	Upper part of section beneath thick sandstone	Mudstone for geochemistry analysis
07-HB-21	Hilt Bed (Blue Gulch Mudstone)	Hilt Exit off of I-5 on private road	Concretion within upper turbidite sequence	Sandstone for detrital zircon analysis, thin section
07-HB-28	Blue Gulch Mudstone	Dead Indian Memorial Rd. 5 km E of Ashland	Upper Section	Sandstone, hand sample, thin section
07-HB-27	Blue Gulch Mudstone	Dead Indian Memorial Rd. 5 km E of Ashland	Upper Section	Mudstone for geochemistry analysis
07-HB-26	Blue Gulch Mudstone	Dead Indian Memorial Rd. 5 km E of Ashland	Middle section	Sandstone for detrital zircon analysis, thin section
07-HB-25	Blue Gulch Mudstone	Dead Indian Memorial Rd. 5 km E of Ashland	Lower-Middle Section	Sandstone, hand sample, thin section
07-HB-24	Blue Gulch Mudstone	Dead Indian Memorial Rd. 5 km E of Ashland	Lower Section	Sandstone, hand sample
07-HB-23	Blue Gulch Mudstone	Dead Indian Memorial Rd. 5 km E of Ashland	Lower Section	Mudstone for geochemistry analysis
07-HB-06	Rancheria Gulch Beds (Rocky Gulch Sandstone)	Quarry along CDF Fire Road; W of I-5 and Henley-Hornbrook exit	Upper section	Sandstone, hand sample, thin section
07-HB-08	Rancheria Gulch Beds (Rocky Gulch Sandstone)	Quarry along CDF Fire Road; W of I-5 and Henley-Hornbrook exit	Lower section	Sandstone, hand sample; fossiliferous
07-HB-07	Rancheria Gulch Beds (Rocky Gulch Sandstone)	Quarry along CDF Fire Road; W of I-5 and Henley-Hornbrook exit	Lower section	Sandstone, hand sample; fossiliferous
07-HB-05	Rancheria Gulch Beds (Rocky Gulch Sandstone)	Quarry along CDF Fire Road; W of I-5 and Henley-Hornbrook exit	Middle section	Sandstone for detrital zircon analysis, thin section
07-HB-04	Rancheria Gulch Beds (Rocky Gulch Sandstone)	Quarry along CDF Fire Road; W of I-5 and Henley-Hornbrook exit	Lower section	Sandstone; hand sample, thin section
06-KS-11	Rocky Gulch Sandstone	Eagle Mill Rd. 1.8 km S of Valley View Rd. Exit off I-5	Lower-Middle Section	Sandstone for detrital zircon analysis, thin section
07-HB-29	Rocky Gulch Sandstone	Eagle Mill Rd. 1.8 km S of Valley View Rd. Exit off I-5	Lower-Middle Section	Mudstone for geochemistry analysis
07-HB-18	Unknown possibly Rocky Gulch Sandstone	Ditch Creek Rd. adjacent to Ditch Creek	First stop	Sandstone, hand sample
07-HB-19	Unknown	Ditch Creek Rd.	Second stop; thick sand	Siltstone for geochemisty analysis
07-HB-20	Unknown	Ditch Creek Rd.	Second stop; below thick sand	Sandstone, hand sample
07-HB-16	Ditch Creek Silstone	N of Siskiyou Summit along I-5	Uppermost section of Outcrop	Sandstone, hand sample, thin section
07-HB-15	Osburger Gulch Sandstone	N of Siskiyou Summit along I-5	Upper Section of Osburger Gulch Member	Sandstone, hand sample
07-HB-17	Osburger Gulch Sandstone	N of Siskiyou Summit along I-5	Middle Section of Osburger Gulch Member	Sandstone for detrital zircon analysis, thin section
07-HB-14	Osburger Gulch Sandstone	N of Siskiyou Summit along I-5	Upper Section of Osburger Gulch Member	Sandstone, hand sample, thin section
07-HB-13	Osburger Gulch Sandstone	N of Siskiyou Summit along I-5	Middle Section of Osburger Gulch Member	Sandstone for detrital zircon analysis, thin section
07-HB-12	Osburger Gulch Sandstone	N of Siskiyou Summit along I-5	Middle Section of Osburger Gulch Member	Sandstone, hand sample; fossiliferous
07-HB-11	Osburger Gulch Sandstone	N of Siskiyou Summit along I-5	Lower Section of Osburger Gulch Member	Sandstone for detrital zircon analysis, thin section
07-HB-10	Klamath River Conglomerate	N of Siskiyou Summit along I-5	Lowest section of overall outcrop	Sandstone, hand sample; fossiliferous
07-HB-09	Klamath River Conglomerate	N of Siskiyou Summit along I-5	Lowest section of overall outcrop	Sandstone, hand sample; fossiliferous, thin section
07-HB-01	Klamath River Conglomerate	Roadcut along Oberlin Rd. 3 km SE of Yreka	Lower section; turbidite cycle two	Quartzite clasts for detrital zircon analysis, thin section
07-HB-03	Klamath River Conglomerate	Roadcut along Oberlin Rd. 3 km SE of Yreka	Lower section; turbidite cycle one	Mudstone for geochemistry analysis
06-KS-06	Klamath River Conglomerate	Roadcut along Oberlin Rd. 3 km SE of Yreka	Lower section; turbidite cycle one	Sandstone for detrital zircon analysis, thin section

Table 1: The location and rock type of the samples show in Figure 6. The location of the outcrops can be found using Nilsen's Field Guide (1984).

One idea, summarized by Irwin and Wooden (1999), suggests that the Klamath Mountains went through a series of eight accretionary episodes during which various allochthonous terranes subsequently accreted onto the Klamath Mountains. These terranes were sutured together with plutons and stocks ranging in composition from ultramafic to silicic (Snoke and Barnes, 2006). Traditionally, the progressive tectonic accretion of oceanic the Klamath Mountains has been the archetypal example of this type of mountain belt (Snoke and Barnes, 2006). In contrast, Hacker et al. (1995) propose that changes in the speed of subduction led to alternating periods of subduction and magmatism, contraction, and short-lived extension substantial enough to create oceanic crust in situ. Hacker et al. (1995) hypothesize that oceanic crust found within the Klamath Mountains was caught in between two terranes as they contracted. Hacker et al. (1995) also suggest that this model can also be applied to the Cascade Range, Blue Mountains, and northern Sierra Nevada Mountains.

If the Klamath Mountains are a source region for the Hornbrook Formation, sediment characteristic of the eastern terranes of the Klamath Mountains should be found within the Hornbrook Formation. The nearby Rattlesnake Creek terrane, Eastern Hayfork subterrane, and Eastern Klamath terrane (Trinity, Yreka, and Redding subterranes) are all possible sources (Fig. 4). I have focused on the ages of the plutons within these terranes because intermediate and felsic plutons supply the most zircon in the sediment. The Rattlesnake Creek terrane consists mostly of mélange of tectonite, ophiolite, and volcaniclastic rock and is intruded by earliest Jurassic plutons (U/Pb age of ~200 Ma) (Fig. 4; Wright, 1981; Petersen, 1982; Gray, 1985). Another pulse of plutonism related to accretion occurred at about ~160 Ma (Fig. 4; Wright and Fahan, 1988; Hacker and Ernst, 1993; Yule, 1996; and Irwin and Wooden, 1999). While most of the plutonism occurred during these two pulses,

Saleeby and Harper (1993) date a plagiogranite within this terrane at about 170 Ma, and Harper et al. (1994) date the Grants Pass pluton as ~140 Ma (Fig. 4).

The Eastern Hayfork subterrane is a mélange of ultramafic rocks, mafic rocks, limestone, and clastic rocks with Silurian and Triassic fossils (Hacker et al, 1995). At 170 Ma, regional contraction and associated metamorphism of the Siskiyou Orogeny (167 to 170 Ma) formed the basement of the Western Hayfork subterrane and intruded the Eastern Hayfork subterrane (Wright and Fahan, 1988). Plutons of gabbroic and more felsic compositions (U/Pb ages of 168 to 177) intruded volcanics during the Middle Jurassic, probably as a result of accretion (Fig. 4; Lanphere et al., 1968; Wright, 1981; Fahan, 1982; Hacker et al, 1995). In the Middle Jurassic, northwest-southeast extension ensued, which Hacker et al. (1995) suggest formed the ophiolite sequences found within the Klamath Mountains (Preston Peak and Josephine ophiolites). By the Late Jurassic, large-scale thrust faulting and metamorphism that has traditionally been associated with the Nevadan Orogeny deformed the Klamath Mountains (Hacker et al., 1995; and references therein). From the Devonian to the Jurassic, over ten kilometers of sediment and volcanics were deposited to make up the Eastern Klamath terranes, which consist of tuffaceous rocks, limestone, shale, and chert (Hacker et al, 1995, and references therein).

Three main subterranes make up the Eastern Klamath Terrane: Trinity, Yreka, and Redding subterranes. The Trinity subterrane dominantly consists of peridotite whose chemistry implies an oceanic origin, but a true ophiolitic origin is debated (Mattinson and Hopson, 1972; Lindsley-Griffen, 1977; 1982; Quick, 1981; Jacobsen et al., 1984; Boudier et al., 1989). A layered gabbro from the Trinity subterrane yielded a zircon age of ~470 Ma (Mattinson and Hopson, 1972). Wallin et al. (1990) also give dikes which intrude these

gabbros zircon ages of ~410 Ma. The lower Paleozoic Yreka subterrane covers the Trinity subterrane to the north with low-grade metasedimentary and metavolcanic rocks, volcaniclastic and quartz-rich sandstone, argillite, and limestone (Rubin et al., 1990). Using zircon U/Pb analysis, Wallin (1990) dated the granitic blocks within the Shookum Gulch mélange of the Trinity subterrane as ~570 Ma. The Antelope Mountain Quartzite, an important facies of the Yreka subterrane, underlies the Hornbrook Formation in the area surrounding Yreka, California and thus is a very likely source of sediment (Fig. 4; Wallin et al., 2000). The Antelope Mountain Quartzite signature contains only Precambrian age zircon (1.3 to 3.0 Ga; Wallin et al., 2000) and should therefore provide a very clear signature if found in the Hornbrook Formation. The Devonian to Middle Jurassic Redding subterrane contains dominantly volcanogenic and sedimentary rocks that overlie the Trinity terranes in the south (Rubin et al., 1990). The Mule Mountain Stock, which intrudes into both the Copley Greenstone and Balaklala Rhyolite, is dated using U/Pb analysis of zircon as ~ 400 Ma (Albers et al., 1981).

The Sierra Nevada Mountains

Much of the plutonism, igneous activity, extension, and dike intrusion in the Sierra Nevada Mountains occurred simultaneously in the Klamath Mountains (Hacker et al., 1995; and references therein). The Sierra Nevadan magmatic arc, which developed during the late Mesozoic as a result of a subduction zone to the west from the Late Jurassic to Early Cretaceous, is commonly linked with the Great Valley Basin but the northern region is also a potential source for the Hornbrook Formation (Fig. 7; Ingersoll, 1978; 1979). The sediment shed off of the Sierra Nevadas into the eastern Great Valley was deposited in a deltaic, shallow marine, and submarine fan environment (Ingersoll, 1979; Haggart and Ward, 1984).

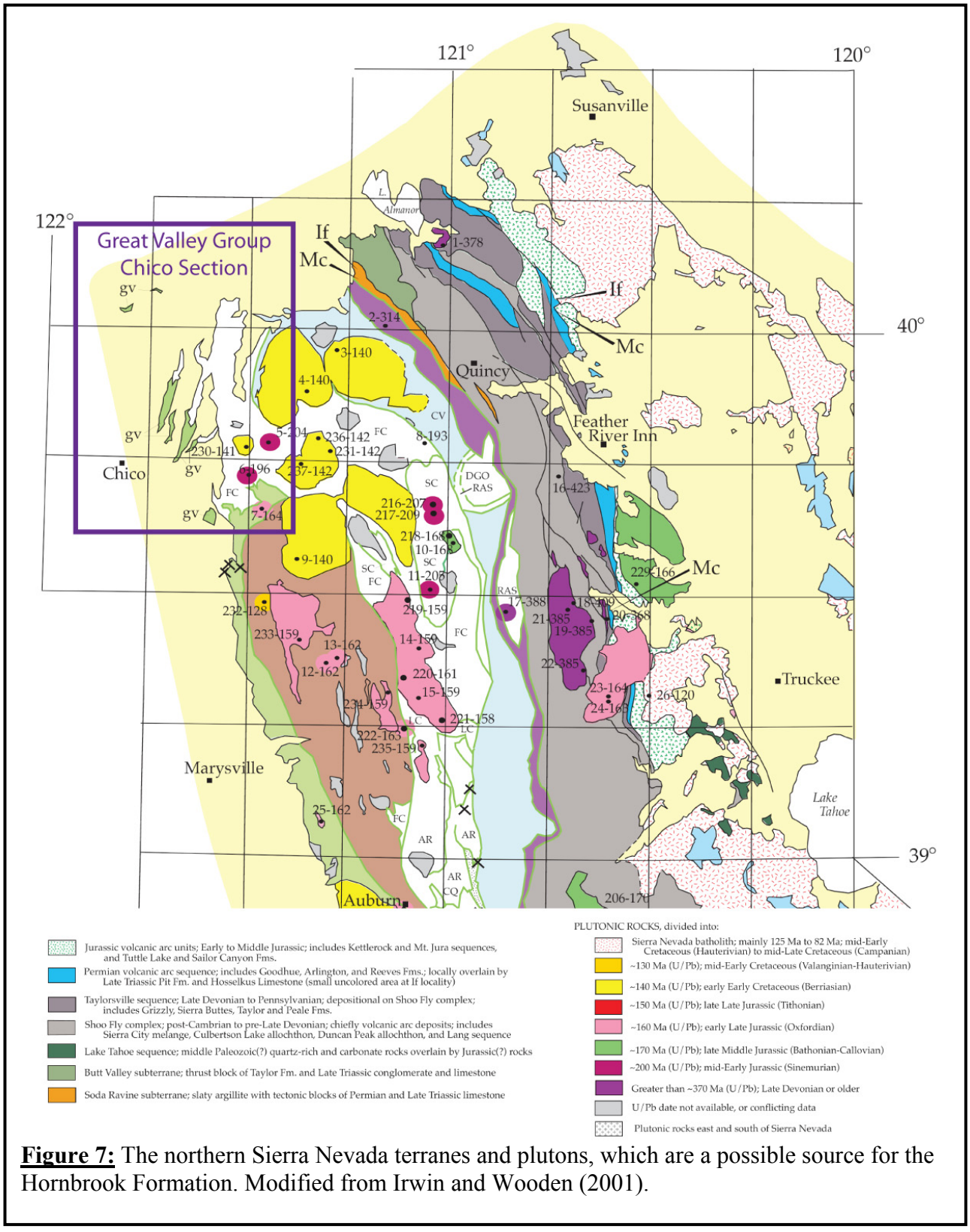

Figure 7: The northern Sierra Nevada terranes and plutons, which are a possible source for the Hornbrook Formation. Modified from Irwin and Wooden (2001).

The Northern Sierra Nevadan terrane is divided into the Shoo Fly Complex, and the overlying Upper Devonian Taylorsville sequence (Schweickert et al., 1984), which are both intruded by the Sierra Nevada batholith (Fig. 7; Bateman, 1981; 1983; Saleeby, 1986). The lower Paleozoic Shoo Fly Complex is dominantly deep water sedimentary rocks, chert, carbonate, basaltic lavas, submarine tuff, and mélange (Schweickert et al., 1984), and has commonly been correlated with the Yreka terrane of the Klamath Mountains as a result of lithological and biological similarities between the terranes (Bond and Devay, 1980; Wallin, 1989; Potter et al.,1990). The Taylorsville sequence contains the Grizzly, Sierra Buttes, and Taylor Formations (Harwood, 1988). At ~380 Ma plutons were intruded into these three formations, and U/Pb zircon analysis has been used to date them (Fig. 7; Hanson et al., 1998; Saleeby et al., 1987). Other important northern Sierra Nevada plutonism occurred at ~140 Ma (Saleeby et al., 1989) and at ~200 Ma (Fig. 7; Edelman et al., 1989; Saleeby et al., 1989).

The Blue Mountains

The Blue Mountains are commonly considered the source of sediment for the Ochoco Basin, which has often been linked in reconstructions (Miller et al., 1992; Wyld et al., 2006) with the Hornbrook Basin. The Blue Mountains of northeastern Oregon began assembling 100 to 105 Ma and ended 90 Ma as magmatism expanded northward from the Sierra Nevadas (Cowan and Bruhn, 1992; and references therein), creating a magmatic arc that is the assumed source of material for the Ochoco forearc basin to the west (Kleinhans et al., 1984). During the Albian and Turonian, sediment was deposited in the Ochoco Basin that ranged from a non-marine to deep marine environment (Kleinhans et al., 1984).

The collision of the Blue Mountain terranes occurred almost simultaneously with collisions within the Sierra Nevada (Schweickert and Cowan, 1975). The four main terranes

of the Blue Mountains, the Wallowa, Baker, Izee, and Olds Ferry terranes, are elongate and east-west trending (Ave Lallemant, 1995). During the Late Triassic to Early Jurassic, the Izee terrane was subducted underneath the Olds Ferry terrane and the Baker terrane was then accreted onto it (Hotz et al., 1977; Ave Lallemant, 1995). The Wallowa terrane formed as result of a volcanic arc active from the Pennsylvanian to the Late Triassic with minor volcanism until the Jurassic (Goldstrand, 1994; White and Vallier, 1994). The research of Walker (1981, 1982, 1986) gives a U/Pb zircon ages of 265 to 233 Ma for the plagiogranite while a gneiss from this terrane has a U/Pb zircon age of 309 Ma (Walker, 1986). During the Late Triassic to Early Jurassic, the Wallowa terrane collided with the Baker-Izee-Olds Ferry terrane, and then from 143 to 120 Ma, the terranes were sutured together by plutons (Armstrong et al., 1977; Walker, 1989).

METHODOLOGY

Field Work

Based on the field guide by Nilsen (1984), six outcrops were chosen in order to sample all members of the Hornbrook Formation. At each outcrop an overall survey was taken in order to assess the best location to collect medium-grained sandstone samples for analyses and to pinpoint the location of the samples within the stratigraphic work done by Nilsen (1984; 1993). Sedimentary structures were documented and fossils collected in order to corroborate Nilsen's (1993) interpretation of the Hornbrook Formation. Sandstone and quartzite samples were collected for detrital zircon analysis and thin section provenance, and mudstone was collected for major and trace element geochemistry. I collected samples of medium-grained sandstone whenever possible as these are the optimal size for detrital zircon analysis.

Petrographic Analysis

The fifteen samples taken from the five members of the Hornbrook Formation were made into thin sections and stained with sodium cobalt nitrate in order to distinguish potassium feldspar from quartz more easily. Point counts were used to determine the percentages of detrital minerals, matrix, cement, and lithic fragments within these thin sections. These percentages were then applied to the fields of provenance calculated by Dickinson et al. (1983). In each sample 400 grains were tallied using a mechanical stage. Depending on the width of the grains within the sample, the distance moved across the sample was adjusted in order ensure that no grain was counted twice. Twelve different compositional categories reflected the types of material found in the Hornbrook Formation: monocrystalline quartz, polycrystalline quartz (including chert), plagioclase, potassium feldspar, chlorite, micas, matrix, cement, unidentifiable grains, and volcanic, metamorphic, and sedimentary lithic grains. The unidentifiable grains include all grains too weathered or diagenetically altered to identify and those grains such as amphibole that formed too small of a percentage of the entire sample to create a separate category.

Geochemical Analysis

Five mudstone and siltstone samples were collected for major and trace element geochemical analysis. Thirty-gram samples were sent to the GeoAnalytical Lab at Washington State University where these samples were analyzed for the fourteen rare earth elements and Ba, Th, Nb, Y, Hf, Ta, U, Pb, Rb, Cs, Sr, Sc, and Zr. The GeoAnalytical Lab uses inductively coupled plasma emission mass spectrometry and an x-ray fluorescence spectrometer to determine the parts per million concentrations of these elements in the bulk rock composition. Vanadium-scandium and zirconium-thorium plots as well as plots of rare

earth elements normalized to the North America Shale Composite (NASC) are all useful for determining the history of provenance changes within sedimentary formations (Rollinson, 1993; Ryan and Williams, 2007). I analyzed my geochemical data using these three types of plots to demonstrate the relative changes between members of the Hornbrook Formation and to support the conclusions made from the petrographic and detrital zircon analysis.

Detrital Zircon Analysis

Sampling Strategy and Laboratory Techniques

In order to achieve representative sampling, nine 3-5 kg samples were collected from the various members of the Hornbrook Formation for detrital zircon analysis (Fig. 6). By sampling the top and bottom of each member, any changes in provenance within members and between members will be documented. To separate zircon from the sandstone, the samples were ground using a jaw crusher and disk grinder to reduce the sandstones to their original grain size. The crushed samples were then run through a Gemini table to remove the lighter portion of the sandstone. The heavy fraction was then soaked in 10% acetic acid to remove any carbonate material until the sample no longer reacted. These samples were then washed with de-ionized water and placed in a 3% solution of hydrogen peroxide until the sample no longer reacted to eliminate organic material. The samples were then washed again with de-ionized water and dried. A large hand-sized magnet was used to draw off the iron filings and mafic minerals. The non-magnetic portion was then sieved to remove the largest rock fragments, but not the smallest fraction, to avoid biasing the sample by removing tiny detrital zircons. The remaining sample was then placed in Sodium polytungstate (SPT) with a specific gravity of 2.89 which removed the lighter fraction. The remaining heavy fraction was then run through a slope Franz at 20° slope and at 0.1, 0.5, 0.7, and 1.0. amperes,

respectively, to remove additional magnetic grains. The nonmagnetic fraction was then run through methylene iodide (MEI), which has a specific gravity of 3.3. The zircon within the heavy MEI split were picked under a stereoscope to achieve a "pure" split by removing pyrite and other non-zircon grains that remained after the MEI separation. This did not bias the sample as no zircon grains were removed. The final zircon split was then poured and mounted in a 1-inch diameter epoxy plug and polished until the interior of most of the zircon grain was exposed.

Geochronology using Laser Ablation Multicollector ICP Mass Spectrometry

Detrital zircon can be radiometrically dated by using a Multicollector Inductively Couple Plasma Mass Spectrometer and a 193 nm Excimer laser ablation system to measure the U/Th/Pb isotope ratios that are produced as the uranium decays (Gehrels et al., 2006; 2007). Using a wavelength of 193 nm produces well-defined pits with a 35 to 25 μm diameter and depth of about 15 μm in silicate materials such as zircon and enough ablated material to analyze (Gehrels et al., 2006; 2007). For the first 20 seconds, data are collected to determine peak background intensities, and then the laser ablates the zircon grain for 20 one-second iterations (Gehrels et al., 2006; 2007). Simultaneously, the ablated material is carried into the mass spectrometer using helium gas where the U, Th, and Pb isotopes are measured (Gehrels et al., 2006; 2007). For the next 30 seconds, the machine clears out the previous sample and resets for the next sample (Gehrels et al., 2006; 2007). One precisely dated standard grain of SL3 (Sri Lankan zircon) is analyzed after every 5 unknown grains are analyzed (Gehrels et al., 2006; 2007). In each sample I endeavored to analyze 100 zircon grains, which statistically gives an accurate representation of at least 6% of all the ages within that sample that exist in the source region (Vermeesch, 2004) The resulting data were

then processed using the Isoplot Add-in to Microsoft Excel (Ludwig, 2003) to generate concordia plots, cumulative age probability plots, normalized age probability plots, age probability density curves, and age histograms. The concordia plots were used to determine discordant ages within the sample, and if the age was more than 5% discordant, the data were discarded according to procedure by Gehrels et al. (2006; 2007).

RESULTS

Petrology and Stratigraphy of the Hornbrook Formation

Klamath River Conglomerate Member

The Klamath River Conglomerate member forms the basal section of the Hornbrook Formation, which lies on a nonconformity above Paleozoic and Mesozoic igneous and metamorphic rocks and is conformably overlain by the Osburger Gulch Mudstone Member (Nilsen, 1993). The thickness of the Klamath River Conglomerate is variable and ranges from several meters to about 90 m and is absent in some areas. In the type section studied by Nilsen (1993), the Klamath River Conglomerate Member is 36.50 m thick (Fig. 6). The Klamath River Conglomerate contains alternating beds of conglomerate and pebbly mudstone with some sandstone and siltstone inter-bedded (Figs. 8 and 9; Nilsen, 1993). In the coarse grained strata, plant fragments such as leaves, branches, and trunks are common in the southern region, and roots are found in the finer grained strata (Nilsen, 1993). Units often form lens-shaped beds with medium to large-scale cross bedding and fining upward conglomerate cycles (Figs. 8 and 9; Nilsen, 1993). The Klamath River Conglomerate was deposited by debris-flows and mud-flows within alluvial fans and braided meandering fluvial environments (Nilsen, 1993). The Klamath River Conglomerate member overlies Jurassic felsic plutons in the Klamath Mountains but could range in age from latest Jurassic

to earliest Cretaceous (Nilsen, 1993). It is more likely that the Klamath River Conglomerate is Albian to Turonian because the conformable contact with the Osburger Gulch, which is time-transgressive from northwest to southwest, has been dated as Albian to Coniacian in age (Nilsen, 1993). Limited fossil data has prevented scientists from determining if the Klamath River Conglomerate also follows a time-transgressive pattern (Nilsen, 1993).

Barats et al. (1984) conducted three clast counts on the Klamath River Conglomerate at the type section of Nilsen (1993) at different heights in the section: the basement contact,

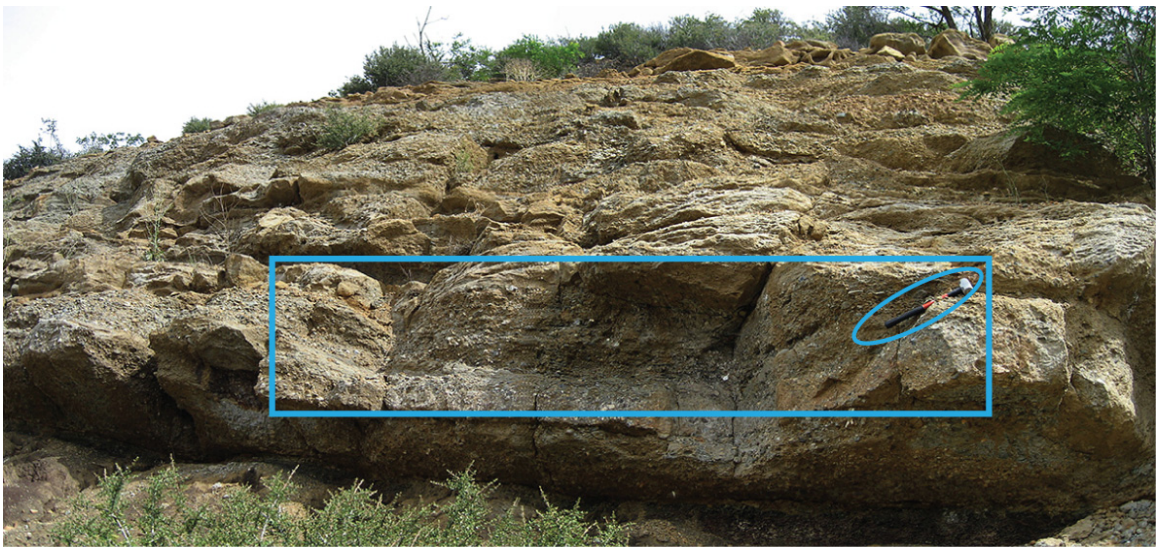

Figure 8: Turbidite cycle two of the lower section of the Klamath River Conglomerate. A clast count was conducted in the area inside the blue box. Notice the hammer circled for scale.

Figure 9: Cross-bedding in the sandstone of the Klamath River Conglomerate. The pebble stringers in the lower half of the picture are common throughout the sandstone beds.

3.8 m, and 35.3 m (Table 1). Barats et al. (1984) chose clasts larger than 2 cm in the longest dimension at random and counted 100 clasts for each sampling. These clast counts yielded greater than 90% metavolcanic rocks, less than 10% chert, and almost no quartzite (Table 2; Barats et al., 1984). I conducted a clast count of the Klamath River Conglomerate in the lower section of turbidite cycle two (Fig. 8). The

Composition of Conglomerate Clasts in Type Section of the Klamath River Conglomerate Member

	Basement Contact	3.8 m above basal contact	35.3 m above basal contact
Metavolcanic rocks	31	35	93
Metasedimentary	0	1	1
Quartzite	1	0	0
Chert (including jasper)	8	4	3
Sandstone	0	0	3
Total	100	100	100

Table 2: Conglomerate clast count conducted by Barats et al. (1984) yielded much less quartzite than found in my clast count, which was not located in Nilsen's (1993) type section. See Fig. 5 for location of the clast count by Barats et al. (1984). Table modified from Barats et al., (1984).

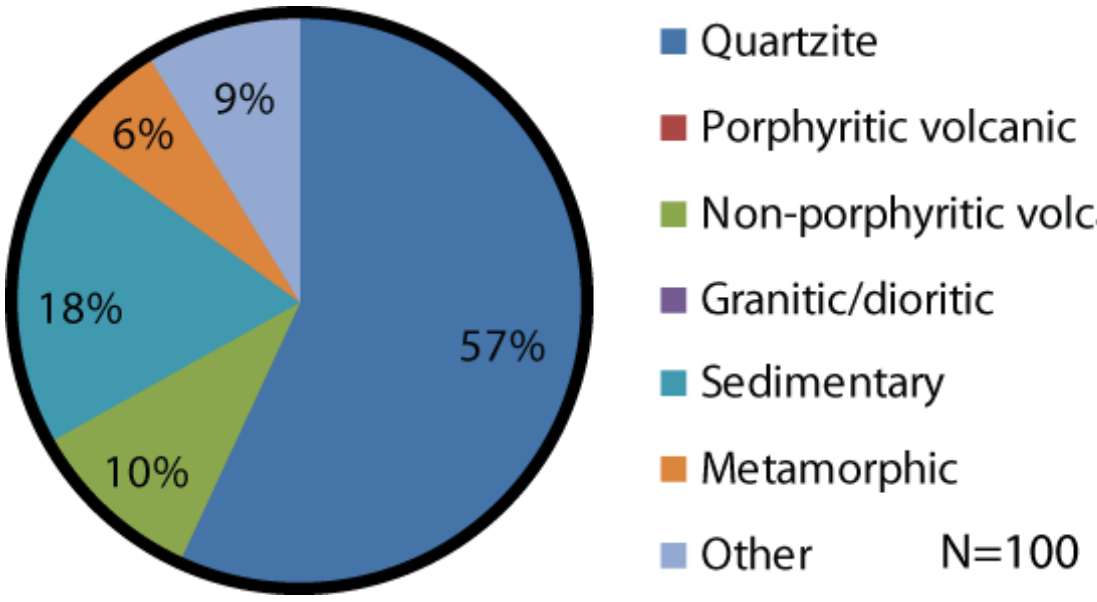

Figure 10: Quartzite makes up the majority of the clasts within the Klamath River Conglomerate, and very little chert was found. See Fig. 5 for the location of the conglomerate clast count.

largest clasts ranged from 2 mm to 8 cm, but were typically 1.5 to 2 cm in diameter with a coarse sand matrix (Fig. 8). To ensure a random sampling of the Klamath River Conglomerate, every 8 horizontal cm a clast was identified and categorized into one of 7 different groups. 100 clasts were identified; over half of the clasts were quartzite, and very little chert was found (Fig. 10). This conglomerate clast count from the Klamath River Conglomerate member is broadly consistent with sandstone petrography from the same member, but yielded more quartzite and fewer volcanic clasts than the sand-sized fraction. This reflects the different susceptibility to weathering and diagenesis of these rock types.

Three samples from the Klamath River Conglomerate were collected for petrographic analysis. Sample 07-HB-01 (See Fig. 6 for sample locations) is a quartzite clast collected during the conglomerate clast count, which consists mostly of polycrystalline quartz, with minimal potassium feldspar and plagioclase (Fig. 11). Sample 07-HB-02 is a feldspathic

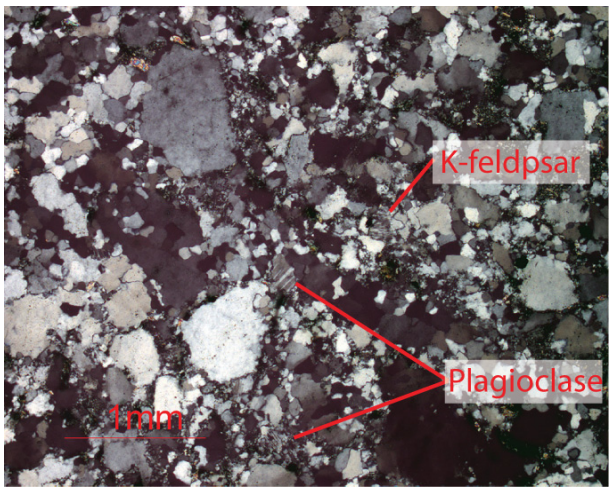

Figure 11: A photomicrograph of quartzite clast sample 07-HB-01 from the Klamath River Conglomerate at 4X crossed polars. Mostly polycrystalline quartz with minimal amounts of potassium feldspar and plagioclase as indicated in the figure. See Figure 6 for stratigraphic location.

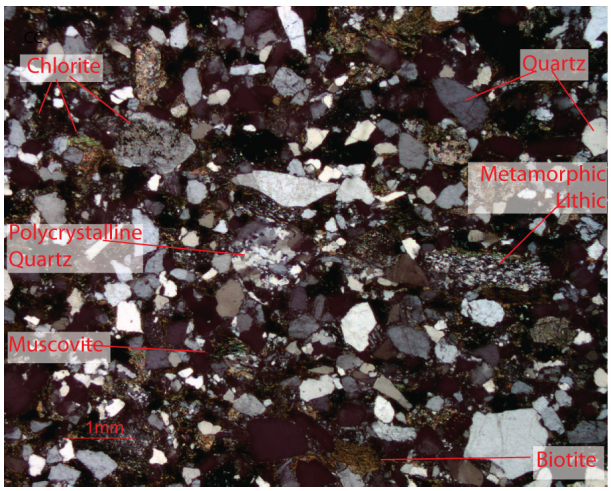

Figure 12: A photomicrograph of sandstone sample 07-HB-02 from the Klamath River Conglomerate at 2X crossed polars. The sandstone matrix has been significantly altered to chlorite. Other common detritus is indicated on the figure. See Figure 6 for sample location within the stratigraphy.

sandstone, which is dominated by monocrystalline quartz (Fig. 12). Other common detritus includes polycrystalline quartz, muscovite, biotite, metamorphic lithics, and plagioclase. The sample has also been altered significantly, as shown by abundant chlorite (Fig. 12). The sample is poorly sorted with angular grains, and a preferred orientation of the micas and large quartz grains can be seen in Figure 12. This sample falls into the recycled orogen provenance field of Dickinson et al. (Fig. 13; 1983). Sample 07-HB-09 is a feldspathic sandstone whose provenance falls in the basement uplift provenance field (Figs. 13 and 14; Dickinson et al., 1983). Monocrystalline quartz is the most abundant mineral, but significant detrital micas, feldspar, and plagioclase were found, and the matrix of the sample has also been notably altered to chlorite. These classic wavy detrital micas indicate a close source of sediment and

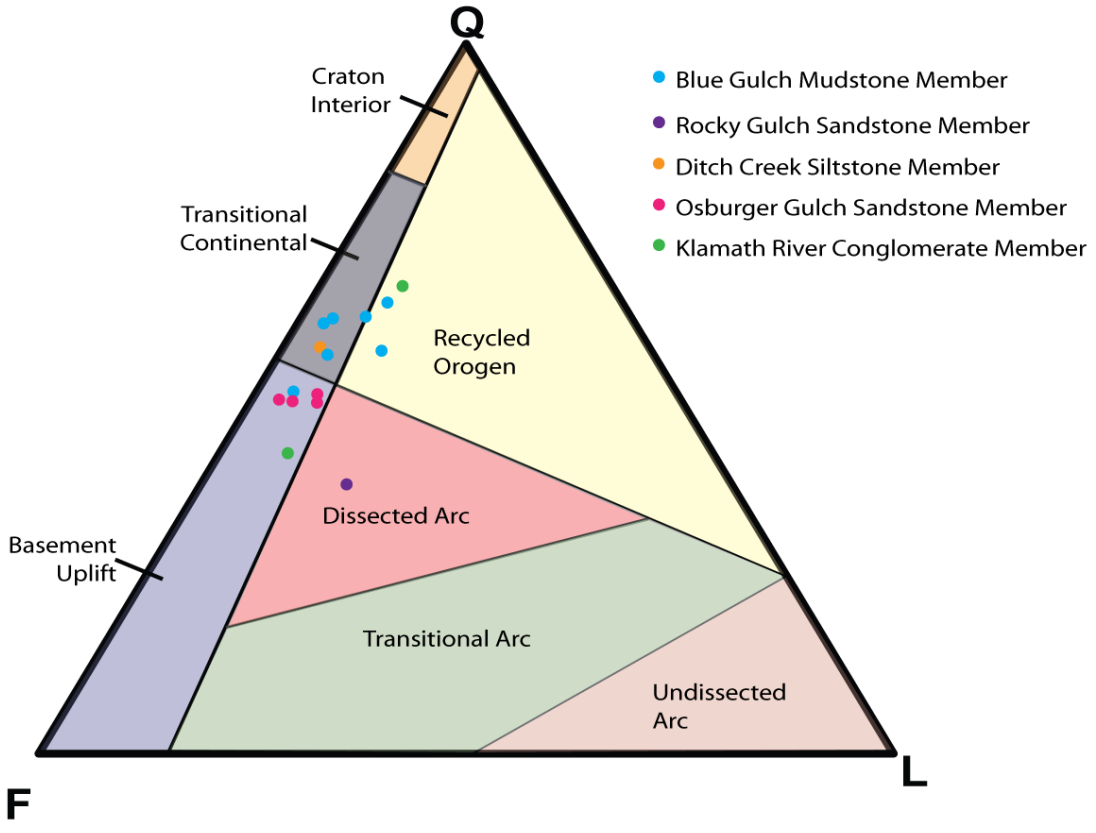

Figure 13: Sandstone petrography of the Hornbrook Formation using fields determined by Dickinson et al. (1983).

show the preferred orientation of the micas (Fig. 14). The sample is poorly sorted with subrounded to subangular grains and quartz overgrowths and sutures can be seen on some grains (Fig. 14). The transition into the Osburger Gulch Sandstone marks a change from non-marine to marine depositional environments (Nilsen, 1993).

Osburger Gulch Sandstone Member

The Osburger Gulch Sandstone usually forms a conformable contact with the Klamath River Conglomerate, and rests on Paleozoic and Mesozoic igneous and metamorphic rocks where the Klamath River conglomerate is absent (Nilsen, 1993). The Osburger Gulch Sandstone is a generally grey, calcareous sandstone with lenses of conglomerate, coquina, and inter-bedded siltstone (Figs. 15, 16, and 17; Nilsen, 1993). The carbonaceous and micaceous siltstone is often laminated or ripple-laminated and heavily bioturbated (Nilsen, 1993).

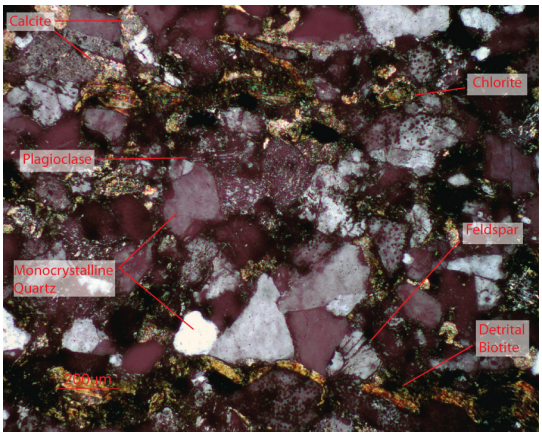

Figure 14: Photomicrograph of feldspathic sandstone sample 07-HB-09 of the Klamath River Conglomerate at 10X crossed polars. Notice the classic wavy detrital biotite at the bottom of the photomicrography. See Figure 6 for stratigraphic location.

Figure 15: Thick laterally continuous sand beds of the Osburger Gulch Sandstone. See Fig. 6 for stratigraphic location of outcrop.

The lower section of the Osburger Gulch Sandstone is characterized by thick beds, large-scale cross-stratification, and medium to very coarse-grained sandstone, while the middle section can be parallel-stratified, trough cross-stratified, or massive (Fig. 15; Nilsen, 1993). The Osburger Gulch Sandstone fines upward through the section as bioturbation increases in abundance (Nilsen, 1993). The member is usually 75 to 150 m thick but averages about 100 m and can range from zero to an estimated 250 m as much of the Osburger Gulch Sandstone is covered (Fig. 5; Nilsen, 1993). The Osburger Gulch Sandstone was deposited in a mostly marine shelf environment with abundant hummocky cross-stratification and changed from a very high-energy environment to an offshore environment of lower energy (Nilsen, 1993). In other areas, the Osburger Gulch Sandstone was part of a transgressive Cretaceous shoreline with lagoonal environments, which is further demonstrated by the fossils found in the Osburger Gulch Sandstone (Nilsen, 1993). Oysters, turritellas, gastropods, and pelecypods all suggest shallow marine conditions of high energy

Figure 16: Shell hash commonly found throughout the Osburger Gulch Sandstone. Some bivalve shells are still intact but all have been replaced by sparry calcite. The concentration of broken shells indicates a high energy environment such as a beach. Notice the pencil in left corner for scale.

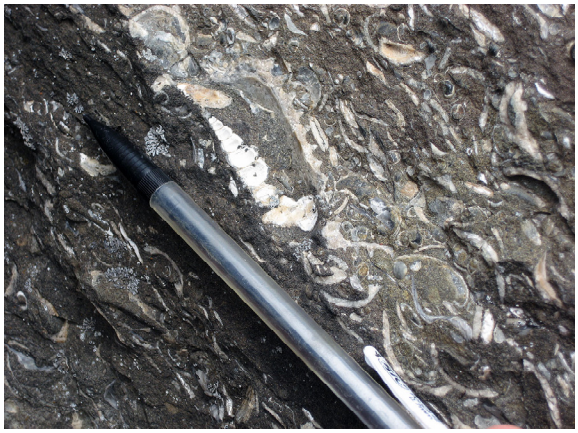

Figure 17: A close up of shell hash commonly found throughout the Osburger Gulch Sandstone. Note the turritella fossil near the center of photograph.

environment (Fig. 17; Nilsen, 1993). The fossils also indicate a Middle Turonian age, but the age of the Osburger Gulch Sandstone ranges from Late Albian to Early Coniacian.

Point counts of four sandstone samples from the lower, middle, and upper Osburger Gulch Sandstone section along Interstate 5 indicate a basement uplift source (Fig. 13; Dickinson et al., 1983). Samples 07-HB-11, 07-HB-13, 07-HB-14, 07-HB-17 all have very similar provenance (See Fig. 6 for stratigraphic location). All of these samples are feldspathic sandstones with a heavily chloritized matrix (Figs. 18, 19, and 20), moderate to poor sorting, subrounded to angular

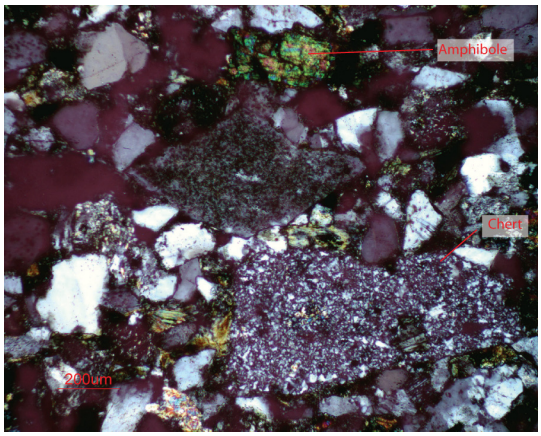

Figure 18: Photomicrograph of feldspathic sandstone sample 07-HB-14 at 10X crossed polars. The chert and amphibole shown here are good examples of such grains found throughout these samples.

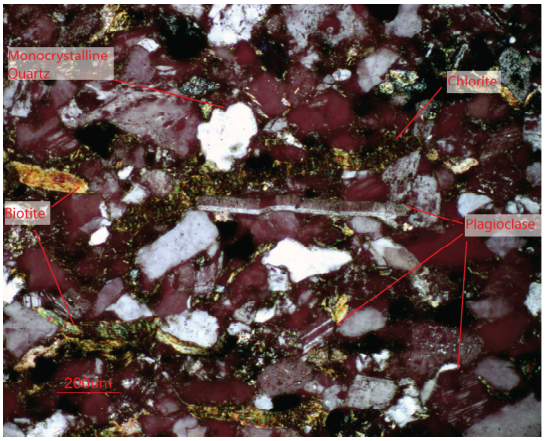

Figure 19: Photomicrograph of feldspathic sandstone sample 07-HB-11 at 10X crossed polars. The micas and elongate plagioclase and quartz crystals demonstrate the preferred orientation of this sample, which is typical of other samples in the Osburger Gulch Sandstone.

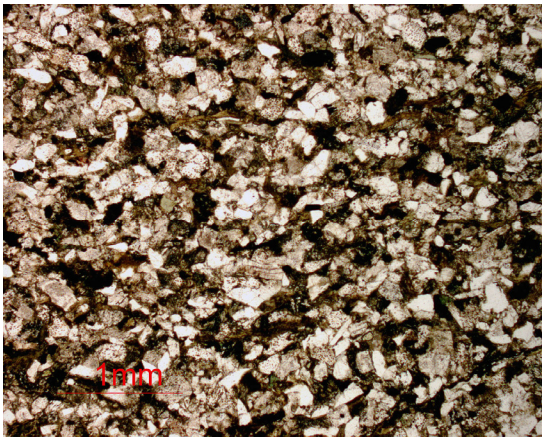

Figure 20: Photomicrograph of feldspathic sandstone sample 07-HB-13 at 4X uncrossed polars. The green, chloritized matrix is easily distinguished in the uncrossed polars of this sample.

grains, and a preferred orientation defined by micas and elongate plagioclase and quartz (Fig. 19). There are a few slight differences between the samples, however. The transition into the Ditch Creek Siltstone is marked by a gradational change from well-stratified and well-sorted sandstone to poorly stratified siltstone and very fine-grained silty sandstone (Nilsen, 1993)

Ditch Creek Siltstone Member

Generally, the Ditch Creek Siltstone forms a conformable but gradational contact with the Osburger Gulch Sandstone where the Hornbrook Formation changes from resistant, cross-bedded, and fine-grained sandstone to a non-resistant and bioturbated, very-fine grained, silty sandstone or siltstone (Fig. 21; Nilsen, 1993). The Rocky Gulch Sandstone overlies the Ditch Creek Siltstone conformably, but some unconformities exist where it is overlain by Tertiary non-marine sedimentary rocks (Nilsen, 1993). This is the first member in the Hornbrook Formation without any conglomerate (Nilsen, 1993). Molluscan fossils are abundant in the Ditch Creek Siltstone and are found in both living positions and as transported fragments (Nilsen, 1993). The organisms found in the Ditch Creek Siltstone created bioturbation that destroyed most of the sedimentary structure in the beds (Nilsen, 1993).

Figure 21: The Ditch Creek Siltstone member is easily eroded and outcrops poorly. The outcrop shown here is not siltstone, but rather thinly laminated sandstone of mostly vfL sand.

Overall, the Ditch Creek Siltstone consists of massive and bioturbated siltstone or very fine grained-sandstone with some rippled lamination (Nilsen, 1993). It is 20 to 80 m thick and is present in

every outcrop but can become very thin in some areas (Fig. 6; Nilsen, 1993). Nilsen (1993) suggests that the Ditch Creek Siltstone was deposited in a low energy outer-shelf environment with slower sedimentation rates that allowed for the extensive bioturbation (Nilsen, 1993). He also proposes that the Ditch Creek Siltstone was deposited in deeper marine conditions in the north that shallowed to the south where a lagoonal environment allowed for coal deposits and shallow marine fossils (Nilsen, 1993). The age of the Ditch Creek Siltstone ranges from Early Turonian to Early Coniacian (Nilsen, 1993). One sandstone sample (07-HB-16) was collected from the Ditch Creek Siltstone. The sample is intensely oxidized with lots of hematite cement, subrounded to angular in shape, and moderately sorted (Fig. 22). Massive and very thick beds of sandstone mark the transition into the Rocky Gulch Mudstone Member.

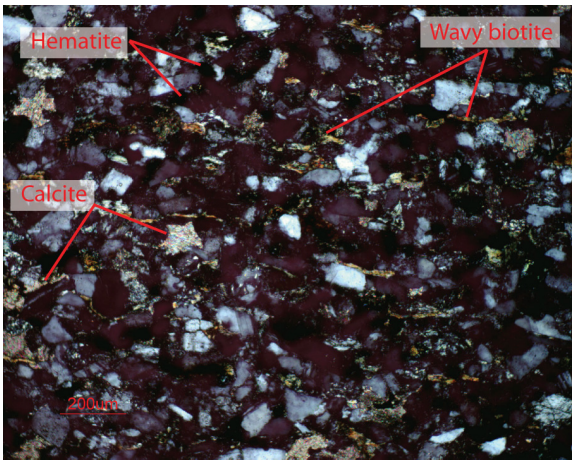

Figure 22: Photomicrograph of sandstone sample 07-HB-16 at 10X crossed polars. The sample has been heavily altered by hematite and calcite cement.

Rocky Gulch Sandstone Member

The Rocky Gulch Sandstone in most cases conformably overlies the Ditch Creek Siltstone, but some contacts may be erosional while others grade into thick beds of sandstone (Nilsen, 1993). These fining upward and thinning upward beds are organized into turbidite cycles of 5 to 10 fine to medium grained sandstone beds per cycle and separated by thin shale beds less than 1 m thick (Fig. 23; Nilsen, 1993). The lower section of this member is commonly amalgamated and contains sole marks such as flute casts, groove casts, and load

Figure 23: The Rocky Gulch Sandstone Member formed from turbidity flows. Each sandstone bed represents a different flow and Bouma sequence.

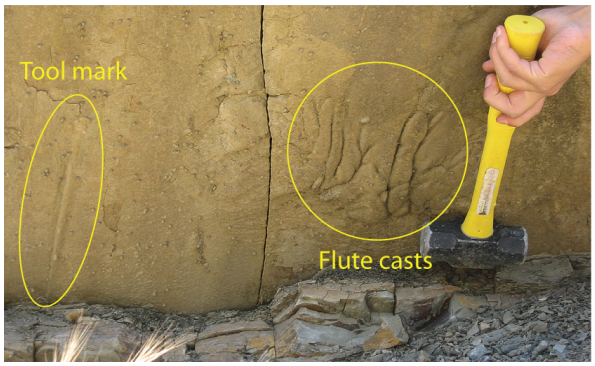

Figure 24: Flute casts and tool markings measured to determine the paleoflow direction of the turbidity currents (See Fig. 25).

casts, along with rip-up clasts from underlying shale beds (Figs. 23 and 24; Nilsen, 1993). The 13°N measurement of flute casts and one tool mark I collected are consistent with those collected by Nilsen (Fig. 6; 1993) and a Klamath Mountain (southern) source of sediment (Fig. 25). The units are generally 115 to 225 m thick and normally graded (Fig. 6; Nilsen, 1993). The Rocky Gulch Sandstone was deposited as deep marine sediment gravity flows, high-concentration turbidity currents, sandy debris flows, or grain flows, forming a turbidite apron on

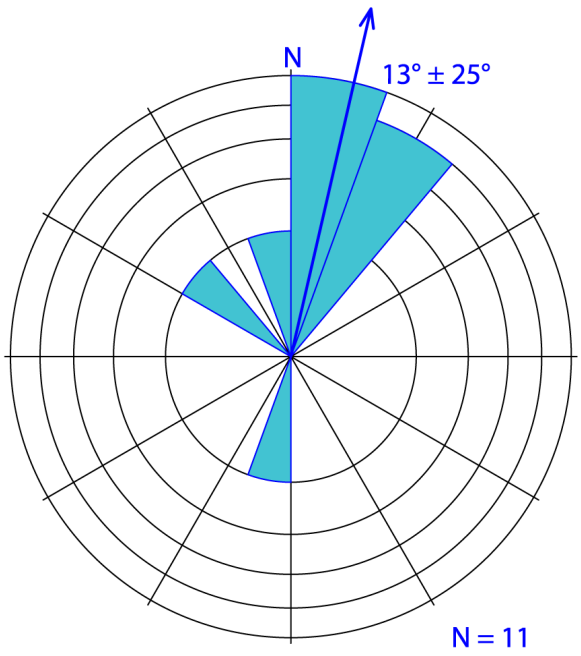

Figure 25: The measurements taken from flute casts and one tool mark give a paleoflow direction of 13° N. This is consistent with previous studies (e.g., Nilsen, 1993) and indicates a potential source for the Hornbrook Formation was to the south, possibly the Klamath Mountains.

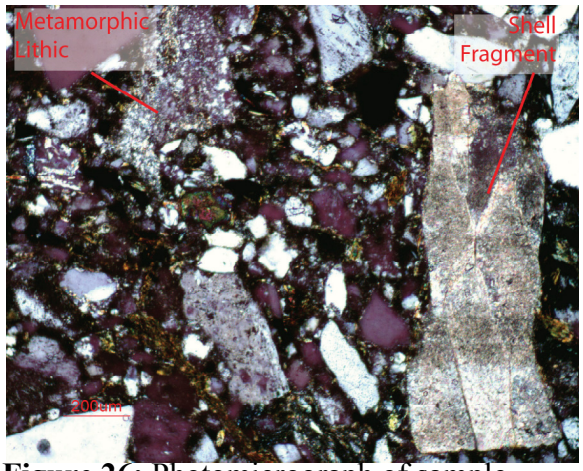

Figure 26: Photomicrograph of sample 07-HB-30 at 10X crossed polars. The metamorphic lithic is characteristic of those found throughout the Hornbrook Formation.

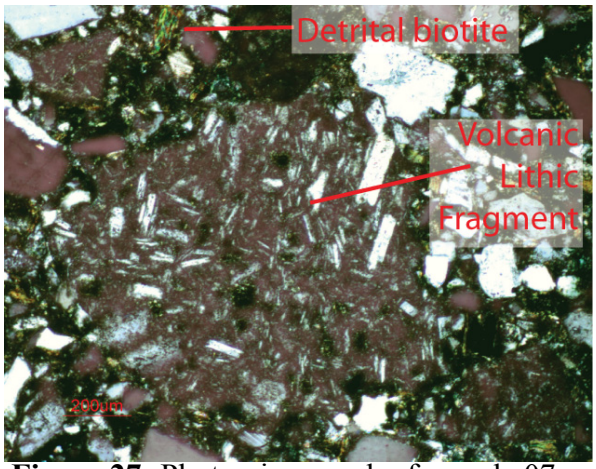

Figure 27: Photomicrograph of sample 07-HB-30 at 10X crossed polars. The volcanic lithic is representative of those found throughout the Hornbrook Formation.

the submarine slope of the Klamath Mountains (Nilsen, 1993). Fossils in the Rocky Gulch Sandstone are limited in number and so the age of this member is not very well defined. Foraminiferas from the middle Turonian are found in the Rocky Gulch Sandstone, giving the member an age range from Turonian to Campanian (Nilsen, 1993). One sample from the lower middle section of the outcrop in Fig. 23 was collected for petrographic analysis. The sample (07-HB-30) was derived from a recycled orogen source of sediment (Fig. 13). It is poorly sorted with subangular to angular shaped grains, and preferred orientation of the grains is defined by micas (Fig. 26). Figures 26 and 27 also demonstrate good examples of shell fragments and volcanic lithic fragments found throughout the Hornbrook Formation.

Blue Gulch Mudstone Member

The Blue Gulch Mudstone Member is the thickest member of the Hornbrook Formation and contains two distinct beds within it, the Rancheria Sandstone Bed and the Hilt Bed (Fig. 6; Nilsen, 1993). The Blue Gulch Mudstone overlies the Rocky Gulch Sandstone conformably everywhere it exists, but the Rocky Gulch is missing in some areas and

therefore the Blue Gulch Mudstone probably lies on top of the Ditch Creek unconformably (Nilsen, 1993). The transition from the Rocky Gulch Sandstone into the Blue Gulch Mudstone is marked by bioturbated mudstone with interbedded siltstone and very fine-grained sandstone rather than the graded beds of fine to medium-grained sandstone characteristic of the Rocky Gulch Sandstone (Nilsen, 1993). The upper contact of the Blue Gulch Mudstone is unconformable as Tertiary nonmarine strata or Tertiary volcanic rocks eroded or altered this contact (Nilsen, 1993).

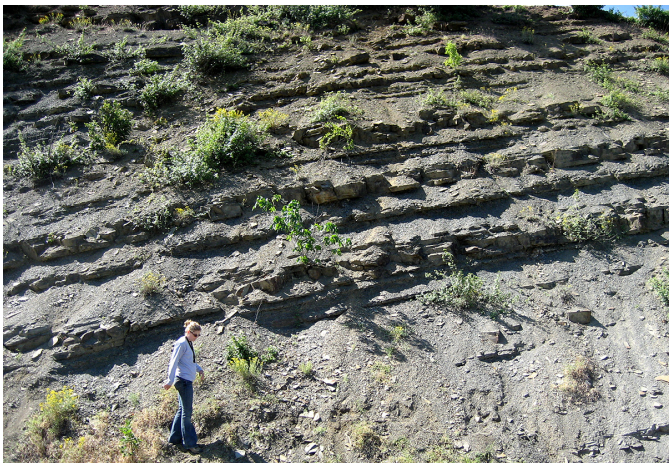

Figure 28: Turbidites of the Blue Gulch Mudstone in the lower middle section of the member. While these flows seem very regular, other areas of the outcrop show greater variations in sandstone thickness as more or less sand came into the system.

Overall the Blue Gulch Mudstone is characterized by mostly silty and nonfissile mudstone, but there are distinct changes between the lower, middle, and upper section (Nilsen, 1993). The lower section is characterized by thin beds of very fine-grained sandstone interbedded with massive bioturbated siltstone (Fig. 28; Nilsen, 1993). In the middle section, the Blue Gulch Mudstone changes from massive siltstone to silty mudstone to

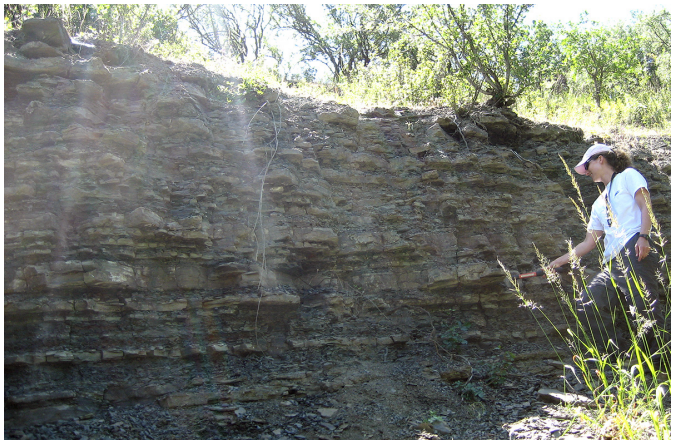

Figure 29: The upper section of the outcrop with much thinner turbidite beds that indicate a deeper, more distal environment.

mudstone as bioturbation and the number of plant fragments and carbonate concretions decreases (Nilsen, 1993). The upper section is characterized by a laterally continuous massive mudstone interbedded with siltstone and very fine-grained sandstone (Fig. 29; Nilsen, 1993). Many sole markings characteristic of turbidite deposits can be found in the Blue Gulch Mudstone, including flute casts and groove casts that provide paleocurrent direction (Nilsen, 1993). The Blue Gulch Mudstone is typically 800 to 900 m thick (Fig. 6; Nilsen, 1993).

The depositional environments of the Blue Gulch Mudstone are variable throughout the section (Nilsen, 1993). The lower and uppermost sections, including the Rancheria Sandstone Bed, were deposited in a shallow marine environment (Nilsen, 1993). The middle and upper sections were deposited in a deep-marine environment, as indicated by the benthic foraminifers that are from at least bathyal depths (Nilsen, 1993). No fossils have been found below the

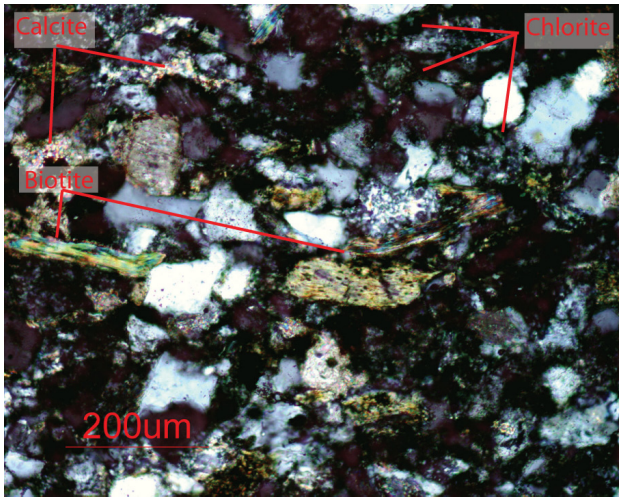

Figure 30: A photomicrograph of sample 07-HB-25 at 20X crossed polars. Both chlorite and calcite have taken over the matrix in some areas. Notice the preferred orientation of the grains demonstrated by the micas.

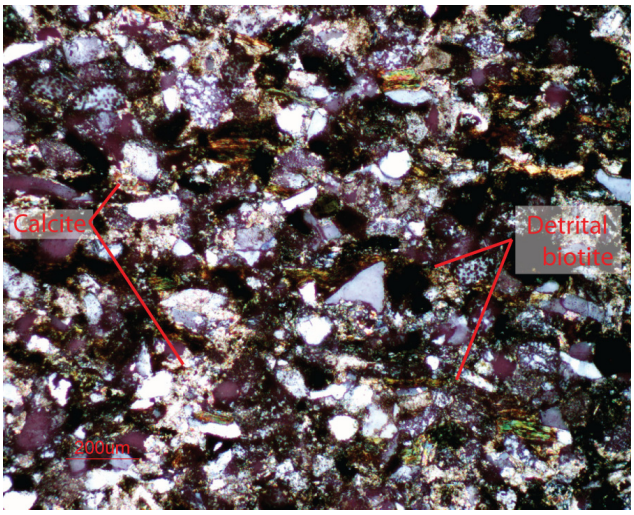

Figure 31: Photomicrograph of sample 07-HB-28 at 10X crossed polars. This classic wavy detrital biotite is concentrated within the laminae shown in Figure 32.

Rancheria Sandstone Bed, resulting in a poor lower time constraint for the Blue Gulch Mudstone (Nilsen, 1993). Also, the ammonites and foraminifers found do not always correlate, giving a possible age range of Late Turonian to early Maastrichtian (Nilsen, 1993).

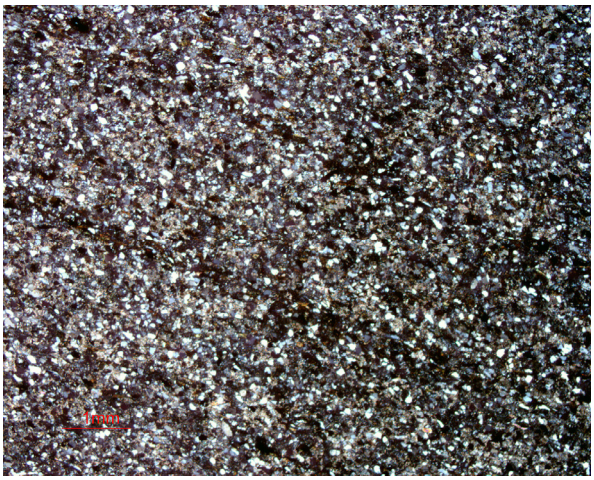

Figure 32: Photomicrograph of sample 07-HB-28 at 4X crossed polars. Notice the laminae, which are defined by higher concentrations of biotite seen in Figure 31 and less calcite than in the lighter areas.

Three samples were taken for petrographic analysis in the Blue Gulch Mudstone. Both samples 07-HB-25 and 07-HB-28 were derived from a transitional continental source of sediment while sample 07-HB-26 was derived from a recycled orogen, based on the provenance field by Dickinson et al. (Fig. 13; 1983). The samples are all moderately to poorly sorted with subrounded to angular shaped grains and a preferred orientation defined by micas and elongate quartz and micas (Figs. 30, 31, and 32). The matrix has been altered by both chlorite and calcite cement in samples 07-HB-25 and 07-HB-26 (Figs. 30 and 31). The micas throughout sample 07-HB-28 show wavy biotite, characteristic of a close sediment source (Fig. 31). Laminae can also be seen in this sample and are defined by more biotite and less calcite cement than in the darker laminae (Fig. 32).

Rancheria Sandstone Bed

The Rancheria Sandstone Bed forms a conformable lens of sandstone within the Blue Gulch Mudstone with siltstone and mudstone interbedded (Fig. 6; Nilsen, 1993). The bed extends for 8 km before pinching out to the northwest and southeast (Nilsen, 1993). Some

Figure 33: In the Rancheria Sandstone beds of the Blue Gulch Mudstone Member, the beds are laterally continuous and contain fossils such as bivalves, gastropods, and burrows.

beds are amalgamated, massive, or hummocky cross-bedded, but all are bioturbated (Figs. 33 and 34; Nilsen, 1993). Some burrows were discovered along with fossils such as pelecypods and gastropods found in living position and as transported fragments (Fig. 35; Nilsen, 1993). The Rancheria Sandstone ranges in thickness from 0 to at least 85 m in thickness, and was deposited in an outer-shelf environment by storm-wave action that formed the hummocky cross-bedding and contains fossils that prefer sand substrates and energetic coastal waters (Nilsen, 1993). Based on the fossils found in the Rancheria Sandstone, this bed is Late Campanian in age (Nilsen, 1993).

Three samples were collected from the Rancheria Sandstone Bed for petrographic analysis. Samples 07-HB-04 and 07-HB-05 have a transitional continental source of sediment

Figure 34: Hummocky cross-stratification found in the middle section of the outcrop, which indicates a storm-dominated shelf environment.

Figure 35: A large bivalve shell fragment approximately 10 cm long.

as defined by Dickinson et al. (1983), while sample 07-HG-06 was derived from a basement uplift source (Fig. 13). All three petrographic samples are moderately sorted and subrounded to angular in shape with a preferred orientation of the grains defined by micas and elongate quartz grains (Fig. 36).

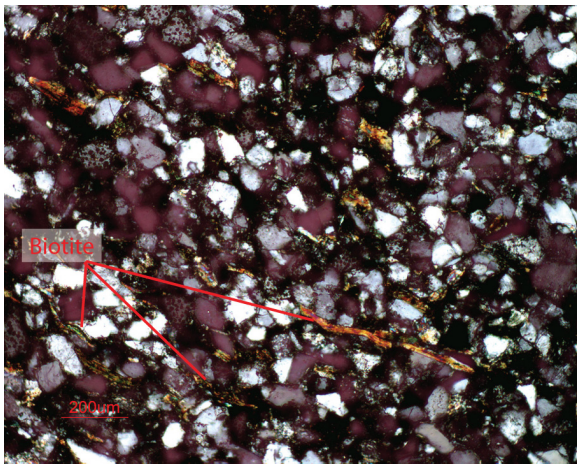

Figure 36: Photomicrograph of sample 07-HB-04 at 10X crossed polars. The biotite in this sample clearly defines the preferred orientation of the grains and is representative of other samples taken from this location.

Hilt Bed

The Hilt Bed is a 2 to 5 m thick sandstone bed within the Blue Gulch Mudstone that formed as a result of compound turbidite sequences in a deep marine environment and extends about 45 km (Nilsen, 1993). The lateral continuity, erosional basal contacts, sole markings, and graded beds all point to Bouma sequences and a deep marine basin environment (Fig. 37; Nilsen, 1993). Based on benthic fauna found in the Hilt Bed, it was probably deposited during the Late Campanian (Nilsen, 1993). Petrographic analysis of the Hilt Bed (07-HB-21) indicates a recycled orogen source of sediment (Fig.13). The grains are moderately sorted and subangular to angular in shape, and the preferred orientation of the grains is defined by micas, chlorite, quartz, and plagioclase (Fig. 39). Almost all of the matrix has been replaced by calcite cement (Fig. 39).

Figure 37: A typical Bouma sequence of the Hilt Bed.

Figure 38: Mudstone beneath the Bouma sequence in Fig. 37 collected for geochemical analysis.

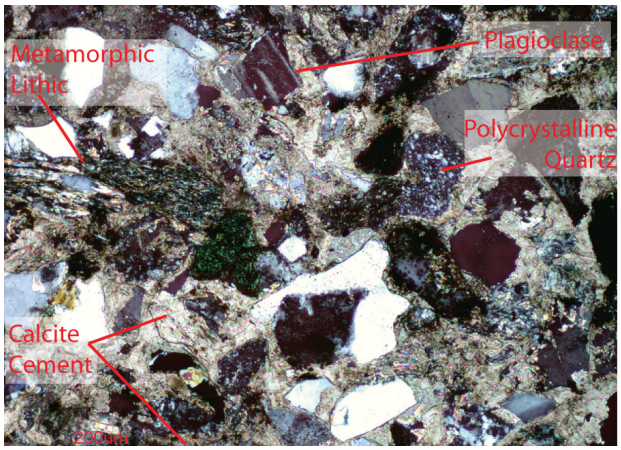

Figure 39: Photomicrograph of sample 07-HB-21 at 10X crossed polars. Calcite cement has completely replaced the matrix in this sample.

Results of Geochemistry

The use of geochemistry to determine the provenance of sedimentary rocks is controversial, and in many instances samples from known origins do not plot in the provenance fields first determined by Bhatia and Crook (1986) (Ryan and Williams, 2007). In the case of the Hornbrook Formation, I am using geochemical data to highlight changes between members that might not be demonstrated by petrographic analysis and to provide additional support for my interpretation of the petrographic analysis, rather than using the geochemistry to determine tectonic provenance. Five mudstone and siltstone samples were collected from the Klamath River Conglomerate, Rocky Gulch Sandstone, and the Blue

Gulch Mudstone Members. Four different types of plots demonstrate the geochemistry of these samples. The NASC-normalized multi-element diagram is organized in order of most compatibility to least compatibility from left to right (Fig. 40). The samples in the legend are organized so that the stratigraphically lowest sample is at the bottom to show the changes in geochemistry between the different members. The Klamath River Conglomerate sample (07-HB-03) is characterized by extremely high concentrations of nickel, chromium, and scandium, but a depletion of rubidium, barium, cesium, thorium, uranium, and hafnium. In the other four samples, these minerals are enriched compared to the North American Shale Composite. The Rocky Gulch Sandstone sample (07-HB-29) is enriched in strontium and uranium, but the other elements have similar concentrations to those remaining samples (07-HB-23, 07-HB-27, and 07-HB-22). The Rocky Gulch Sandstone sample has been depleted of barium, but depletions of other elements are similar to those in the Blue Gulch Mudstone samples. The Blue Gulch Mudstone samples are all very similar to each other, being enriched in barium, cesium, strontium, scandium, and uranium, but also being depleted in nickel, chromium, thorium, and hafnium.

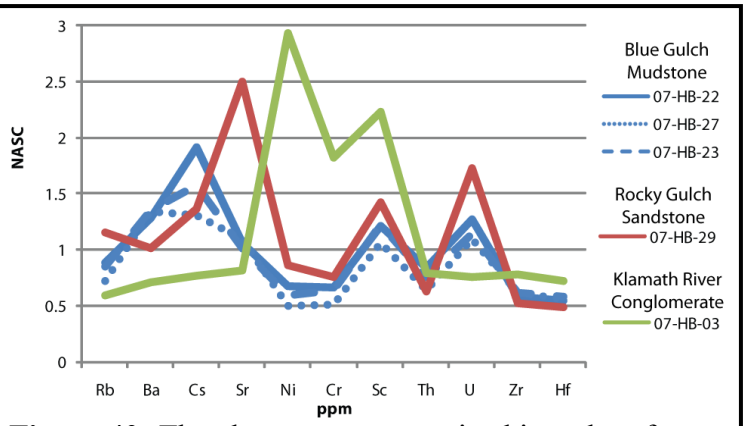

Figure 40: The elements are organized in order of most compatibility to least compatibility from left to right. The legend is organized so that the stratigraphically lowest sample is at the bottom to show the changes in geochemistry between the different members. Notice the stark contrast between sample 07-HB-03 (Klamath River Conglomerate) and the other four samples. See Fig. 6 for the stratigraphic location of these samples.

The NASC-normalized rare earth element diagram demonstrates a relatively similar concentration of these elements throughout the Hornbrook Formation (Fig. 41). This diagram shows the similarities between the members, but also the change from a somewhat depleted concentration to a somewhat enriched concentration relative to NASC. Sample 07-HB-03 (Klamath River Conglomerate) has been heavily enriched in scandium compared to other samples within the Hornbrook Formation and is also enriched in neodymium, samarium, and europium compared to the NASC. Both samples 07-HB-29 (Rocky Gulch Sandstone) and 07-HB-27 (Blue Gulch Mudstone) are depleted in

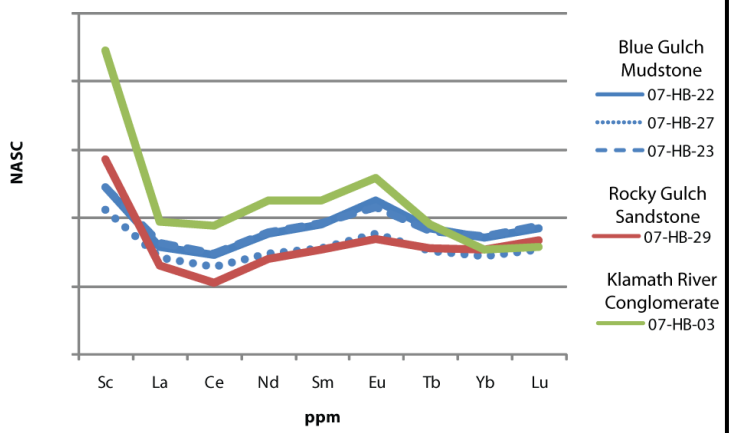

Figure 41: The rare earth elements are organized from most compatible to least compatible from left to right. The legend is organized so that the stratigraphically lowest sample is at the bottom to illustrate the changes in geochemistry between the different members. Notice the high nickel concentration in sample 07-HB-03 (Klamath River Conglomerate). See Figure 6 for stratigraphic location of sample.

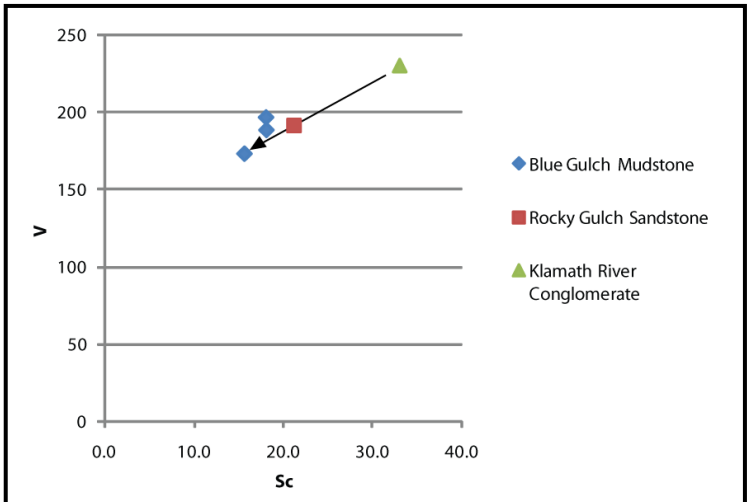

Figure 42: Vanadium-scandium diagram plotted using the actual concentrations of the trace elements in ppm. The samples are organized stratigraphically from bottom to top. The arrow marks the general decreasing trend of the volcanic component stratigraphically up-section.

every element except scandium compared to the NASC. Samples 07-HB-23 and 07-HB-22 (Blue Gulch Mudstone) follow a similar pattern but have elevated amounts of europium as well as scandium.

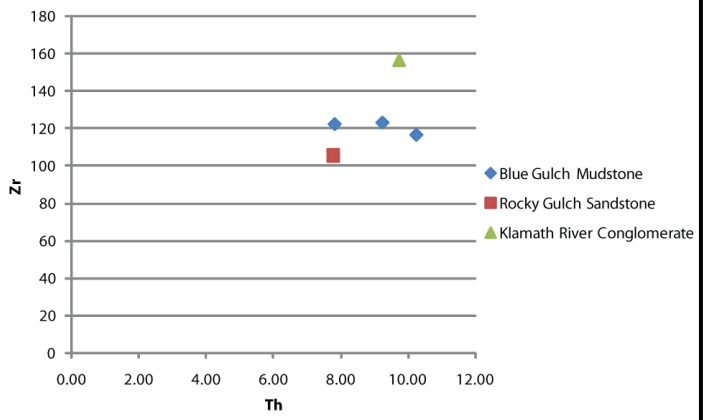

Figure 43: Zirconium-Thorium diagram plotted using the actual concentrations of the trace elements in ppm. The samples are organized stratigraphically from bottom to top.

Ryan and Williams (2007) showed that vanadium and scandium are good discriminators for highlighting sediment enriched by a volcanic source because they are concentrated in the mafic portion of the provenance. Based on the enrichment of vanadium within the Klamath River Conglomerate and decreasing amounts in the Rocky Gulch Sandstone and the Blue Gulch Mudstone, the Hornbrook Formation has decreasing volcanic input the younger it becomes (Fig. 42). The Zr-Th diagram further demonstrates the geochemical differences between the members of the Hornbrook Formation. Although the members do not show a consistent trend as in the V-Sc Diagram, the figure does reveal the very high concentration of zirconium in the Klamath River Conglomerate compared to the other two members (Fig. 43). The members of the Hornbrook Formation also do not clearly fall in any provenance field defined by Bhatia and Crook (1986); however, the low average ratio of Zr to Th, 13.95 ± 1.91, is indicative of active continental margins.

Results of Geochronology

The detrital zircon analysis of the Hornbrook Formation demonstrates the diversity of sediment input between the five members. The quartzite clasts of the Klamath River

Conglomerate (07-HB-01) contain a Precambrian detrital zircon age distribution, but most of these Precambrian ages are absent in the sandstone sample from the same member (06-KS-06; Figs. 44 and 45). Other Hornbrook samples contain a few Precambrian grains, but there are not enough grains to form a peak in any single sample distribution, nor do they follow any discernable trend (Fig. 44). When combined into a normalized cumulative probability plot, the Precambrian grains demonstrate an important difference between the Klamath River Conglomerate and the rest of the members of the Hornbrook Formation (Fig. 45). With the exception of the quartzite clasts in the basal Klamath River Conglomerate member, Precambrian ages are rare. The only clear Paleozoic grouping of grains occurs in samples 07-HB-21 and 07-HB-26 (Blue Gulch Mudstone) between ~ 400 Ma and ~ 500 Ma (Early Devonian to Early Ordovician; Fig. 44). The Klamath River Quartzite clasts closely resemble the Antelope Mountain Quartzite of the Yreka subterrane of the eastern Klamath Mountains (Fig. 45). The combined Hornbrook data does not correlate with the quartzite clasts or the Antelope Mountain Quartzite, but rather more closely resembles the adjacent terranes in the northern Sierra Nevadas such as the Shoo Fly Complex and the Paleozoic Nevada miogeocline (Fig. 45).

Mesozoic grains are abundant throughout the Hornbrook Formation, but the source of sediment was not consistent. For example, an Early Jurassic age peak (~190 Ma) occurs in the basal and upper members of the Hornbrook, but it is absent in the middle strata (07-HB-1, 07-HB-21, 07-HB-26; Fig. 46). A Late Jurassic-Early Cretaceous peak (~150 Ma), prominent in the basal two members (06-KS-06, 07-HB-11, and, 07-HB-13), is minor in the fourth member and gradually disappears altogether from the youngest member of the Hornbrook Formation (Fig. 46). Completely absent until the middle Osburger Gulch Sandstone, a Late

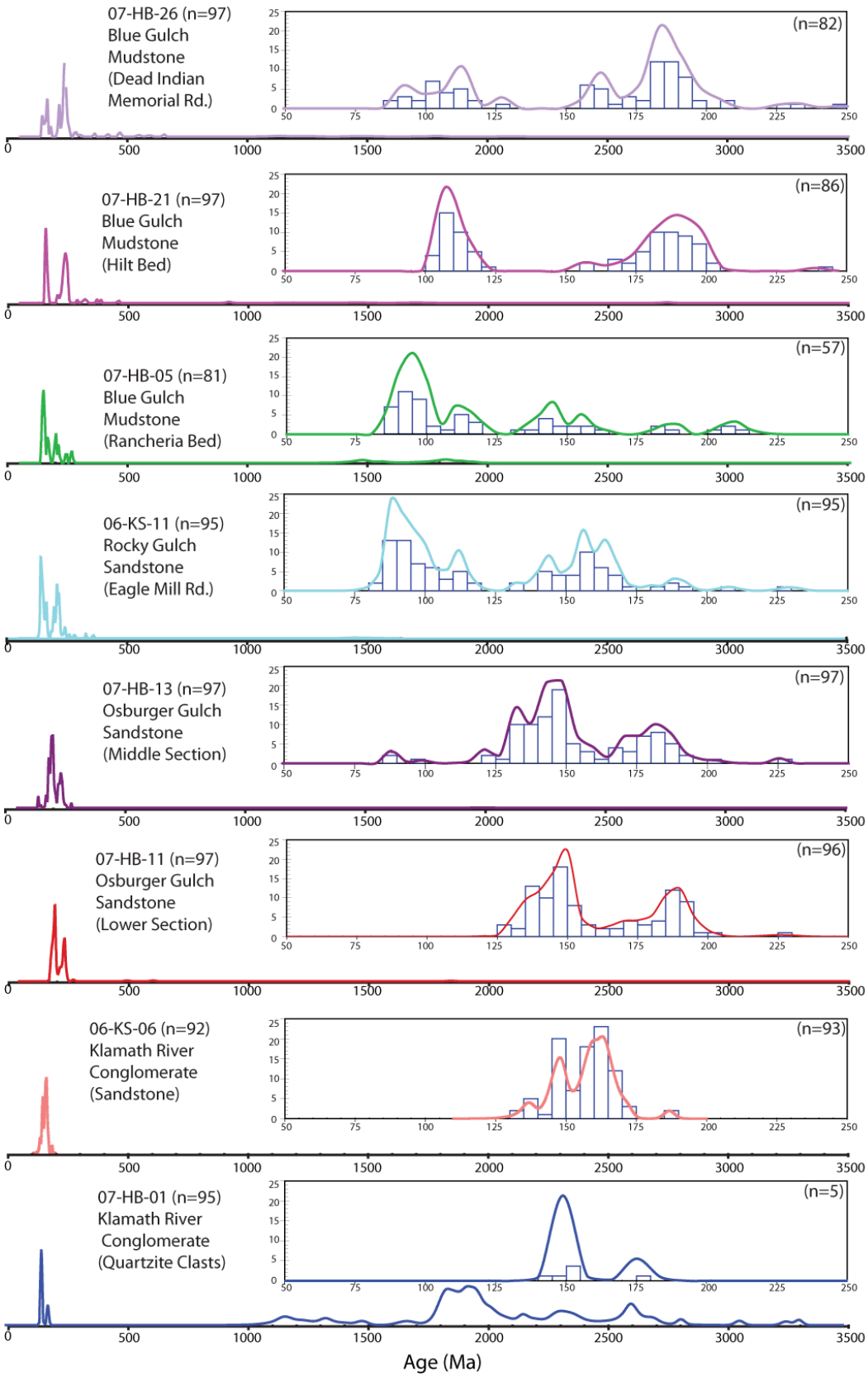

Figure 44: Probability density plots of the members of the Hornbrook Formation. Each member is plotted using the entire distribution and as a close-up of the Mesozoic distribution with histograms.

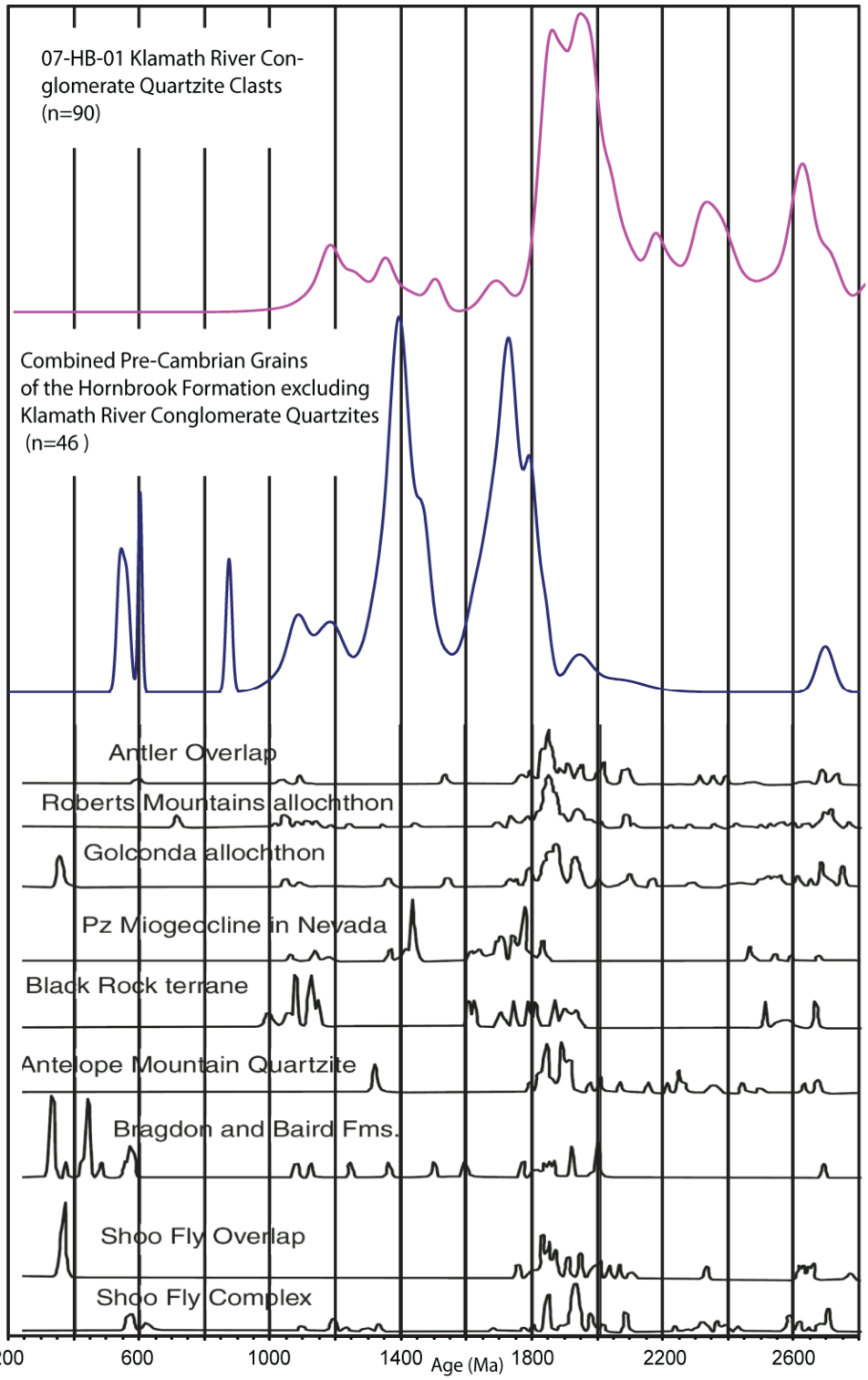

Figure 45: Normalized cumulative probability plot of Precambrian grains in the Hornbrook Formation and in surrounding and adjacent terranes. Notice the clear differences between the combined Hornbrook data and the quartzite clasts, which resemble the Antelope Mountain Quartzite. References for other detrital zircon distributions are: Bragdon and Baird formations, Eastern Klamath Terrane, Gehrels and Miller (2000); Antelope Mountain Quartzite, Wallin et al. (2000); Shoo Fly Complex, Harding et al. (2000); Shoo Fly Overlap, Gehrels and Dickinson (2000); Roberts Mountain allochthon, Gehrels et al. (2000); Black Rock terrane, Darby et al. (2000); Paleozoic Nevada miogeocline, Gehrels et al. (1995).

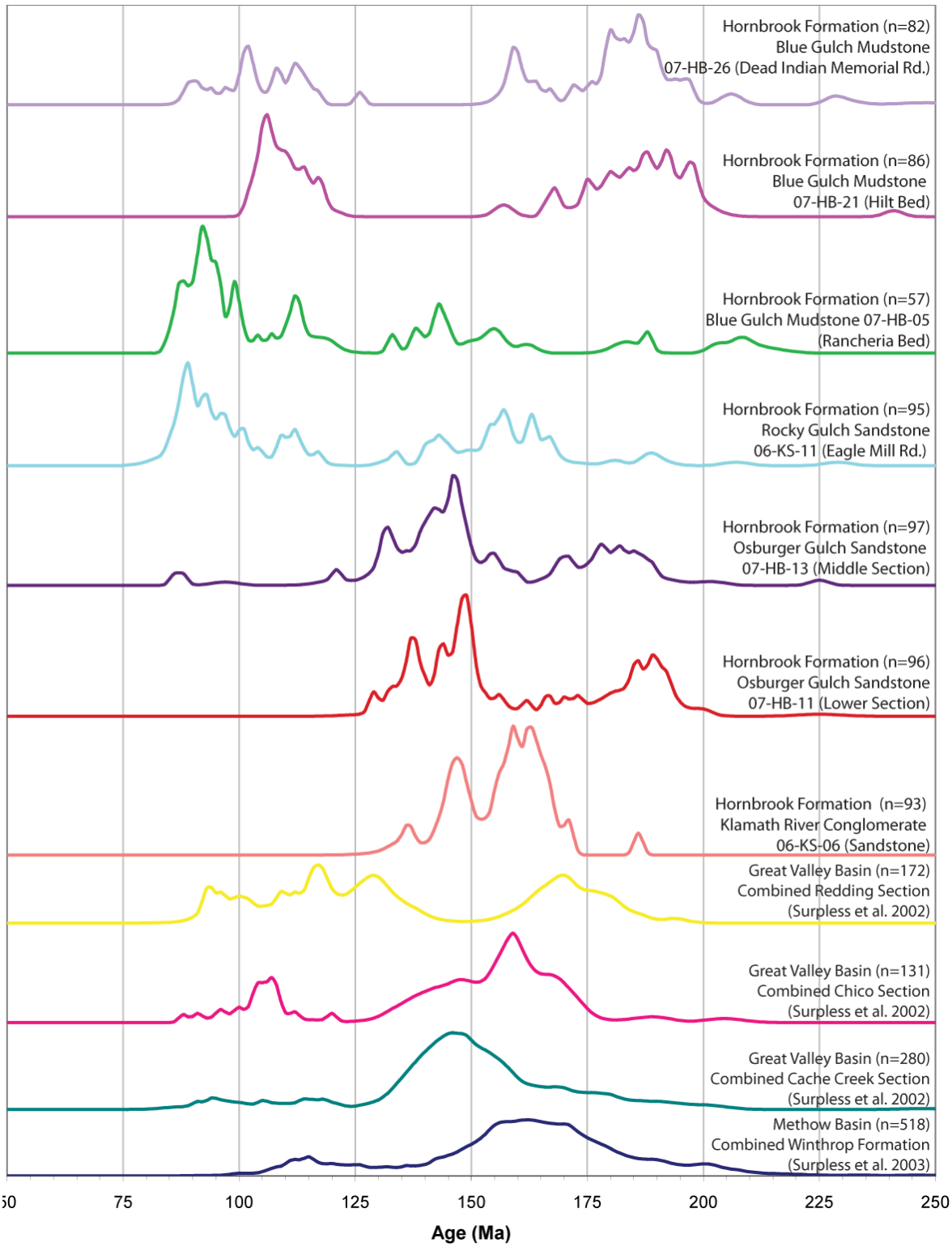

Figure 46: Normalized cumulative probability plot of only Mesozoic grains in the Hornbrook Formation and other Mid to Late Cretaceous basins. The normalized data from Surpless et al. (2002; 2003) is combination of all detrital zircon ages younger than 250 Ma from each region. Based on this summary of ages from the Methow and Great Valley Basins, the Hornbrook Formation more closely resembles the Great Valley Basin.

Cretaceous peak (~90 Ma) dominates the Rocky Gulch Sandstone and the Rancheria Sandstone Bed of the Blue Gulch Mudstone, and then nearly disappears in the upper samples of the Blue Gulch Mudstone (Fig. 46). The normalized data from Surpless et al. (2002; 2003) is a summary of the ages from the Methow and Great Valley Basins where all of the detrital zircons younger than 250 Ma were combined in order to demonstrate which basin the Hornbrook Formation more closely resembles (Fig. 46). The members of the Hornbrook Formation more closely correlate with the Chico and Redding Sections of the Great Valley Basin. The Early Jurassic, Late Jurassic-Early Cretaceous, and Late Cretaceous peaks found in the Hornbrook Formation are also found in the Chico and Redding Sections.

Even with all the changes in age distribution and therefore sediment input, there are similarities between samples collected within each member of the Hornbrook Formation. A cumulative probability plot of the Hornbrook Formation better demonstrates these changes (Fig. 47). Both Osburger Gulch Sandstone samples follow a parallel curve along with a

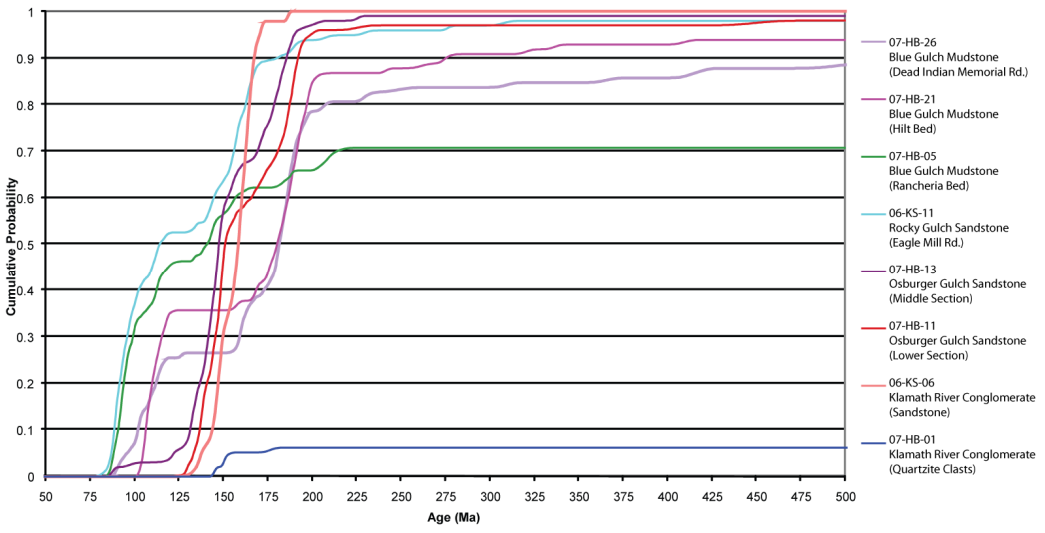

Figure 47: Cumulative probability plot of the Hornbrook Formation. Samples are organized stratigraphically from bottom to top and the colors correlate with the samples shown in Figures 44 and 46. Notice the similarities within the Blue Gulch Mudstone samples and the Osburger Gulch samples. Samples 07-HB-01 and 07-HB-05 contain several grains older than 500 Ma.

somewhat similar curve from the sandstone sample in the Klamath River Conglomerate (Fig. 47). The youngest Blue Gulch Mudstone samples also show many similarities while the older Blue Gulch Mudstone sample and the Rocky Gulch Sandstone sample are much more alike (Fig. 47).

DISCUSSION

The petrographic, geochemical, and geochronologic results provide insight into the paleogeography and changing provenance of the Hornbrook Formation. The detrital zircon analyses require revision of past interpretations about the source of the Hornbrook Formation as the youngest ages indicate that the formation did not have solely a Klamath Mountains source, as suggested by Nilsen (1993). If the Hornbrook Formation was exclusively derived from the Klamath Mountains, the Early Cretaceous peak (~90 Ma) that occurs in the middle and upper members would not be possible because the Klamath Mountains contain no plutons younger than 136 Ma (Shasta Bally batholith; Fig. 4; Irwin and Wooden, 1999; and references therein). Conversely, the Sierra Nevada magmatic arc contains many plutons emplaced during the Early and Late Cretaceous (Fig. 7; Irwin and Wooden, 2001); however, prior to the Cretaceous, many magmatic events occurred simultaneously in the Klamath and Sierran Arcs. As a result a clear differentiation of sources is not possible with the age peaks observed in the Hornbrook Formation.

The Precambrian detrital zircon age distribution found in the quartzite clast sample of the Klamath River Conglomerate is very similar to that found in the Antelope Mountain Quartzite within the Yreka subterrane of the eastern Klamath Mountains (Fig. 45; Wallin et al., 2000). This distribution suggests that sediment was eroding from the Klamath Mountains, at least in the basal Hornbrook; however, these older ages found abundantly in the Klamath

River Conglomerate quartzite cobbles are rarely found in the other members, implying that a different and/or additional source supplied sediment for the rest of the Hornbrook Formation. This inference is further supported by the fact that Precambrian ages are absent in the sandstone sample from the same outcrop of the Klamath River Conglomerate member, signifying that the Precambrian zircon grains of the quartzite clasts were derived exclusively from the Antelope Mountain Quartzite.

When the rare Precambrian grains (excluding the Klamath River Conglomerate quartzite clasts) are combined into a normalized cumulative probability plot and compared with the Klamath River Conglomerate quartzite clasts, the two plots show very different trends (Fig. 45). Where the Klamath River Conglomerate contains age peaks, the rest of the Hornbrook samples demonstrate little to none of that age and vice versa (Fig. 45). The fact that a few small peaks correlate with the Klamath River Conglomerate quartzite clasts suggests that perhaps some of the Antelope Mountain Quartzite has been recycled, but very little. In contrast, the combined Precambrian zircon grains from the remaining Hornbrook Formation members, with ages that more closely resemble cratonal basement provinces from much further south, seem have to been recycled through the northern Sierra Nevada terranes. Throughout Western North America, there are Precambrian basement provinces with characteristic age signatures (Gehrels et al., 1995; Gehrels and Miller, 2000). The combined Precambrian signature of the Hornbrook Formation, excluding the Klamath River Conglomerate quartzite clasts, correlates with four of these distinctive Precambrian basement provinces: the anorogenic igneous (1.34 to 1.48 Ga), Mazatzal (1.65 to 1.72 Ga), Yavapai (1.72 to 1.80 Ga), and Mojave provinces (1.63 to 1.80 Ga and 2.0 to 2.3 Ga) (Fig. 45; Gehrels and Miller, 2000). These age peaks also appear in the Shoo Fly Formation and

overlap assemblage within the northern Sierran terranes, suggesting that they were recycled from basement provinces into sediments of the northern Sierras and then into the Hornbrook Formation.

The Klamath River Conglomerate provides key insights into the changing provenance of the Hornbrook Formation, as the conglomerate clast counts of this member yielded a range in results depending on sampling location and thus demonstrate the compositional variability of the Klamath River Conglomerate. The clast count conducted by Barats et al. (1984) has almost 90% metavolcanics while my clast count from a more southern location yielded greater than 50% quartzite but very few volcanic or metamorphic clasts (Table 2; Figs. 5 and 10). The variability of the Klamath River Conglomerate is further demonstrated by the differences between the conglomerate clast composition and the sand-sized fraction (Figs. 10 and 13). While the clast count is broadly consistent with sandstone petrography, it yielded much more quartzite and fewer volcanic clasts than the sand-sized fraction. This suggests that the quartzite was not reduced to sand-sized grains during transport, but rocks from plutonic arc sources were disaggregated. The quartzite clasts may be less susceptible to weathering and diagenesis or have a closer source rock than the sand-sized fraction. This conclusion is also supported by the very different zircon distributions found between the Klamath River Conglomerate quartzite clasts and sandstone fraction.

My petrographic data from the other members of the Hornbrook Formation and data from Golia and Nilsen (1984) show a complicated provenance containing elements of basement uplift, recycled orogen, and dissected arc (Fig. 13). Because the petrography is so variable, a clear linear trend up-section cannot be discerned, but the distinction between members is apparent (Fig. 13). With the exception of the Osburger Gulch Sandstone, the

lower members have a more variable provenance than the upper members (Golia and Nilsen, 1984). Golia and Nilsen (1984) suggest that this is a result of the mixing of turbidites in the upper members, which more evenly distribute the different sources than the alluvial, fluvial, and shallow marine systems of the lower members. This variability is also a result of the complication of more than one source of sediment and the integration or disruption of the fluvial system as the Cordilleran terranes were transported, mixing the signal left behind in the rocks. Golia and Nilsen (1984) suggest that this signal can be explained solely by a Klamath Mountain source, which the Early Cretaceous detrital zircon age peak discounts but does not rule out (Fig. 46). My Rocky Gulch Sandstone paleoflow measurements, and those presented by Nilsen (1993) are consistent with a Klamath Mountain source, demonstrating that the Klamath Mountains did contribute some sediment (Figs. 6 and 25).

The complicated provenance of the Hornbrook Formation is further reflected in the geochemical analyses conducted on three of the members and supports the age data that suggest a Sierra Nevada source of sediment. The geochemical analyses on the clay-sized fraction of the Hornbrook Formation cannot assign the sediment to a specific provenance, only the relative change between members. Both Figures 40 and 41 demonstrate the continued differences between the Klamath River Conglomerate member and the rest of the Hornbrook Formation, regardless of the size of the grain analyzed. Figure 42 clearly shows decreasing volcanic input from the basal Klamath River Conglomerate to the upper Blue Gulch Mudstone.

Because the disappearance of old ages from the younger strata found in the Klamath River Conglomerate quartzite clasts might suggest more volcanic input from the Sierra Nevada volcanic arc, the geochemical analyses seem to contradict the detrital zircon results.

This is not inconsistent with the age spectra if the Sierra Nevada arc was being dissected at the time. Ingersoll (1983) discusses this phenomenon in the Great Valley Basin, to which the Sierra Nevada arc contributed a great deal of sediment. Based on petrographic analysis, the sediment of the Great Valley Group became increasingly rich in K-feldspar as the volcanic arc was dissected down into the plutons (Ingersoll, 1983). Because of the complexity of the provenance in the Hornbrook Formation, the volcanic signature does not clearly appear in the petrographic analysis of the sand-sized fraction, but the geochemistry of the clay-sized fraction does exhibit this phenomenon. In the geochemical data of the Hornbrook Formation, the volcanic signature decreased as the arc dissected (Fig. 42), but the plutonic signature increased (Fig. 43). Because zircon does not form in abundance in volcanic rocks, the basal members of the Hornbrook Formation demonstrate a volcanic signature with very few younger zircons. The distribution of young zircons increases in the younger members of the Hornbrook Formation as the arc dissected to reveal plutonic rocks, which are rich in zircon.

Based on the petrographic, geochemical, and geochronological data, the Hornbrook Formation could not have been deposited by one (Klamath) source, but nor does its provenance support the reconstruction done by Wyld et al. (2006). The Hornbrook Formation contains no clear age peaks that correlate with age peaks in the Methow Basin (Fig. 46; Surpless et al., 2003). Instead Early Jurassic, Late Jurassic-Early Cretaceous, and Late Cretaceous peaks found in the Hornbrook Formation are also found in the Chico and Redding Sections of the Great Valley Group (Fig. 46; Surpless et al., 2002). This suggests that the reconstruction presented by Miller et al. (1992) that connects the Great Valley, Hornbrook, and Ochoco basins, is more plausible (Fig. 2) than the Wyld et al. (2006) reconstruction, which connects the Methow, Ochoco, and Hornbrook Basins, while leaving the Great Valley

basin a separate and discrete basin (Fig. 3). However, very little data are available for the Ochoco Basin and further research is needed to determine whether the Ochoco Basin is part of this potentially continuous forearc basin.

CONCLUSIONS

Although the complexity of Cordilleran geology presents a challenge in reconstructing the tectonics and paleogeography of the region, the Hornbrook Formation provides critical information that will aide in our understanding of the Late Cretaceous. The Mesozoic detrital zircon distribution helps to pinpoint the location of the Hornbrook Basin in relation to its potential sources and rules out a connection with the Methow Basin. Specifically, the Late Cretaceous peak contradicts the assertion that the Hornbrook Formation was derived solely from a Klamath Mountains source rather than the nearby Sierra Nevada arc. In addition, the Mesozoic distribution from the Hornbrook Basin more closely matches the Great Valley Basin as opposed to the Methow Basin, and therefore, it is possible that the Hornbrook Basin was linked with the Great Valley Group and the Ochoco Basin (where further research is needed). The Precambrian zircon age data also support this conclusion, as the Klamath River Conglomerate clast distribution, which resembles the Antelope Mountain Quartzite of the Klamath Mountains, clearly differs from the combined Precambrian distribution of the Hornbrook Formation. The rare Precambrian grains from the Hornbrook Formation much more closely correspond with cratonal sources further south that likely have been recycled through terranes within the northern Sierra Nevada Mountains. The composition of the Hornbrook Formation also supports a combined Klamath Mountains and Sierra Nevada arc source, as the petrography of the Hornbrook Formation is highly variable in composition. In addition, the geochemistry is similar to the Great Valley Group and shows

evidence of a dissecting Sierra Nevada arc. In conclusion, the petrographic, geochemical, and geochronological signatures preserved in the Hornbrook Formation locate an extensive Cretaceous Great Valley-Hornbrook forearc basin nearby both the Klamath Mountains and the Sierra Nevada Mountains, which both contributed sediment.

ACKNOWLEDGEMENTS

This research was supported by the American Chemical Society - Petroleum Research Fund awarded to Dr. Kathleen D. Surpless, the GSA Cordilleran Section Student Travel Grant, and the Trinity University Herndon Scholarship Funds. Special thanks to George Gehrels, Victor Valencia, and the National Science Foundation for the use of the Arizona LaserChron Center. Thank you to Gregory Augsburger for all his help and humor, and to my parents for their constant encouragement in all of my endeavors. I also would like to particularly thank my thesis advisor, Dr. Kathleen Surpless, for all the support she has given me, thesis-related and otherwise.

References

Ague, J.J. and Brandon, M.T., 1996, Regional tilt of the Mount Stuart batholiths, Washington, determined using aluminum in hornblende barometry: Implications for northward translation of Baja British Columbia: Geological Society of America Bulletin, v. 108, p. 471-488.

Albers, J. P., Kistler, R. W., and Kwak, L., 1981, The Mule Mountain stock, an early Middle Devonian pluton in northern California: Isochron/West, no. 31, p. 17.

Armstrong, R.L., Taubeneck, W.H., and Hales, P.O., 1977, Rb-Sr and K-Ar geochronometry of Mesozoic granitic rocks and their Sr isotope composition, Oregon, Washington, and Idaho: Geological Society of America Bulletin, v. 88, p. 397-411.

Barats, G. M., Nilsen, T.H., and Golia, R.T., 1984, Conglomerate clast composition of the Upper Cretaceous Hornbrook Formation, Oregon and California, *in* Nilsen, T.H., ed., Geology of the Upper Cretaceous Hornbrook Formation, Oregon and California: Pacific Section, Society of Economic Paleontologists and Mineralogists, v. 42, p. 111-122.

Bateman, P.C., 1981, Geologic and geophysical constraints on models for the origin of the Sierra Nevada batholith, California, *in* Ernst, W.G., ed., The geotectonic development of California: Englewood Cliffs, New Jersey, Prentice-Hall, p. 71-86.

Bateman, P.C. 1983, A Summary of critical relations in the central part of the Sierra Nevada batholith, California, U.S.A., *in* Roddick, J.A., ed., Circum-Pacific plutonic terranes: Geological Society of America Memoir 159, p. 241-254.

Beck, M.E. Jr., 1976, Discordant paleomagnetic pole positions as evidence of regional shear in the western Cordillera of North American: American Journal of Science, v. 276, p. 471-492.

Beck, M.E. Jr., Burmeister, R.F., and Schoonover, R., 1981, Paleomagnetism and tectonics of the Cretaceous Mt. Stuart batholiths of Washington: Translation or tilt?: Earth and Planetary Science Letters, v. 56, p. 336-342.

Bhatia, M.R. and Crook, K. A. W., 1986, Trace element characteristics of greywackes and tectonic setting discrimination of sedimentary basins: Contributions to Mineralogy and Petrology, v. 92, p. 181-193.

Bond, G.C., and Devay, J.C., 1980, Pre-Upper Devonian quartzose sandstones in the Shoo Fly Formation, northern California; Petrology, provenance, and implications for regional tectonics: Journal of Geology, v. 88, p. 285-388.

Boudier, R., Le Suerur, E., and Nicolas, A., 1989, Structure of an atypical ophiolites; The Trinity complex, eastern Klamath Mountains, California: Geological Society of America Bulletin, v. 101, p. 820-833.

Burchfiel, B.C., Cowan, D.S., and Davis, G.A., 1992, Tectonic overview of the Cordilleran orogen in the western United States, in Burchfiel, B.C., Lipman, P.W. and Zoback, M.L., eds., The Geology of North America: The Cordilleran Orogen: Conterminous U.S. Boulder, Colorado, The Geology Society of America, p. 407-479.

Butler, R.F., Gehrels, G.E., and Kodama, K.P., 2001, A Moderate Translation Alternative to the Baja British Columbia Hypothesis: GSA Today, v. 11, p. 4-10.

Cowan, D.S., and Bruhn, R.L., 1992, Late Jurassic to early Late Cretaceous geology of the U.S. Cordillera, in Burchfiel, B.C., Lipman, P.W. and Zoback, M.L., eds., The

Geology of North America: The Cordilleran Orogen: Conterminous U.S. Boulder, Colorado, The Geological Society of America, p. 169-189.

Darby, B.J., Wyld, S.J., and Gehrels, G.E., 2000, Provenance and paleogeography of the Black Rock terrane, northwestern Nevada, in Soreghan, M.J., and Gehrels, G.E., eds., Paleozoic and Triassic paleogeography and tectonics of western Nevada and northern California: Geological Society of America Special Paper 347, p. 77-88.

Dickinson, W.R., Beard, S.L., Brakenridge, G.R., Erjavec, J.L., Ferguson, R.C., Inman, K.F., Knepp, R.A., Lindberg, F.A., and Ryberg, P.T., 1983, Provenance of North American Phanerozoic sandstones in relation to tectonic setting: Geological Society of America Bulletin, v. 94, p. 222-235.

Edelman, S. H., Day, H. W., and Bickford, M. E., 1989, Implications of U-Pb zircon ages for the tectonic settings of the Smartville and Slate Creek complexes, northern Sierra Nevada, California: Geology, v. 17, p. 1032-1035.

Fahan, M. R., 1982, Geology and geochronology of a part of the Hayfork terrane, Klamath Mountains, northern California: Berkeley, California University, M. S. thesis, 127 p.

Gehrels, G.E. and Dickinson, W.R, 2000, Detrital zircon and geochronology of the Antler overlap and foreland basin assemblages, Nevada, in Soreghan, M.J., and Gehrels, G.E., eds., Paleozoic and Triassic paleogeography and tectonics of western Nevada and northern California: Geological Society of America Special Paper 347, p. 57-64.

Gehrels, G.E., Dickinson, W.R., Riley, B.C.D., Finney, S.C., and Smith, M.C., 2000, Detrital zircon geochronology of the Roberts Mountain allochthon, Nevada, in Soreghan, M.J., and Gehrels, G.E., eds., Paleozoic and Triassic paleogeography and tectonics of western Nevada and northern California: Geological Society of America Special Paper 347, p. 19-42.

Gehrels, G.E., Dickinson, W.R., Ross, G.M., Stewart, J.H., and Howell, D.G., 1995, Detrital zircon reference for Cambrian to Triassic miogeoclinal strata of western North America: Geology, v. 23, p. 831-834.

Gehrels, G.E., and Juiz, J., 2007, U-Th-Pb geochronology of zircon by Laser-Ablation Multicollector ICP Mass Spectrometry at the Arizona LaserChron Center: Journal of Analytical Atomic Spectrometry, v. what to do?, .

Gehrels, G.E., and Miller, M.M., 2000, Detrital zircon geochronologic study of upper Paleozoic strata in the eastern Klamath terrane, northern California, in Soreghan, M.J. and Gehrels, G.E., eds., Paleozoic and Triassic paleogeography and tectonics of western Nevada and northern California: Boulder, Colorado, Geological Society of America Special Paper 347, p. 99-107.

Gehrels, G.E., Valencia, V., and Pullen, A., 2006, Detrital Zircon Geochronology by Laser-Ablation Multicollector ICPMS at the Arizona LaserChron Center, in Olszewski, T., ed., Geochronology: Emerging Opportunities: The Paleontological Society Papers, p. 67-76.

Golia, R.T., and Nilsen, T.H., 1984, Sandstone petrography of the upper Cretaceous Hornbrook Formation, Oregon and California, in Nilsen, T.H., ed., Geology of the Upper Cretaceous Hornbrook Formation, Oregon and California: 42, Pacific Section S.E.P.M., p. 99-109.

Goldstrand, P.H., 1994, The Mesozoic geologic evolution of the northern Wallowa terrane, northeastern Oregon and western Idaho, *in* Vallier, T.L., and Brooks, H.C., eds., Geology of the Blue Mountains region of Oregon, Idaho, and Washington-

Stratigraphy, physiography, and mineral resources of the Blue Mountains region: U.S. Geological Survey Professional Paper 1439, p. 29-53.

Gray, G. G., 1985, Structural, geochronological, and depositional history of the western Klamath Mountains, California and Oregon: Implications for the early to middle Mesozoic evolution of the western North American Cordillera: Austin, University of Texas, Ph.D. dissertation, 162 p.

Hacker, B.R., Donato, M.M., Barnes, C.G., McWilliams, M.O., and Ernst, W.G., 1995, Timescales of orogeny: Jurassic construction of the Klamath Mountains: Tectonics, v. Vol. 14 No. 3, p. 677-703.

Hacker, B.R., and Ernst, W.G., 1993, Jurassic Orogeny in the Klamath Mountains: A Geochronological Analysis: Mesozoic Paleogeography of the Western United States-II, v. Book 71, p. 37-60.

Haggart, J.W., and Ward, P.D., 1984, Late Cretaceous (Santonian-Campanian) stratigraphy of the northern Sacramento Valle, California: Geological Society of America Bulletin, v. 95, p. 618-627.

Hanson, R. E., Saleeby, J. B., and Schweickert, R. A., 1988, Composite Devonian island-arc batholith in the northern Sierra Nevada, California: Geological Society of America Bulletin, v. 100, no. 3, p. 446-457.

Harding, J.P., Gehrels, G.E., Harwood, D.S., and Girty, G.H., 2000, Detrital zircon geochronology of the Shoo Fly complex, northern Sierra terrane, northeastern California, in Soreghan, M.J., and Gehrels, G.E., eds., Paleozoic and Triassic paleogeography and tectonics of western Nevada and northern California: Geological Society of America Special Paper 347, p. 43-56.

Harper, G. D., Saleeby, J. B., and Heizler, 1994, Formation and emplacement of the Josephine ophiolite and the Nevadan orogeny in the Klamath Mountains, California-Oregon: U/Pb 40Ar/39Ar geochronology: Journal of Geophysical Research, v. 99, no. B3, p. 4293-4321.

Harwood, D.S., 1983, Tectonism and metamorphism in the northern Sierra terrane, northern California, *in* Ernest, W.G., ed., Metamorphism and crustal evolution of the western United States; Rubey Volume 7: Englewood Cliffs, New Jersey, Prentice-Hall, p. 764-788.

Hotz, P.E., Lanphere, M.A., and Swanson, D.A., 1977, Triassic blueschist from northern California and north-central Oregon: Geology, v. 5, p. 659-663.

Ingersoll, R.V., 1978, Petrofacies and petrologic evolution of the Late Cretaceous forearc basin, northern and central California: Geological Society of America Bulletin, v. 89, p. 335-352.

Ingersoll, R.V., 1979, Evolution of the Late Cretaceous forearc basin, northern and central California: Geological Society of America Bulletin, v. 90, part I, p. 813-826.

Ingersoll, R.V., 1983, Petrofacies and Provenance of a Late Mesozoic Forearc Basin, Northern and Central California: The American Association of Petroleum Geologists Bulletin, v. 67, p. 1125--1142.

Irving, E., Woodsworth, G.J., Wynne, P.J., and Morrison, A., 1985, Paleomagnetic evidence for displacement from the south of the Coast plutonic complex, British Columbia: Canadian Journal of Earth Sciences, v. 22, p. 584-598.

Irwin, W.P., and Wooden, J.L., 1999, Plutons and accretionary episodes of the Klamath Mountains, California and Oregon: U.S. Geological Survey Open File Report 01-229, 1 sheet.

Jacobsen, S.B., Quick, J.E., and Wasserburg, G.J., 1984, A Nd and Sr isotopic study of the Trinity peridotite; implications for mantle evolution: Earth and Planetary Science Letters, v. 68, p. 361-378.

Kim, B., and Kodama, K.P., 1999, Magnetic anisotropy of Nanaimo Group sedimentary rocks from Hornby Island: Eos (Transactions, American Geophysical Union), v. 80, p. F299-F300.

Kleinhans, L.C., Balcells-Baldwin, E.A., and Jones, R.E., 1984, A paleogeographic reinterpretation of some middle Cretaceous units, north-central Oregon; Evidence for a submarine turbidite system, *in* Nilsen, T.H., ed., Geology of the Upper Cretaceous Hornbrook Formation, Oregon and California: Pacific Section, Society of Economic Paleontologists and Mineralogists, v. 42, p. 239-257.

Lallemant, H.G.A., 1995, Pre-Cretaceous tectonic evolution of the Blue Mountain province, northeastern Oregon, *in* Vallier, T.L., and Brooks, H.C. eds., Geology of the Blue Mountains region of Oregon, Idaho, and Washington: Petrology and tectonic evolution of Pre-Tertiary rocks of the Blue Mountains region, U.S. Geological Survey Professional Paper 1438, p. 271-304.

Lanphere, M. A., Irwin, W. P., and Hotz, W.P., 1968, Isotopic age of the Nevadan orogeny and older plutonic and metamorphic events in the Klamath Mountains, California: Geological Society of America Bulletin, v. 79, no. 8, p. 1027-1052.

Lindsley-Griffen, N., 1977, The trinity ophiolites, Klamath Mountains, California, *in* Coleman, R.G., and Irwin, W.P., eds., North American ophiolites: Oregon Department of Geology and Mineral Industries Bulletin 95, p. 107-120.

Lindsley-Griffen, 1982, Structure, stratigraphy, petrology, and regional relationships of the Trinity ophiolites, eastern Klamath Mountains, California [Ph.D. thesis]: Davis, University of California, 445 p.

Ludwig, K. R., 2003, Isoplot 3.00: Berkeley Geochronology Center, Special Publication No. 4, 70 p.

Mankinen, E.A., and Irwin, W.P., 1990, Review of paleomagnetic data from the Klamath Mountains Blue Mountains, and Sierra Nevada; Implications for paleogeographic reconstructions, in Harwood, D.S. and Miller, M.M., eds., Paleozoic and early Mesozoic paleogeoprahic relations; Sierra Nevada, Klamath Mountains, and related terranes: Boulder, Colorado, Geological Society of America Special Paper 255, p. 397-407.

Mattinson, J.M., and Hopson, C.A., 1972, Paleozoic ophiolites complexes in Washington and northern California: Carnegie Institution of Washington Yearbook, no. 71, p. 578-583.

Miller, D.M., Nilsen, T.H., and Bilodeau, W.L., 1992, Late Cretaceous to early Eocene geologic evolution of the U.S. Cordillera, in Burchfiel, B.C., Lipman, P.W. and Zoback, M.L., eds., The Geology of North America: The Cordilleran Orogen: Conterminous U.S. Boulder, Colorado, The Geological Society of America, p. 205-260.

Miller, M.M., 1987, Dispersed remnants of a northeast Pacific fringing arc; Upper Paleozoic terranes of Permian McCloud faunal affinity, western U.S. Tectonics, v. 6, p. 807-830.

Miller, R.B., Mattinson, J.M., Hopson, C.A., and Treat, C.L., 1993, Tectonic Evolution of Mesozoic Rocks in the Southern and Central Washington Cascades: Mesozoic Paleogeography of the Western United States-II, v. Book 71, p. 81-98.

Monger, J.W.H., 1975, Correlation of eugeosynclinal tectonostratigraphic belts in the North American Cordillera: Geoscience Canada, v.2, p. 4-9.

Monger, J.W.H., 1977, Upper Paleozoic rocks of the western Canadian Cordillera and their bearing on Cordilleran evolution: Canadian Journal of Earth Sciences, v. 14, p. 1832-1859.

Monger, J.W.H., and Price, R.A., 1996, Paleomagnetism of the Upper Cretaceous strata of Mount Tatlow: Evidence for 3000 km of northward displacement of the eastern Coast Belt, British Columbia, by P.J. Wynne et al., and Paleomagnetism of the Spences Bridge Group and northward displacement of the Intermontane Belt, British Columbia: A second look, by E. Irving et al.: Discussion and reply: Journal of Geophysical Research, v. 101, p. 13,793-13,800.

Nilsen, T.H., ed., 1984, Geology of the Upper Cretaceous Hornbrook Formation, Oregon and California: Pacific Section, Society of Economic Paleontologists and Mineralogists, v. 42.

Nilsen, T.H., 1993, Stratigraphy of the Cretaceous Hornbrook Formation, Southern Oregon and Northern California: U.S. Geological Survey Professional Paper, p. 1-89.

Panuska, B.C., 1985, Paleomagnetic evidence for a post-Cretaceous accretion of Wrangellia: Geology, v. 13, p. 880-883.

Potter, A.W., Boucot, A.J., Bergstrom, S.M., Blodgett, R.B., Dean, W.T., Flory, R.A., Ormiston, A.R., Pedder, A.E.H., Rigby, J.K., Rohr, D.M., and Savage, N.M., 1990, Early Paleozoic stratigraphic, paleogeographic, and biogeographic relations of the eastern Klamath belt, northern California, in Harwood, D.S. and Miller, M.M., eds., Paleozoic and early Mesozoic paleogeographic relations; Sierra Nevada, Klamath Mountains, and related terranes: Boulder, Colorado, Geological Society of America Special Paper 255, p. 57-73.

Quick, J.E., 1981, Petrology and petrogenesis of the Trinity peridotite, an upper mantle diapir in the eastern Klamath Mountains, northern California: Journal of Geophysical Research, v. 86, p. 11837-11863.

Rollinson, H.R., 1993, Using geochemical data: evaluation, presentation, interpretation: London, England, Longman Group UK Ltd.

Rubin, C.M., Miller, M.M., and Smith, G.M., 1990, Tectonic development of Cordilleran mid-Paleozoic volcano-plutonic complexes; Evidence for convergent margin tectonism, in Harwood, D.S. and Miller, M.M., eds., Paleozoic and early Mesozoic paleogeographic relations; Sierra Nevada, Klamath Mountains, and related terranes: Boulder, Colorado, Geological Society of America Special Paper 255, p. 1-15.

Ryan, K.M and Williams, D.M., 2007, Testing the reliability of discrimination diagrams for determining the tectonic depositional environment of ancient sedimentary basins: Chemical Geology, v. 212, p. 103-125.

Saleeby, J.B., 1986, C-2 Central California offshore to Colorado Plateau: Boulder, Colorado, Geological Society of America, Centennial Continent/ Ocean Transect no. 10, 2 sheets with text, scale 1:500,000.

Saleeby, J. B., Hannah, J. L., and Varga, R. J., 1987, Isotopic age constraints on middle Paleozoic deformation in the northern Sierra Nevada, California: Geology, 15, no. 8, p. 757-760.

Saleeby, J. B., Shaw, H. F., Niemeyer, S., Moores, E. M., and Edelman, S. H., 1989, U/Pb, Sm/Nd and Rb/Sr geochronological and isotopic study of northern Sierra Nevada ophiolitic assemblages, California: Contributions to Mineralogy and Petrology, v. 102, no. 2, p. 205-220

Saleeby, J.B., and Harper, G.D., 1993, Tectonic relations between the Galice Formation and the Condrey Mountain Schist, Klamath Mountains, northern California, in Mesozoic paleogeography of the western United States-II, Dunn, G., and McDougall, K., eds.: Society of Economic Paleontologists and Mineralogists, Pacific Section, Book 71, p. 61-80.

Schweickert, R.A., and Cowan, D.S., 1975, Early Mesozoic tectonic evolution of the western Sierra Nevada, California: Geological Society of America Bulletin, v. 86, p. 1329-1336.

Schweickert, R.A., Harwood, D.S., Girty, G.A., and Hanson, R.E., 1984, Tectonic development of the northern Sierra terrane; An accreted late Paleozoic island arc and its basement, *in* Lintz, J., ed., Geological excursions; Geological Society of America Cordilleran Section Meeting Guidebook: Reno, Nevada, Mackay School of Mines, p. 1-65.

Snoke, A.W., and Barnes, C.G., 2006, The development of tectonic concepts for the Klamath Mountains province, California and Oregon, in Snoke, A.W. and Barnes, C.G., eds., Geological studies in the Klamath Mountains province, California and Oregon: A volume in honor of William P. Irwin: Boulder, Colorado, Geological Society of America Special Paper 410, p. 1-29.

Surpless, K. D., Mahoney, J.B., Wooden, J.L., and McWilliams, M.O., 2003, Lithofacies control in detrital zircon provenance e studies: Insights from the Cretaceous Methow basin, southern Canadian Cordillera: GSA Bulletin, v. 115, p. 899-915.

Surpless, K. D., Wooden, J.L., and McWilliams, M.O., 2002, Detrital zircon provenance analysis of the Great Valley Group, California: Evolution of an arc-forearc system: GSA Bulletin, v. 12, p. 1564-1580.

Umhoefer, P.J., 1987, Northward translation of "Baja British Columbia" along the Late Cretaceous to Paleocene margin of western North America, Tectonics, v. 6, p. 377-395.

Vandall, T.A. 1993, Cretaceous Coast Belt paleomagnetic data from the Spetch Creek pluton, B.C.: Evidence for the "tilt and moderate displacement" model: Canadian Journal of Earth Science, v. 30, p. 1037-1048.

Vermeesch, P., 2004, How many grains are needed for a provenance study?: Earth and Planetary Science Letters, v. 224, p. 441-451.

Wallin, E.T. 1989, Provenance of lower Paleozoic sandstones in the eastern Klamath Mountains and the Roberts Mountains allochthon, California and Nevada [Ph.D. thesis]: Lawrence, University of Kansas, 152 p.

Wallin, E. T., 1990, Petrogenetic and tectonic significance of xenocrystic Precambrian zircon in Lower Cambrian tonalite, eastern Klamath Mountains, California: Geology, v. 18, p. 1057-1060.

Wallin, E.T., Noto, R.C., and Gehrels, G.E., 2000, Provenance of the Antelope Mountain Quartzite, Yreka terrane, California: Evidence for large scale late Paleozoic sinistral displacement along the North American Cordilleran margin and implications for the mid-Paleozoic fringing-arc model, in Soreghan, M.J. and Gehrels, G.E., eds., Paleozoic and Triassic Paleogeography and Tectonics of Western Nevada and Northern California: Boulder, Colorado, The Geological Society of America Special Paper 347, p. 119-131.

Walker, N.W., 1981, U/Pb geochronology of ophiolitic and volcanic plutonic arc terranes, northeastern Oregon and westernmost central Idaho [abs]: Eos (American Geophysical Union Transactions), v. 62, no. 45, p. 1087.

Walker, N.W., 1982, Pre-Tertiary plutonic rocks in the Snake River canyon, Oregon/Idaho—Intrusive roots of a Permo-Triassic arc complex [abs.]: Geological Society of America Abstracts with Programs, v. 14, p. 242-243.

Walker, N.W., 1986, U/Pb geochronologic and petrologic studies in the Blue Mountains terrane, northeastern Oregon and westernmost central Idaho—Implications for pre-Tertiary tectonic evolution: Santa Barbara, University of California, Ph.D. dissertation, 224 p.

Walker, N.W., 1989, Early Cretaceous initiation of post-tectonic Plutonism and the age of the Connor Creek fault, northeastern Oregon [abs.]: Geological Society of America Abstracts with Programs, v. 21, p. A-155.

Ward, P., Hurtado, J., Kirschvink, J., and Verosub, K., 1997, Measurements of the Cretaceous paleolatitude of Vancouver Island: Consistent with the Baja-British Columbia hypothesis: Science, v. 277, p. 1642-1645.

White, D.L., and Vallier, T.L., 1994, Geologic evolution of the Pittsburg Landing area, Snake River canyon, Oregon and Idaho, *in* Vallier, T.L., and Brooks, H.C., eds., Geology of the Blue Mountains region of Oregon, Idaho, and Washington-Stratigraphy, physiography, and mineral resources of the Blue Mountains region: U.S. Geological Survey Professional Paper 1439, p. 55-73.

Wright, J. E., 1981, Geology and U-Pb geochronology of the Western Paleozoic and Triassic Subprovince, Klamath Mountains, California: Santa Barbara, California University, Ph.D. dissertation, 300 p

Wright, J. E., and Fahan, M. R., 1988, An expanded view of Jurassic orogenesis in the western United States cordillera: Middle Jurassic (pre-Nevadan) metamorphism and thrust faulting within an active arc environment, Klamath Mountains, California: Geological Society of America Bulletin, v. 100, p. 859-876.

Wyld, S.J., Umhoefer, P.J., and Wright, J.E., 2006, Reconstructing northern Cordilleran terranes along known Cretaceous and Cenozoic strike-slip faults: Implications for the Baja British Columbia hypothesis and other models, in Haggart, J.W., Enkin, R.J. and Monger, J.W.H., eds., Paleogeography of the North American Cordillera: Evidence For and Against Large-Scale Displacements: Geological Association of Canada Special Paper 46, p. 277-298.

Wynne, P.J., Irving, E., Maxson, J.A., and Kleinspehn, K.L., 1995, Paleomagnetism of the Upper Cretaceous strata of Mount Tatlow: Evidence for 3000 km of northward

displacement of the eastern Coast Belt, British Columbia: Journal of Geophysical Research, v. 100, p. 6073-6091.

Yule, J. D., 1996, Geologic and tectonic evolution of Jurassic marginal ocean basin lithosphere, Klamath Mountains, Oregon: Pasadena, California Institute of Technology, Ph.D. dissertation, 308 p.

APPENDIX A: ICPMS Geochmical Data

Sample ID	La ppm	Ce ppm	Pr ppm	Nd ppm	Sm ppm	Eu ppm	Gd ppm	Tb ppm	Dy ppm	Ho ppm	Er ppm
07-HB-03	30.02	62.13	7.98	30.80	6.28	1.51	5.08	0.80	4.66	0.88	2.45
07-HB-22	24.45	48.54	6.08	24.06	5.32	1.32	4.73	0.78	4.82	0.98	2.76
07-HB-23	25.34	49.20	6.26	24.32	5.38	1.27	4.72	0.77	4.67	0.98	2.76
07-HB-27	21.96	42.67	5.30	20.33	4.35	1.04	3.87	0.64	3.92	0.81	2.28
07-HB-29	20.18	34.50	4.88	18.96	4.24	0.99	3.93	0.66	4.03	0.85	2.38

Sample ID	Tm ppm	Yb ppm	Lu ppm	Ba ppm	Th ppm	Nb ppm	Y ppm	Hf ppm	Ta ppm	U ppm	Pb ppm
07-HB-03	0.37	2.33	0.36	450.80	9.74	13.41	20.96	4.51	0.92	2.00	10.27
07-HB-22	0.41	2.60	0.42	816.38	10.25	9.00	25.62	3.43	0.67	3.40	22.56
07-HB-23	0.42	2.63	0.43	863.60	9.24	9.33	24.90	3.62	0.67	3.04	19.98
07-HB-27	0.34	2.19	0.35	852.60	7.82	8.15	20.58	3.55	0.61	2.92	16.96
07-HB-29	0.36	2.34	0.38	649.99	7.79	10.70	21.60	3.09	0.73	4.61	19.52

Sample ID	Rb ppm	Cs ppm	Sr ppm	Sc ppm	Zr ppm
07-HB-03	73.9	3.95	115	33.1	156
07-HB-22	110.3	9.90	150	18.1	116
07-HB-23	105.1	8.13	143	18.2	123
07-HB-27	90.8	6.72	155	15.8	122
07-HB-29	145.0	7.07	355	21.2	105

X-ray Fluorescence Geochemical Data

	07-HB-03	07-HB-22	07-HB-23	07-HB-27	07-HB-29
			Unnormalized Major Elements (Weight %):		
SiO2	47.59	56.16	56.99	60.43	53.45
TiO2	1.152	0.797	0.774	0.692	0.796
Al2O3	22.92	18.45	18.22	16.30	17.49
FeO*	7.03	5.80	5.96	6.73	6.40
MnO	0.057	0.060	0.032	0.036	0.045
MgO	2.75	2.33	2.29	2.79	3.18
CaO	0.91	0.82	0.90	0.82	2.06
Na2O	0.53	1.40	1.36	1.93	1.17
K2O	1.82	2.68	2.65	2.30	3.11
P2O5	0.037	0.147	0.206	0.169	0.168
Sum	84.79	88.64	89.38	92.19	87.85
			Normalized Major Elements (Weight %):		
SiO2	56.13	63.36	63.76	65.55	60.84
TiO2	1.359	0.899	0.866	0.750	0.906
Al2O3	27.03	20.81	20.38	17.68	19.90
FeO*	8.29	6.54	6.66	7.30	7.29
MnO	0.067	0.068	0.035	0.039	0.051
MgO	3.24	2.63	2.56	3.03	3.62
CaO	1.07	0.93	1.01	0.89	2.34
Na2O	0.63	1.58	1.53	2.09	1.33
K2O	2.14	3.02	2.97	2.50	3.54
P2O5	0.043	0.165	0.231	0.183	0.191
Total	100.00	100.00	100.00	100.00	100.00
			Unnormalized Trace Elements (ppm):		
Ni	170	39	34	29	50
Cr	227	82	79	63	95
Sc	32	19	20	17	22
V	230	196	188	173	191
Ba	455	825	882	863	660
Rb	74	111	105	90	147
Sr	114	150	144	155	358
Zr	144	118	124	124	108
Y	19	25	25	21	23
Nb	12.8	8.7	9.4	7.8	9.9

Ga	25	21	21	17	25
Cu	163	69	69	48	75
Zn	117	158	152	145	152
Pb	9	22	19	16	18
La	28	26	25	21	20
Ce	60	49	51	49	32
Th	11	10	9	7	7
Nd	30	23	24	21	17
	07-HB-03	**07-HB-22**	**07-HB-23**	**07-HB-27**	**07-HB-29**
sum tr.	1920	1953	1978	1865	2011
in %	0.19	0.20	0.20	0.19	0.20
sum m+tr	84.98	88.83	89.58	92.37	88.05
M+Toxides	85.04	88.87	89.62	92.41	88.10

			Major elements are normalized on a volatile-free		
			basis, with total Fe expressed as FeO.		
NiO	216.3	49.6	42.7	37.3	64.2
Cr2O3	331.9	119.8	114.7	92.7	139.1
Sc2O3	48.6	29.5	30.2	25.5	33.4
V2O3	338.2	287.6	276.3	254.2	281.4
BaO	508.2	921.6	984.8	963.3	736.8
Rb2O	81.0	121.5	115.2	98.8	160.5
SrO	134.3	177.7	169.9	183.7	423.3
ZrO2	197.1	160.8	169.3	168.6	148.0
Y2O3	24.6	32.1	31.5	26.7	29.0
Nb2O5	18.3	12.4	13.4	11.2	14.2
Ga2O3	33.6	28.8	27.6	22.3	33.1
CuO	204.5	86.5	86.4	60.1	94.4
ZnO	146.3	197.8	190.1	181.1	190.4
PbO	9.3	23.3	20.8	16.7	19.6
La2O3	33.1	31.0	29.4	24.7	23.1
CeO2	73.3	60.4	63.2	59.6	39.6
ThO2	11.8	11.0	9.9	7.9	8.2
Nd2O3	34.6	27.1	27.5	24.4	19.5
U2O3	0.0	0.0	0.0	0.0	0.0
Bi2O5	0.0	0.0	0.0	0.0	0.0
Cs2O	0.0	0.0	0.0	0.0	0.0
As2O5	0.0	0.0	0.0	0.0	0.0
W2O3	0.0	0.0	0.0	0.0	0.0

sum tr.	2445.3	2378.4	2402.9	2258.7	2457.7
in %	0.2	0.2	0.2	0.2	0.2

FeO*	8.29	6.54	6.66	7.30	7.29
MgO	3.24	2.63	2.56	3.03	3.62
FeO* + MgO	11.53	9.17	9.22	10.32	10.91
TiO2	1.36	0.90	0.87	0.75	0.91
Al2O3	27.03	20.81	20.38	17.68	19.90
SiO2	56.13	63.36	63.76	65.55	60.84
Al2O3/SiO2	0.48	0.33	0.32	0.27	0.33
K2O	2.14	3.02	2.97	2.50	3.54
Na2O	0.63	1.58	1.53	2.09	1.33
log (K2O/Na2O)	0.53	0.28	0.29	0.08	0.43

APPENDIX B: Detrital Zircon Age Data

Sample	U (ppm)	Th (ppm)	238U /232Th	±(%)	Total 206 /238	±(%)	Total 206 /207	±(%)	206Pb /238U Age	1s err	206Pb /207Pb Age	1s err
H1 -1	168	44	0.17981	2.01	0.47192	4.36	5.386	1.47	2492	90	2704	24
H1-2	221	91	0.07526	3.79	0.26691	1.12	8.307	1.29	1525	15	1962	23
H1-3	40	24	0.15453	2.22	0.47837	1.35	5.803	1.45	2520	28	2580	24
H1-5	168	115	0.06161	21.4	0.38425	1.22	6.649	2.83	2096	22	2351	48
H1-4	166	57	0.10059	8.15	0.31883	1.73	9.047	1.72	1784	27	1808	31
H1-6	127	112	0.10243	1.01	0.33594	6.50	8.240	1.89	1867	105	1976	34
H1-7	108	76	0.13958	2.2	0.41301	1.00	6.878	1.63	2229	19	2292	28
H1-9	187	68	0.10499	5.43	0.41714	2.05	5.975	2.84	2247	39	2531	48
H1-8	44	51	0.14288	2.8	0.43639	2.00	6.060	2.72	2334	39	2508	46
H1-10	130	102	0.12508	3.42	0.51671	1.00	5.340	4.84	2685	22	2718	80
H1-11	56	25	0.00486	9.62	0.02387	1.79	19.075	21.24	152	3		
H1-12	90	46	0.12041	3.2	0.38445	1.31	7.160	2.78	2097	23	2223	48
H1-13	114	70	0.09289	6.75	0.34579	1.00	8.286	3.24	1914	17	1966	58
H1-14	143	60	0.11675	3.75	0.43464	1.00	6.548	3.74	2327	20	2376	64
H1-15	34	27	0.02397	1.61	0.20377	1.42	11.263	3.12	1196	15	1400	60
H1-16	133	57	0.08923	6.16	0.39142	1.00	6.729	3.76	2129	18	2330	64
H1-17	9	3	0.09221	4.07	0.38315	1.31	7.678	3.66	2091	23	2101	64
H1-18	98	39	0.11432	2.41	0.44997	1.06	6.343	2.48	2395	21	2431	42
H1-19	135	47	0.00626	7.18	0.02368	1.00	20.348	9.68	151	1		
H1-20	122	75	0.11376	1.56	0.47658	1.00	5.652	2.80	2512	21	2624	47
H1-21	96	44	0.09117	4.59	0.42993	1.00	6.787	1.98	2305	19	2315	34
H1-22	103	64	0.09844	3.77	0.42973	1.00	6.837	1.67	2305	19	2303	29
H1-23	56	89	0.08172	3.15	0.34103	1.00	8.164	7.08	1892	16	1993	126
H1-25	33	23	0.07222	7.51	0.31763	1.00	8.879	2.89	1778	16	1842	52
H1-24	136	57	0.08184	4	0.35786	1.00	8.265	1.62	1972	17	1971	29
H1-26	131	117	0.08770	3	0.34552	1.30	8.341	2.78	1913	22	1954	50
H1-27	25	24	0.08551	4.12	0.36534	1.00	8.015	2.63	2007	17	2025	47
H1-28	114	103	0.08201	8.61	0.35917	1.38	8.155	2.71	1978	24	1995	48
H1-29	83	67	0.08291	6.16	0.32251	2.23	8.902	1.00	1802	35	1837	18
H1-30	202	225	0.08193	7.01	0.34307	1.00	8.482	1.19	1901	16	1925	21
H1-31	152	70	0.08319	2.6	0.33558	1.28	8.549	1.03	1865	21	1911	18
H1-32	85	61	0.11502	6.07	0.50388	1.66	5.669	1.30	2630	36	2619	22
H1-33	111	57	0.08185	5.71	0.32864	2.12	8.869	1.75	1832	34	1844	32
H1-34	93	77	0.07871	3.38	0.36248	1.00	7.741	1.88	1994	17	2087	33
H1-35	78	52	0.14643	5.38	0.64844	1.21	3.695	1.00	3222	31	3310	16
H1-36	68	150	0.08889	2.07	0.35920	1.36	8.037	1.18	1978	23	2021	21
H1-37	71	34	0.07044	2.63	0.33253	2.60	8.707	1.03	1851	42	1877	19
H1-38	142	119	0.10237	3.08	0.43667	1.90	5.719	1.00	2336	37	2605	17

H1-39	992	820	0.01060	16.6	0.12002	1.00	8.678	1.14	731	7	1884	21
H1-40	24	18	0.04106	4.57	0.17554	1.86	13.064	5.38	1043	18	1109	107
H1-41	81	65	0.07521	3.29	0.32873	1.02	8.924	1.03	1832	16	1833	19
H1-42	30	11	0.12515	1.49	0.59106	1.84	4.324	1.18	2994	44	3061	19
H1-43	199	126	0.07846	1.89	0.30652	4.90	8.759	1.57	1724	74	1867	28
H1-44	86	70	0.09518	3.06	0.35106	1.00	7.186	3.23	1940	17	2217	56
H1-45	118	83	0.08960	3.03	0.34393	1.00	8.497	1.00	1906	16	1921	18
H1-47	66	56	0.13295	1.42	0.55049	1.00	5.029	1.00	2827	23	2817	16
H1-46	91	46	0.00487	9.67	0.02290	1.17	18.111	9.36	146	2		
H1-48	195	19	0.04343	7.29	0.18042	1.69	12.988	2.16	1069	17	1121	43
H1-49	86	46	0.04508	8.49	0.19240	1.17	12.735	1.48	1134	12	1160	29
H1-50	130	57	0.08360	2.39	0.34258	1.54	8.358	1.00	1899	25	1951	18
H1-51	183	149	0.05873	1.53	0.22928	1.00	11.650	1.14	1331	12	1334	22
H1-52	216	59	0.07640	4.37	0.32098	1.28	9.042	1.00	1795	20	1809	18
H1-53	230	63	-0.04359	5.38	0.17650	####	7.370	30.25	1048	166	2173	541
H1-54	75	61	0.11830	1.01	0.46777	1.82	5.667	1.49	2474	37	2620	25
H1-55	87	88	0.17060	1.74	0.64934	1.00	3.825	1.39	3226	25	3255	22
H1-56	52	29	0.00496	9.7	0.02363	1.00	22.791	11.66	151	1		
H1-57	293	80	0.05932	3.77	0.19418	1.00	12.691	1.35	1144	10	1167	27
H1-58	150	172	0.08493	3.78	0.30090	1.00	8.462	1.00	1696	15	1929	18
H1-59	45	80	0.09227	1.01	0.35864	1.00	8.271	1.25	1976	17	1970	22
H1-60	69	59	0.05608	2.54	0.21068	1.00	12.219	1.58	1232	11	1242	31
H1-61	58	30	0.13617	3.39	0.38498	1.00	7.437	1.00	2100	18	2157	17
H1-62	62	64	0.12297	3.55	0.40009	1.11	7.433	2.07	2169	20	2158	36
H1-63	218	138	0.14954	2.93	0.50413	1.40	5.469	1.66	2632	30	2679	27
H1-64	93	56	0.09092	1.6	0.31460	1.11	8.734	2.62	1763	17	1872	47
H1-65	227	147	0.07795	6.08	0.30822	1.00	8.860	1.79	1732	15	1846	32
H1-66	49	39	0.09745	3.1	0.33419	1.00	8.773	1.39	1859	16	1864	25
H1-67	75	44	0.13499	4.81	0.43824	3.27	6.631	2.20	2343	64	2355	38
H1-68	49	65	0.09775	3.04	0.32773	1.00	8.850	2.07	1827	16	1848	37
H1-69	53	59	0.09065	1.73	0.33930	1.75	7.932	2.34	1883	29	2044	41
H1-70	108	50	0.05902	6.25	0.21812	1.00	11.821	2.04	1272	12	1306	40
H1-71	76	61	0.13754	2.67	0.49504	1.00	5.686	1.83	2592	21	2614	30
H1-72	153	150	0.08922	3.21	0.31517	1.16	9.138	1.72	1766	18	1790	31
H1-73	126	41	0.12727	2.75	0.49237	1.25	5.716	2.55	2581	27	2605	42
H1-74	106	65	0.08085	3.19	0.31952	1.00	8.845	2.36	1787	16	1849	43
H1-75	118	48	0.08160	9	0.44979	1.89	5.222	9.08	2394	38	2755	150
H1-76	59	32	0.08080	6.27	0.28472	1.00	9.745	2.55	1615	14	1672	47
H1-77	89	166	0.06719	2.81	0.31209	1.00	8.587	2.26	1751	15	1902	41
H1-78	109	30	0.09690	5.61	0.43161	1.00	6.577	1.83	2313	19	2369	31
H1-79	63	90	0.09869	3.31	0.32080	1.06	8.649	1.30	1794	17	1890	23
H1-80	158	77	0.08078	1.95	0.28605	2.01	9.743	1.85	1622	29	1672	34
H1-81	86	52	0.08442	5.59	0.32195	1.00	8.932	1.51	1799	16	1831	27

H1-82	313	277	0.00646	4.18	0.02768	2.30	17.274	4.91	176	4		
H1-83	96	30	0.10139	3.74	0.43447	1.00	6.682	2.34	2326	20	2342	40
H1-84	257	92	0.06950	1.02	0.29323	4.16	8.293	1.00	1658	61	1965	18
H1-85	245	110	0.05536	4.78	0.26287	1.00	10.747	1.20	1504	13	1489	23
H1-86	167	67	0.09238	4.41	0.32560	1.66	8.843	1.55	1817	26	1850	28
H1-87	351	26	0.05374	12.7	0.30366	3.64	8.042	2.54	1709	55	2019	45
H1-88	40	41	0.09464	3.3	0.33993	1.23	8.541	2.55	1886	20	1912	46
H1-89	131	42	0.00801	3.1	0.02265	1.35	22.202	8.95	144	2		
H1-90	390	201	0.07574	6.65	0.25463	2.11	8.531	3.44	1462	28	1914	62
H1-91	350	217	0.02845	6.66	0.24958	1.66	7.752	6.31	1436	21	2084	111
H1-92	143	99	0.11320	5.65	0.36679	1.00	7.265	2.11	2014	17	2198	37
H1-93	56	28	0.10566	8.81	0.34830	1.00	8.427	2.53	1926	17	1936	45
H1-94	211	53	0.06258	3.7	0.19770	1.01	12.429	1.98	1163	11	1208	39
H1-95	196	64	0.06919	2.88	0.21019	1.14	11.368	2.86	1230	13	1382	55
H1-97	88	104	0.09811	2.99	0.34661	1.62	8.322	2.86	1918	27	1959	51
H1-96	76	52	0.09291	4.65	0.35066	1.00	8.502	1.71	1938	17	1920	31
~~xx~~	~~1243~~	~~1452~~	~~0.00868~~	~~7.08~~	~~0.04995~~	~~2.89~~	~~8.770~~	~~10.54~~	~~314~~	~~9~~	~~1864~~	~~191~~
H1-99	180	47	0.09276	2.96	0.30758	1.23	7.988	2.59	1729	19	2031	46
H1-100	104	83	0.14535	8.16	0.49518	1.00	5.767	3.18	2593	21	2591	53
H5-1	154	63	0.00526	7.33	0.02179	1.00	21.476	5.72	139	1		
H5-3	641	505	0.00613	5.42	0.02279	1.00	19.801	2.60	145	1		
H5-2	89	26	0.00154	22.2	0.01780	1.50	23.469	16.39	114	2		
H5-4	979	380	0.00359	3.29	0.01439	1.34	20.869	3.07	92	1		
H5-5	406	289	0.05407	1	0.23947	2.25	11.250	1.00	1384	28	1402	19
H5-6	392	274	0.00291	8.37	0.01330	1.00	20.129	4.63	85	1		
H5-7	579	371	0.00353	7.67	0.01753	1.00	17.914	9.27	112	1		
H5-8	1071	340	0.00609	13.5	0.02894	2.05	20.063	1.00	184	4		
H5-9	238	106	0.08479	8.82	0.31051	3.66	8.900	1.00	1743	56	1838	18
H5-10	226	102	0.00364	13.8	0.01866	1.78	16.625	5.41	119	2		
H5-11	726	238	0.07072	1.78	0.22200	8.23	9.541	1.27	1292	96	1711	23
H5-12	458	141	0.08043	2.9	0.28785	2.65	9.426	1.19	1631	38	1733	22
H5-13	386	95	0.00388	4.14	0.01802	1.77	20.459	5.21	115	2		
H5-14	826	547	0.00528	3.2	0.02095	1.02	20.518	2.55	134	1		
H5-15	688	352	0.00581	13.8	0.03200	1.01	19.223	2.84	203	2		
H5-16	655	129	0.05494	2.37	0.21672	1.34	11.514	2.99	1265	15	1357	58
H5-17	179	132	0.00233	7.38	0.01515	1.00	17.414	12.57	97	1		
H5-18	215	134	0.00431	9.84	0.01684	1.25	18.495	12.04	108	1		
H5-19	819	285	0.00310	7.81	0.01366	1.00	20.028	3.73	87	1		
~~xx~~	~~171~~	~~105~~	~~0.05261~~	~~12.5~~	~~0.47656~~	~~1.00~~	~~4.853~~	~~3.09~~	~~2512~~	~~21~~	~~2875~~	~~50~~
H5-21	474	234	0.00347	7.19	0.01462	1.00	18.834	3.94	94	1		
H5-22	275	238	0.00261	6.64	0.01401	1.00	15.306	10.25	90	1		
H5-23	260	97	0.00677	3.58	0.03305	1.52	19.040	5.05	210	3		
H5-24	1095	305	0.00315	6.66	0.01548	1.44	20.578	1.53	99	1		

H5-25	394	294	0.00752	11.1	0.03288	1.18	19.326	5.98	209	2		
H5-26	396	74	0.00259	11.8	0.01726	1.00	20.153	5.86	110	1		
H5-27	362	405	0.00218	3.6	0.01487	1.00	20.695	8.51	95	1		
H5-28	351	93	0.06525	5.58	0.31663	2.30	9.132	1.00	1773	36	1791	18
H5-29	285	87	0.00262	13.3	0.01408	1.55	18.560	7.83	90	1		
H5-30	297	180	0.00221	5.07	0.01587	1.29	17.351	4.98	102	1		
H5-31	456	185	0.06159	6.83	0.23565	2.18	10.610	2.74	1364	27	1513	52
H5-32	1707	1067	0.05429	9.04	0.23892	1.66	11.379	3.06	1381	21	1380	59
H5-33	357	218	0.00371	3.81	0.01381	1.00	21.831	5.12	88	1		
H5-34	870	209	0.04859	4.25	0.19380	5.74	10.003	3.12	1142	60	1623	58
~~xx~~	~~128~~	~~80~~	~~0.00629~~	~~9~~	~~0.03000~~	~~1.61~~	~~9.537~~	~~9.18~~	~~191~~	~~3~~	~~1712~~	~~169~~
H5-36	349	213	0.00303	5.06	0.01755	1.43	18.596	5.66	112	2		
H5-37	1265	536	0.00841	3.23	0.02548	1.47	19.927	1.55	162	2		
H5-38	477	366	0.05560	3.86	0.29032	1.00	9.985	1.70	1643	15	1627	32
H5-39	1311	138	0.06677	1.58	0.28745	1.63	9.600	1.35	1629	23	1700	25
H5-40	1086	114	0.06709	5.37	0.22592	1.69	11.047	2.60	1313	20	1437	50
H5-41	829	213	0.02283	5.36	0.15568	1.28	10.628	3.29	933	11	1510	62
H5-42	122	51	0.00721	9.59	0.03379	1.97	20.203	5.86	214	4		
H5-43	670	299	0.03340	14.7	0.22396	1.25	9.450	1.21	1303	15	1729	22
H5-44	2560	651	0.00424	8.55	0.01562	1.00	20.458	1.52	100	1		
H5-45	157	77	0.00422	3.52	0.01629	1.60	21.293	11.96	104	2		
H5-46	216	138	0.00632	8.2	0.02226	1.80	20.711	3.02	142	3		
H5-47	57	49	0.06395	3.06	0.20288	3.37	11.359	1.36	1191	37	1383	26
H5-48	522	246	0.00682	5.72	0.02436	1.80	19.062	2.74	155	3		
H5-49	246	137	0.05182	12.5	0.25663	1.28	10.868	1.00	1473	17	1468	19
H5-50	1355	80	0.00369	8.14	0.01444	1.57	20.622	2.59	92	1		
H5-51	849	98	0.05542	2.01	0.15758	1.30	11.641	1.68	943	11	1336	32
H5-52	337	237	0.00271	2.88	0.01445	1.13	18.324	5.39	92	1		
H5-53	132	150	0.06674	2.33	0.28549	1.66	9.691	2.71	1619	24	1682	50
H5-54	358	247	0.00528	2.97	0.02204	3.01	20.716	3.54	141	4		
H5-55	887	349	0.00389	9.52	0.01553	1.00	20.457	3.94	99	1		
H5-56	491	345	0.00529	6.79	0.02248	1.00	20.410	2.86	143	1		
H5-57	214	101	0.00502	5.06	0.02421	1.45	20.121	9.05	154	2		
H5-58	180	101	0.00559	2.13	0.02366	1.90	19.352	8.70	151	3		
H5-59	1185	155	0.00338	3.84	0.01448	1.00	20.166	2.28	93	1		
H5-60	403	202	0.00682	5.21	0.02908	1.92	19.705	2.31	185	3		
H5-61	645	376	0.00447	1.17	0.01863	3.43	18.668	4.03	119	4		
H5-62	636	333	0.06523	4.02	0.30715	1.74	9.107	1.85	1727	26	1796	34
H5-63	447	256	0.00834	1.53	0.02974	1.05	20.434	4.66	189	2		
H5-64	107	51	0.00339	8.22	0.01755	3.14	18.873	8.50	112	3		
H5-65	1012	560	0.00406	4.55	0.01490	1.00	18.640	4.39	95	1		
H5-66	235	174	0.00533	3.77	0.02290	2.79	19.500	4.62	146	4		
H5-67	301	172	0.07342	1	0.30442	1.50	9.248	1.48	1713	23	1768	27

H5-68	268	127	0.07727	6.35	0.29470	1.00	9.281	1.69	1665	15	1762	31
H5-69	1454	448	0.04837	9.62	0.18981	3.57	9.883	1.00	1120	37	1646	19
H5-70	262	99	0.08693	3.61	0.30762	1.00	9.479	1.27	1729	15	1723	23
H5-71	387	244	0.00370	5.07	0.01472	1.73	17.776	6.50	94	2		
H5-72	399	289	0.00259	4.87	0.01430	1.00	17.850	4.76	92	1		
H5-73	503	170	0.00372	11.1	0.01563	1.49	21.428	2.90	100	1		
H5-74	696	315	0.00470	4.21	0.01494	1.48	20.563	4.69	96	1		
H5-75	859	74	0.08275	3.22	0.23157	1.00	11.381	1.02	1343	12	1380	20
H5-76	505	264	0.07324	5.57	0.27813	1.41	9.731	1.17	1582	20	1675	22
H5-77	362	198	0.00367	4.3	0.01364	1.36	20.349	8.03	87	1		
H5-78	144	63	0.00385	4.53	0.01460	1.52	16.449	8.41	93	1		
H5-79	314	37	0.00580	11.7	0.01508	1.00	10.339	4.33	97	1	1562	81
H5-80	3173	271	0.05482	5.8	0.16457	3.91	11.407	2.10	982	36	1375	40
H5-81	1792	1119	0.00480	1.2	0.01435	1.43	19.565	2.72	92	1		
H5-82	1240	184	0.00549	4.51	0.01463	1.93	19.711	2.52	94	2		
H5-83	188	77	0.00544	7.24	0.02251	1.00	20.389	7.05	144	1		
H5-84	371	277	0.00305	3.73	0.01368	1.00	18.837	6.10	88	1		
H5-85	372	241	0.00635	5.05	0.02457	1.57	17.725	7.09	156	2		
H5-86	284	137	0.00335	3.62	0.01402	1.36	19.809	8.69	90	1		
H11-1	230	85	0.00686	2.95	0.02976	1.00	20.289	4.27	189	2		
H11-2	431	207	0.00501	6.28	0.02324	1.00	20.006	3.44	148	1		
H11-3	490	550	0.00536	2.53	0.02084	1.37	20.268	5.00	133	2		
H11-4	918	501	0.00614	5.4	0.02985	1.00	20.153	1.20	190	2		
H11-5	120	76	0.00491	5.77	0.02342	1.32	19.908	11.95	149	2		
H11-6	529	201	0.00623	4.18	0.02703	1.60	19.947	2.16	172	3		
H11-7	163	114	0.00613	3.54	0.02557	1.00	19.779	7.35	163	2		
H11-8	133	73	0.00468	8.49	0.02366	2.26	21.488	6.40	151	3		
H11-9	473	492	0.00511	8.57	0.03038	1.00	19.536	2.04	193	2		
H11-10	135	74	0.00400	12.4	0.02355	1.00	21.833	9.17	150	1		
H11-11	86	25	0.02160	4.92	0.09044	2.15	17.024	2.00	558	11		
H11-12	477	334	0.00633	1.8	0.02458	1.62	20.701	2.62	157	3		
H11-13	141	74	0.00413	4.71	0.02318	1.00	17.587	15.23	148	1		
H11-14	224	149	0.00536	5.39	0.02140	2.01	21.534	4.86	137	3		
H11-15	122	60	0.00582	9.42	0.02930	1.00	19.439	5.31	186	2		
H11-16	237	181	0.00555	10.6	0.02287	1.94	20.182	10.83	146	3		
H11-17	400	252	0.00664	5.42	0.02178	3.09	20.828	3.83	139	4		
H11-18	296	223	0.00597	3.75	0.02369	1.77	20.339	3.80	151	3		
H11-19	115	79	0.00403	8.22	0.02033	1.09	21.600	17.78	130	1		
~~xx~~	~~104~~	~~69~~	~~0.00673~~	~~8.88~~	~~0.02854~~	~~2.34~~	~~11.898~~	~~19.70~~	~~181~~	4	~~1294~~	~~387~~
H11-21	295	230	0.00482	18.7	0.02163	1.00	20.618	4.86	138	1		
H11-22	205	102	0.00503	13.3	0.02410	1.00	21.339	5.28	154	2		
H11-23	257	155	0.00669	8.75	0.02835	1.41	20.920	4.71	180	3		
H11-24	342	212	0.00793	2.43	0.02994	1.43	20.092	2.24	190	3		

H11-25	153	99	0.00537	6.02	0.02315	1.62	21.968	8.82	148	2		
H11-26	116	69	0.00764	8.21	0.03037	1.43	14.510	10.44	193	3		
H11-27	156	112	0.00777	1.73	0.02623	1.00	20.943	5.67	167	2		
H11-28	209	196	0.00604	4.6	0.02151	1.15	20.762	4.60	137	2		
H11-29	74	41	0.00482	5.87	0.02380	4.76	22.691	13.24	152	7		
H11-30	531	695	0.00682	1.24	0.02255	1.00	20.732	1.92	144	1		
H11-31	247	69	0.00840	2.84	0.03162	1.49	20.047	2.81	201	3		
H11-32	303	169	0.00602	2.25	0.02166	1.28	20.620	3.59	138	2		
H11-33	143	102	0.00614	4.91	0.02357	2.01	19.247	7.97	150	3		
H11-34	419	212	0.00608	2.75	0.02336	1.00	20.449	2.73	149	1		
H11-35	210	123	0.00580	3.45	0.02357	1.00	19.743	5.15	150	1		
H11-36	333	159	0.00821	2.83	0.02917	1.00	20.314	2.79	185	2		
H11-37	250	182	0.00526	2.75	0.02176	1.41	21.275	5.39	139	2		
H11-38	822	537	0.00777	1.9	0.02920	1.13	19.987	1.50	186	2		
H11-39	270	193	0.00530	3.9	0.02324	1.00	20.371	3.86	148	1		
H11-40	742	419	0.00767	2.63	0.02719	2.08	20.436	2.13	173	4		
H11-41	426	218	0.00765	1.28	0.02914	2.10	19.550	1.84	185	4		
H11-42	423	208	0.00722	3.68	0.02379	1.00	19.955	3.17	152	1		
H11-43	523	209	0.08259	2.96	0.32336	2.41	9.092	1.00	1806	38	1799	18
H11-44	583	431	0.00661	3.62	0.02354	1.32	19.074	2.26	150	2		
H11-45	251	153	0.00536	3.11	0.02130	1.22	21.061	3.69	136	2		
H11-46	100	69	0.00553	22.2	0.02802	7.82	16.883	17.14	178	14		
H11-48	264	310	0.00549	1.76	0.02327	1.64	21.021	4.55	148	2		
H11-47	166	131	0.00414	7.49	0.02152	1.00	21.575	7.54	137	1		
H11-49	130	97	0.00409	8.61	0.02274	1.07	19.049	8.98	145	2		
H11-50	1431	1103	0.00724	1.08	0.02683	1.00	20.153	1.22	171	2		
H11-51	117	83	0.00457	11.1	0.02013	4.29	21.667	7.10	128	5		
H11-53	173	130	0.00775	3	0.02859	1.79	19.741	4.82	182	3		
H11-54	232	213	0.00580	4.77	0.02208	1.41	20.689	5.82	141	2		
H11-55	353	122	0.00763	10.2	0.03023	1.45	19.718	1.92	192	3		
H11-52	256	156	0.00701	5.33	0.02560	2.18	19.904	4.45	163	4		
H11-57	399	225	0.00734	5.16	0.02997	1.00	19.635	3.28	190	2		
H11-56	277	65	0.01760	13.8	0.07224	2.67	17.867	2.14	450	12		
H11-58	166	63	0.00728	7.26	0.03566	2.65	19.507	2.89	226	6		
H11-59	1508	946	0.00711	6.83	0.02639	1.18	20.180	1.13	168	2		
H11-60	304	203	0.00648	8.09	0.02898	2.51	20.299	4.05	184	5		
H11-61	207	161	0.00624	3.05	0.02295	2.19	20.004	7.64	146	3		
H11-62	239	124	0.00663	8.75	0.03081	2.02	20.283	2.55	196	4		
H11-64	330	143	0.00801	2.93	0.02943	1.73	19.212	2.57	187	3		
H11-63	177	128	0.00589	5.3	0.02216	2.15	21.637	7.42	141	3		
H11-65	493	400	0.00903	5.21	0.02973	1.00	20.271	1.76	189	2		
H11-66	149	140	0.00606	2.35	0.02312	1.10	19.937	8.12	147	2		
H11-67	180	217	0.00555	5	0.02161	2.04	21.612	7.25	138	3		

H11-68	200	103	0.00625	3.46	0.02476	2.49	18.764	2.97	158	4	
H11-69	320	140	0.00553	5.67	0.02165	1.00	20.168	3.53	138	1	
H11-70	880	283	0.00916	2.55	0.03015	1.49	19.369	1.40	191	3	
H11-71	501	294	0.00845	5.92	0.03046	2.68	20.601	3.70	193	5	
H11-72	288	192	0.00830	4.91	0.02936	1.00	20.443	3.20	187	2	
H11-73	179	183	0.00531	3.89	0.02097	1.00	20.181	6.20	134	1	
H11-74	138	72	0.00391	10.9	0.02460	1.00	20.871	5.52	157	2	
H11-75	786	290	0.00897	6.48	0.03055	2.06	19.977	1.19	194	4	
H11-76	207	130	0.00643	8.72	0.03032	1.17	20.087	3.81	193	2	
H11-77	125	109	0.00614	5.89	0.02850	1.35	20.673	9.62	181	2	
H11-78	391	231	0.00842	2.33	0.02914	1.27	19.941	2.55	185	2	
H11-79	77	42	0.00356	12.1	0.02256	4.35	19.490	9.30	144	6	
H11-80	249	192	0.00573	4.42	0.02340	1.00	21.511	6.30	149	1	
H11-81	261	170	0.00532	5.2	0.02028	1.22	21.187	4.35	129	2	
H11-82	219	233	0.00617	1.39	0.02250	1.00	20.810	5.81	143	1	
H11-84	126	56	0.00764	4.99	0.02926	3.32	17.478	10.49	186	6	
H11-83	274	200	0.00598	3.4	0.02311	1.19	20.957	4.74	147	2	
H11-85	144	123	0.00591	5.49	0.02163	2.00	21.925	6.79	138	3	
H11-86	433	207	0.00992	3.37	0.02911	2.38	19.671	1.80	185	4	
H11-87	167	102	0.00780	2.17	0.02272	1.01	20.103	6.99	145	1	
H11-88	132	58	0.00839	4.58	0.02247	1.00	17.398	4.56	143	1	
H11-89	145	66	0.00675	4.76	0.02283	2.05	20.378	5.98	146	3	
H11-90	263	166	0.00928	1.29	0.02342	1.00	20.214	3.59	149	1	
H11-91	160	138	0.00783	1.38	0.02198	1.00	21.477	6.36	140	1	
H11-92	197	97	0.00980	7.73	0.02782	1.45	20.364	3.89	177	3	
H11-93	62	40	0.00873	7.05	0.02261	1.75	24.909	19.51	144	2	
H11-94	287	271	0.00775	10.6	0.02351	1.00	14.801	17.93	150	1	
H11-95	81	36	0.00608	7.22	0.02341	1.93	23.024	13.51	149	3	
H11-96	141	73	0.00786	4.19	0.02284	1.00	20.850	6.28	146	1	
H11-97	118	81	0.00814	7.08	0.02126	2.41	22.393	10.58	136	3	
H11-98	404	250	0.00993	5.35	0.02736	1.00	17.252	12.94	174	2	
H11-99	135	80	0.00702	5.38	0.02125	2.40	21.553	5.35	136	3	
H11-100	534	334	0.01014	1.98	0.02804	2.11	20.492	1.97	178	4	
H13-1	205	84	0.00634	5.06	0.02989	1.00	18.307	6.56	190	2	
H13-2	959	659	0.00632	1.26	0.02864	1.00	19.565	3.12	182	2	
H13-3	314	127	0.00529	4.86	0.02269	4.04	17.358	4.07	145	6	
H13-4	407	91	0.00503	11.3	0.02809	1.57	18.586	3.30	179	3	
H13-5	147	100	0.00428	8.58	0.02181	1.00	20.745	18.47	139	1	
H13-6	135	65	0.00652	6.08	0.02311	1.19	21.120	7.36	147	2	
H13-7	95	41	0.00625	2.56	0.02064	1.40	23.093	16.35	132	2	
H13-8	375	124	0.00933	3.14	0.02890	1.32	20.148	2.45	184	2	
H13-9	143	76	0.00530	3.47	0.02071	1.08	19.541	6.55	132	1	
H13-10	121	92	0.00348	4.09	0.02250	1.04	20.241	11.45	143	1	

H13-11	139	71	0.00588	5.08	0.02207	2.38	22.352	9.56	141	3		
H13-12	212	139	0.00626	4.76	0.02096	1.00	21.614	5.23	134	1		
H13-13	92	62	0.00588	5.08	0.02460	1.00	21.327	21.55	157	2		
H13-14	253	114	0.00920	2.4	0.02954	1.00	19.665	4.72	188	2		
H13-15	126	43	0.00749	15.3	0.03003	1.82	19.858	6.39	191	3		
H13-16	174	58	0.00630	13.4	0.03066	2.23	19.340	20.93	195	4		
H13-17	275	81	0.07702	14.3	0.34497	1.42	8.413	2.16	1911	23	1939	39
H13-18	231	130	0.00658	4.27	0.02226	1.19	20.904	11.96	142	2		
H13-19	220	133	0.00627	24.2	0.02649	1.82	20.950	6.62	169	3		
H13-20	188	91	0.00537	3.77	0.02057	2.39	20.974	11.38	131	3		
H13-21	392	239	0.00690	5.91	0.02940	2.31	19.545	1.72	187	4		
H13-22	191	89	0.00557	6.08	0.02294	1.06	20.386	5.56	146	2		
H13-24	399	257	0.00766	6.57	0.02866	1.44	20.384	4.36	182	3		
H13-23	290	157	0.00542	8.49	0.02317	1.12	21.161	6.49	148	2		
H13-25	158	131	0.00552	5.21	0.02326	1.00	22.245	9.25	148	1		
H13-26	578	693	0.00729	4.64	0.02904	3.17	19.792	3.23	185	6		
~~xx~~	~~57~~	~~46~~	~~0.00688~~	~~12.2~~	~~0.02391~~	~~2.27~~	~~6.679~~	~~9.53~~	~~152~~	~~3~~	~~2343~~	~~163~~
H13-29	395	156	0.00590	6.55	0.02643	3.33	19.950	1.79	168	6		
H13-28	332	188	0.00598	4.85	0.02331	2.51	19.943	3.02	149	4		
H13-30	349	237	0.00583	5.86	0.02285	2.13	20.348	3.31	146	3		
H13-31	520	290	0.00543	6.71	0.02101	1.24	21.039	4.50	134	2		
H13-32	932	468	0.00610	6.9	0.02666	2.06	20.169	2.37	170	3		
H13-33	104	82	0.00508	7.34	0.02223	1.96	22.928	16.99	142	3		
H13-34	1039	590	0.00687	4.84	0.02813	1.00	19.945	2.54	179	2		
H13-35	193	125	0.00534	4.93	0.02161	2.25	21.299	7.92	138	3		
H13-36	220	196	0.00598	5.7	0.02338	1.21	20.835	3.41	149	2		
H13-37	183	85	0.00932	2.77	0.03555	1.00	19.639	3.69	225	2		
H13-38	108	52	0.00496	10.2	0.02390	1.47	20.473	15.95	152	2		
H13-39	224	87	0.00485	4.72	0.02697	1.15	19.383	5.16	172	2		
H13-40	364	185	0.00743	4.82	0.02916	1.00	19.889	2.63	185	2		
H13-41	195	119	0.00524	4.83	0.02524	1.00	20.525	7.72	161	2		
H13-43	161	71	0.00514	8.5	0.02307	1.00	20.801	8.06	147	1		
H13-42	123	82	0.00526	7.07	0.02242	1.27	19.199	16.26	143	2		
H13-44	85	40	0.00476	9	0.02264	1.38	20.481	20.55	144	2		
H13-45	304	138	0.00737	4.96	0.02766	1.86	15.593	8.95	176	3		
H13-46	108	69	0.00469	13.1	0.02118	3.02	21.602	10.61	135	4		
H13-47	160	55	0.00798	7.57	0.02928	1.40	17.657	14.67	186	3		
H13-48	138	77	0.00521	10.7	0.02264	2.14	21.148	10.11	144	3		
H13-49	299	252	0.00390	13.6	0.02074	1.00	21.350	5.22	132	1		
H13-50	232	148	0.00664	12.4	0.02879	1.88	20.093	6.65	183	3		
H13-51	178	121	0.00618	8.43	0.02134	1.31	21.274	4.36	136	2		
H13-52	161	112	0.00467	5.45	0.02047	2.19	21.427	6.77	131	3		
H13-53	101	66	0.00533	11.6	0.02186	2.16	17.790	9.33	139	3		

H13-54	130	71	0.00493	9.49	0.02153	2.72	21.727	6.85	137	4		
H13-55	208	111	0.00465	10.1	0.02045	2.63	21.604	8.24	131	3		
H13-56	157	98	0.00422	6.31	0.02286	1.56	20.890	8.50	146	2		
H13-57	570	580	0.00420	1.71	0.02300	1.02	18.914	4.34	147	1		
H13-58	172	49	0.00639	8.52	0.03186	1.96	19.784	5.12	202	4		
H13-59	228	85	0.00463	14.3	0.02425	1.14	19.386	3.79	154	2		
H13-60	148	118	0.00414	9.93	0.02292	1.00	21.038	6.61	146	1		
H13-61	143	101	0.00442	8.88	0.02289	2.58	18.923	8.13	146	4		
H13-62	1553	1332	0.00479	1.25	0.02060	6.26	18.692	6.69	131	8		
H13-63	302	190	0.00369	5.84	0.02448	1.00	19.014	3.03	156	2		
H13-64	644	120	0.00645	4.56	0.02850	3.71	18.688	2.73	181	7		
H13-65	660	560	0.00408	3.82	0.02127	8.84	15.669	6.63	136	12		
H13-66	417	310	0.00461	3.04	0.02062	1.00	19.094	5.36	132	1		
H13-67	499	294	0.00475	19.9	0.02339	1.00	20.149	3.65	149	1		
H13-68	747	271	0.00625	4.45	0.02669	1.14	20.115	1.68	170	2		
H13-69	1055	435	0.00887	9.05	0.02794	1.94	19.772	4.34	178	3		
H13-70	163	990	0.00427	6.25	0.02341	2.41	12.862	2.93	149	4	1140	58
H13-71	249	184	0.00561	4.57	0.02198	1.14	22.087	8.96	140	2		
H13-73	369	217	0.00475	11.3	0.02232	1.23	20.678	3.49	142	2		
H13-72	253	159	0.00535	7.66	0.02283	1.67	20.515	5.33	145	2		
H13-74	209	138	0.00755	5.18	0.02897	1.83	20.177	6.21	184	3		
H13-75	1244	1545	0.00654	11.2	0.02772	1.66	19.799	1.57	176	3		
H13-76	257	117	0.00568	4.35	0.02194	3.56	20.126	3.36	140	5		
H13-77	296	230	0.00646	6.63	0.02767	3.07	20.592	3.30	176	5		
H13-78	507	279	0.00667	3.96	0.02690	1.60	20.367	2.43	171	3		
H13-80	129	80	0.00401	24.9	0.02014	6.63	18.384	32.16	129	8		
H13-79	201	146	0.00637	3.8	0.02244	1.79	19.587	10.38	143	3		
H13-81	284	148	0.00570	4.65	0.02263	1.62	20.122	8.16	144	2		
H13-82	179	91	0.00473	6.69	0.02293	1.17	20.323	4.89	146	2		
H13-83	778	536	0.00852	2.36	0.02833	1.57	19.385	4.07	180	3		
H13-84	309	114	0.00851	4.6	0.02744	4.35	19.003	8.40	174	7		
H13-85	286	166	0.00572	6.29	0.02189	3.20	20.454	7.76	140	4		
H13-86	103	83	0.00289	14.8	0.01896	1.02	23.776	16.24	121	1		
H13-87	146	203	0.00347	10.6	0.01516	3.17	22.266	8.15	97	3		
H13-88	123	109	0.00186	13.4	0.01385	1.52	24.309	25.04	89	1		
H13-89	64	17	0.00147	34.5	0.02406	2.56	22.877	12.16	153	4		
H13-90	1378	779	0.00576	12.3	0.02802	1.18	20.209	1.50	178	2		
H13-91	98	68	0.00442	12.3	0.02497	1.00	22.334	9.77	159	2		
H13-92	157	103	0.00229	7.3	0.01355	1.14	19.122	11.86	87	1		
H13-93	153	102	0.00570	4.02	0.02404	2.32	21.480	6.17	153	4		
H13-94	100	57	0.00172	48	0.01881	3.15	23.127	12.39	120	4		
H13-95	301	224	0.00456	6.16	0.02312	2.36	21.556	5.69	147	3		
H13-96	240	152	0.00552	3.94	0.02320	1.93	19.809	3.17	148	3		

H13-97	309	237	0.00515	7.73	0.02291	1.91	20.272	2.97	146	3		
H13-98	99	73	0.00420	13.4	0.02319	2.83	18.785	9.33	148	4		
H13-99	448	354	0.00667	1.56	0.02380	1.75	19.652	1.95	152	3		
H13-100	226	195	0.00450	12.1	0.02180	1.87	20.098	3.30	139	3		
H21-1	435	149	0.00806	7.86	0.03085	1.33	20.108	1.73	196	3		
H21-2	412	158	0.00458	4.2	0.01859	1.00	21.161	5.27	119	1		
H21-3	189	94	0.00726	9.14	0.02998	1.12	21.097	6.25	190	2		
H21-4	347	126	0.00809	6.71	0.02975	1.08	20.074	2.99	189	2		
H21-5	123	47	0.00636	7.26	0.02908	2.00	19.502	9.36	185	4		
H21-6	119	36	0.00758	10.2	0.03164	2.13	20.258	6.13	201	4		
H21-7	713	446	0.00697	6.03	0.02944	1.58	20.418	2.06	187	3		
H21-8	327	101	0.05285	5.7	0.18874	1.65	12.776	2.14	1115	17	1154	42
H21-9	375	210	0.00415	9.56	0.01729	2.67	20.966	5.20	111	3		
H21-10	531	216	0.00752	3.66	0.02924	2.58	20.645	2.05	186	5		
H21-11	340	159	0.00743	8.91	0.02916	2.95	20.058	2.10	185	5		
~~xx~~	~~303~~	~~105~~	~~0.02903~~	~~17.9~~	~~0.25433~~	~~2.94~~	~~9.169~~	~~1.78~~	~~1461~~	~~38~~	~~1784~~	~~32~~
H21-13	146	70	0.00430	12.9	0.01702	1.00	21.457	14.20	109	1		
H21-14	425	254	0.00713	12.7	0.02981	1.48	19.390	3.91	189	3		
H21-15	166	105	0.05870	10.4	0.25177	2.02	11.178	1.45	1448	26	1414	28
H21-16	256	144	0.00824	2.83	0.02905	3.45	21.023	4.20	185	6		
H21-17	147	68	0.00371	8.64	0.01683	1.36	19.573	11.10	108	1		
H21-18	163	101	0.00417	7.39	0.01841	1.61	21.873	7.08	118	2		
H21-19	155	103	0.00667	9	0.02612	1.14	20.692	6.79	166	2		
H21-20	557	316	0.00825	6.75	0.02952	1.97	20.492	2.04	188	4		
H21-21	2386	1439	0.00885	3.73	0.02800	1.16	20.102	2.34	178	2		
H21-22	404	236	0.00501	4.66	0.01637	2.83	20.800	4.57	105	3		
H21-23	687	199	0.00835	8.58	0.03039	2.19	19.795	2.99	193	4		
H21-24	256	101	0.00686	12.4	0.02470	1.38	20.832	2.51	157	2		
H21-25	248	91	0.00791	10.4	0.02961	3.06	20.533	2.03	188	6		
H21-26	297	66	0.00825	5.36	0.02757	1.00	19.864	7.51	175	2		
H21-27	388	182	0.00877	7.7	0.03143	1.21	20.055	3.80	199	2		
H21-28	126	70	0.00363	13.5	0.01720	1.00	23.027	17.38	110	1		
H21-29	187	76	0.00867	5.59	0.02987	1.34	20.600	6.02	190	3		
H21-30	121	126	0.01889	11.5	0.06563	1.14	18.242	3.99	410	5		
H21-31	314	81	0.01158	3.28	0.03069	1.25	19.866	2.90	195	2		
H21-32	240	95	0.00637	5.42	0.01801	2.81	21.568	7.63	115	3		
H21-33	159	70	0.00532	16.3	0.01689	1.36	21.718	11.70	108	1		
H21-34	251	108	0.00552	5.93	0.01735	1.00	21.884	7.45	111	1		
H21-35	87	42	0.01349	9.69	0.04370	1.71	19.612	4.49	276	5		
H21-36	1008	320	0.00594	4.9	0.01707	1.00	21.037	2.52	109	1		
H21-37	133	22	0.00783	7.75	0.03120	1.00	21.719	8.38	198	2		
H21-38	165	41	0.00913	11.4	0.03114	1.00	20.132	7.08	198	2		
H21-39	191	73	0.01025	5.52	0.03028	1.00	18.382	9.85	192	2		

H21-40	193	50	0.00771	5.86	0.02794	1.51	20.057	7.43	178	3		
H21-41	35	0	0.03460	157	0.03811	1.00	18.340	26.57	241	2		
H21-42	25	23	0.12806	3.29	0.51098	1.00	5.414	1.00	2661	22	2696	17
H21-43	298	28	0.01433	7.59	0.05099	1.00	18.952	1.60	321	3		
H21-44	257	168	0.00486	2.28	0.01616	1.00	20.788	8.22	103	1		
H21-45	443	434	0.00770	5.13	0.02762	1.00	20.351	1.44	176	2		
H21-46	138	45	0.01009	2.43	0.04141	1.58	20.569	4.73	262	4		
H21-47	329	303	0.03193	3.75	0.14471	1.19	14.519	1.00	871	10		
H21-48	83	50	0.00240	9.06	0.01647	1.02	22.041	26.91	105	1		
H21-49	911	717	0.00392	4.11	0.01649	1.15	21.152	1.50	105	1		
H21-50	334	164	0.00665	6.84	0.02883	1.17	20.467	2.09	183	2		
H21-51	167	58	0.00299	6.83	0.01690	1.82	22.986	11.12	108	2		
H21-52	1134	603	0.00655	2.31	0.02723	1.68	20.222	1.22	173	3		
H21-53	235	87	0.00522	10.2	0.02684	1.50	20.207	4.01	171	3		
H21-54	400	239	0.00633	7.56	0.02897	1.69	20.467	2.45	184	3		
H21-55	216	126	0.00530	10.6	0.02651	1.07	20.014	4.68	169	2		
H21-56	211	89	0.00369	3.38	0.01644	1.21	20.821	7.49	105	1		
H21-57	39	27	0.08309	2.98	0.29210	2.68	9.857	1.77	1652	39	1651	33
H21-58	231	152	0.00685	2.29	0.02863	1.74	19.695	2.29	182	3		
H21-59	593	199	0.00413	5.62	0.01664	1.00	21.202	2.17	106	1		
H21-60	399	129	0.00629	7.44	0.03042	1.50	19.783	2.67	193	3		
H21-61	102	35	0.00547	7.68	0.03125	1.00	18.221	6.32	198	2		
H21-62	78	34	0.00827	5.66	0.04355	1.00	17.759	12.17	275	3		
H21-63	122	63	0.00248	12.4	0.01607	1.41	26.736	11.00	103	1		
H21-64	337	153	0.00666	7.61	0.02847	1.06	16.169	8.51	181	2		
H21-65	285	179	0.00350	8.52	0.01755	1.00	20.473	7.38	112	1		
H21-66	169	127	0.00405	5.26	0.01670	1.00	20.451	6.84	107	1		
H21-67	232	165	0.00694	3.27	0.02903	1.00	20.624	4.87	184	2		
H21-68	122	45	0.06065	1.22	0.22466	3.03	11.738	2.39	1306	36	1320	46
H21-69	81	49	0.00340	8.19	0.01811	1.68	31.038	27.71	116	2		
H21-70	709	405	0.00786	2.89	0.03038	1.02	20.096	1.41	193	2		
H21-71	287	107	0.00693	5.59	0.02969	1.05	19.934	5.70	189	2		
H21-72	177	78	0.00589	4.63	0.01628	####	17.862	5.67	104	19		
H21-73	504	336	0.00419	5.38	0.01664	2.18	21.231	4.21	106	2		
H21-74	731	293	0.00828	3.99	0.03156	1.96	19.656	1.97	200	4		
H21-75	99	48	0.01152	12.5	0.05359	1.00	18.278	3.37	337	3		
H21-76	359	246	0.00638	5.82	0.02800	1.51	20.466	4.22	178	3		
H21-77	124	76	0.00645	3.98	0.03061	1.61	22.080	7.57	194	3		
H21-79	403	308	0.00434	5.74	0.01774	1.00	21.654	5.27	113	1		
H21-78	208	70	0.00667	5.76	0.02906	2.02	19.998	4.03	185	4		
H21-80	537	97	0.00870	8.54	0.03151	2.06	19.919	2.03	200	4		
H21-81	93	46	0.00288	14.7	0.01668	1.12	23.473	33.33	107	1		
H21-82	380	110	0.00659	6.47	0.02854	1.34	20.509	1.40	181	2		

H21-83	121	56	0.00632	3.35	0.02844	1.74	20.282	5.30	181	3		
H21-84	96	52	0.00349	11.4	0.01796	2.45	22.235	25.27	115	3		
H21-85	138	97	0.00352	5.85	0.01747	1.21	20.792	9.64	112	1		
H21-86	401	324	0.00626	3.98	0.02481	1.59	20.506	2.82	158	2		
H21-87	920	611	0.00751	6.98	0.03045	1.00	19.650	3.48	193	2		
H21-88	171	118	0.00401	4.82	0.01796	1.72	20.513	16.04	115	2		
H21-89	297	130	0.00789	5.5	0.03014	1.07	19.844	3.58	191	2		
H21-90	154	88	0.00349	17.6	0.01846	1.65	22.940	11.66	118	2		
H21-91	153	103	0.00374	4.8	0.01787	1.52	20.773	9.18	114	2		
H21-92	274	183	0.00727	2.46	0.02954	1.07	19.305	4.31	188	2		
H21-93	98	31	0.00525	9.08	0.03088	1.00	22.126	7.88	196	2		
H21-94	133	74	0.00452	7.49	0.01638	1.84	22.535	15.45	105	2		
H21-95	403	345	0.00433	3.47	0.01748	1.00	21.346	5.00	112	1		
H21-96	125	64	0.00339	8.12	0.01724	1.20	21.622	8.98	110	1		
H21-97	108	88	0.00412	7.42	0.01649	2.52	22.459	15.99	105	3		
H21-98	331	171	0.00490	3.48	0.01881	1.73	21.299	4.88	120	2		
H21-99	215	168	0.00427	2.37	0.01660	1.14	21.684	8.46	106	1		
H21-100	597	500	0.00795	5.44	0.02647	1.00	18.872	2.33	168	2		
H26-1	222	107	0.01037	2.61	0.02886	1.33	20.146	5.53	183	2		
H26-2	211	121	0.00983	4.98	0.02939	1.94	19.694	3.37	187	4		
H26-3	180	49	0.00971	4.75	0.03000	1.97	20.310	3.82	191	4		
H26-4	332	147	0.12727	10	0.41537	2.14	5.318	6.76	2239	40	2725	112
H26-5	360	159	0.00766	6.51	0.02946	1.00	20.685	5.53	187	2		
H26-6	205	87	0.07635	8.23	0.30638	1.00	9.606	3.87	1723	15	1699	71
H26-7	375	77	0.00460	4.99	0.01582	2.05	20.544	4.25	101	2		
H26-8	490	284	0.00869	8.14	0.02911	1.11	19.575	3.69	185	2		
H26-9	586	274	0.00427	5.71	0.01398	1.00	21.442	4.02	90	1		
H26-10	1448	588	0.00978	2.64	0.02846	1.00	20.020	2.99	181	2		
H26-11	210	99	0.00476	3.77	0.01773	1.41	23.108	7.57	113	2		
H26-12	116	50	0.00303	5.27	0.01670	2.47	23.823	14.51	107	3		
H26-13	123	144	0.00343	6.92	0.01692	1.31	18.374	13.55	108	1		
H26-14	268	137	0.00463	8.33	0.02869	1.00	20.668	5.76	182	2		
H26-15	220	342	0.00717	6.54	0.03616	1.00	15.422	6.76	229	2		
H26-16	681	441	0.00430	3.17	0.01538	1.00	7.912	5.04	98	1	2048	89
H26-17	498	158	0.00954	1.3	0.02932	1.27	19.889	2.56	186	2		
H26-18	234	70	0.00365	5.68	0.01625	1.00	20.525	5.51	104	1		
H26-19	600	240	0.00414	3.58	0.01443	2.54	21.599	4.35	92	2		
H26-20	290	67	0.00790	3.3	0.02500	1.25	20.274	8.50	159	2		
H26-21	464	192	0.00808	2.14	0.02836	1.00	20.438	1.98	180	2		
H26-22	225	359	0.04486	1.27	0.16954	1.00	13.408	2.90	1010	9	1057	58
H26-23	241	110	0.00319	4.53	0.01708	1.00	18.719	12.19	109	1		
H26-24	382	181	0.00666	1.6	0.02776	1.00	20.368	2.01	177	2		
H26-25	1230	1530	0.01974	1	0.06724	1.00	18.051	1.87	419	4		

H26-26	388	156	0.00734	7.53	0.02627	1.00	18.748	4.10	167	2		
H26-27	1073	456	0.00397	2.31	0.01519	1.00	20.812	2.49	97	1		
H26-28	932	442	0.00657	1.54	0.02553	1.71	19.217	4.21	163	3		
H26-29	219	100	0.00676	11	0.03040	1.74	15.612	12.23	193	3		
H26-30	1192	621	0.00380	8.49	0.01595	1.00	19.756	5.54	102	1		
H26-31	288	199	0.00593	3.44	0.02508	1.35	19.402	3.47	160	2		
H26-32	947	546	0.00382	1.13	0.01606	1.00	20.666	2.22	103	1		
H26-33	430	162	0.00842	1.13	0.02929	1.16	20.156	2.68	186	2		
H26-34	241	136	0.00447	2.37	0.01694	1.00	21.048	8.00	108	1		
H26-35	1147	895	0.00585	3.3	0.02842	1.43	19.780	1.99	181	3		
H26-36	101	41	0.06383	2	0.23181	2.45	11.246	2.08	1344	30	1402	40
H26-37	1239	611	0.00880	2.49	0.03001	1.00	19.718	1.68	191	2		
H26-38	284	161	0.01549	2.2	0.04917	1.39	19.039	5.48	309	4		
H26-39	483	242	0.01018	19.7	0.02895	2.09	17.658	32.10	184	4		
H26-40	71	35	0.02749	2.83	0.07968	1.91	16.625	6.08	494	9		
H26-41	209	54	0.00761	3.01	0.03233	1.00	20.425	3.55	205	2		
H26-42	235	98	0.05141	2.44	0.20146	1.35	12.524	1.74	1183	15	1193	34
H26-43	217	47	0.00670	5.79	0.02851	2.06	19.866	2.56	181	4		
H26-44	961	751	0.01002	2.92	0.03064	1.52	19.796	2.80	195	3		
H26-45	167	68	0.08150	1.04	0.31215	1.21	9.416	1.28	1751	19	1735	23
H26-46	193	83	0.00199	20.2	0.01400	2.82	12.992	29.61	90	3	1120	604
H26-47	167	147	0.04435	5.43	0.18062	2.30	13.253	1.34	1070	23	1081	27
H26-48	1047	925	0.01036	2.15	0.03652	1.64	19.602	1.54	231	4		
H26-49	377	208	0.00921	2.51	0.03068	1.37	20.029	3.15	195	3		
H26-50	981	1206	0.00776	4.62	0.02586	2.51	15.525	20.46	165	4		
H26-51	503	435	0.00967	2.17	0.02825	1.00	20.525	2.60	180	2		
H26-52	2068	723	0.01031	5.02	0.02917	1.66	20.116	1.67	185	3		
H26-53	664	345	0.00665	3.7	0.02876	1.19	19.567	1.46	183	2		
H26-54	789	387	0.00760	2.14	0.02707	1.11	20.032	1.61	172	2		
H26-55	159	53	0.00699	4.67	0.02743	2.32	20.806	7.53	174	4		
H26-56	1432	356	0.02708	2.65	0.08700	2.05	16.555	2.72	538	11		
H26-57	268	215	0.00302	9.41	0.01739	1.27	18.857	4.66	111	1		
H26-58	235	121	0.00396	3.15	0.01801	1.00	22.186	4.54	115	1		
H26-59	328	159	0.00610	4.71	0.02938	1.00	18.300	4.76	187	2		
H26-60	1069	560	0.00814	12.1	0.02957	1.00	19.994	3.48	188	2		
H26-61	445	146	0.00987	5.17	0.03016	2.41	19.341	4.18	192	5		
H26-62	292	134	0.00867	5.5	0.02993	1.81	15.999	14.96	190	3		
H26-63	289	75	0.00701	7.93	0.02533	1.85	19.065	9.78	161	3		
H26-64	179	72	0.00880	2.42	0.03273	1.00	18.452	4.57	208	2		
H26-65	271	129	0.00868	3.92	0.02894	1.00	19.515	3.76	184	2		
H26-66	326	182	0.00602	5.1	0.03095	1.40	20.337	2.86	196	3		
H26-67	485	330	0.00677	5.03	0.02943	1.59	20.100	2.20	187	3		
H26-68	258	122	0.00366	5.79	0.01642	2.27	21.102	7.22	105	2		

H26-69	432	329	0.00567	2.58	0.02511	1.00	20.109	2.88	160	2		
H26-70	1090	640	0.00399	2.42	0.01606	1.00	21.115	2.31	103	1		
H26-71	628	866	0.00505	4.82	0.02511	2.58	19.074	4.47	160	4		
H26-72	276	272	0.00645	2.56	0.02881	2.56	20.362	4.41	183	5		
H26-73	210	163	0.00560	3.47	0.02493	2.46	21.176	4.91	159	4		
H26-74	730	240	0.00405	4.23	0.01765	1.17	20.542	1.68	113	1		
H26-75	202	109	0.00348	11.1	0.01791	1.74	15.511	15.02	114	2		
H26-76	353	157	0.00650	5.67	0.02845	1.38	20.293	3.90	181	2		
H26-77	471	294	0.00386	1.32	0.01478	1.00	19.967	6.61	95	1		
H26-78	279	166	0.00025	3732	0.02428	####	12.537	38.60	155	19	1191	792
H26-79	380	142	0.00396	5.99	0.01986	1.00	19.777	3.17	127	1		
H26-80	394	186	0.00715	1.54	0.02996	1.00	19.285	4.14	190	2		
H26-81	280	134	0.00757	1.16	0.02935	1.05	18.280	3.63	186	2		
H26-82	279	207	0.00370	8.07	0.01561	2.26	20.107	12.14	100	2		
H26-83	30	0	-0.01487	68.4	0.03933	2.82	13.181	19.98	249	7	1092	404
H26-84	176	66	0.00763	5.03	0.02913	1.28	19.379	6.32	185	2		
H26-85	593	267	0.00492	2.02	0.01845	1.58	19.736	3.34	118	2		
H26-86	917	736	0.00614	5.52	0.02585	1.00	19.769	1.45	165	2		
H26-87	500	569	0.00361	10.2	0.01590	1.52	21.037	4.82	102	2		
H26-88	494	308	0.02555	1.8	0.09748	1.10	16.047	4.37	600	6		
H26-89	271	79	0.00797	4.23	0.03103	1.00	19.575	4.90	197	2		
H26-90	484	272	0.00731	1.21	0.02525	1.00	18.585	5.34	161	2		
H26-91	233	133	0.00630	5.31	0.02744	1.39	19.617	5.05	175	2		
H26-92	302	191	0.05606	2.15	0.21684	3.01	10.930	2.49	1265	35	1457	47
H26-93	630	602	0.00683	6.47	0.02845	1.00	19.618	2.81	181	2		
H26-94	53	50	0.03143	9.07	0.16071	7.68	12.518	4.90	961	69	1194	97
H26-95	2080	890	0.00854	1.01	0.02989	1.00	19.515	1.28	190	2		
H26-96	273	173	0.00603	3.43	0.02490	1.33	20.048	6.74	159	2		
H26-97	980	578	0.00421	1.4	0.01424	1.00	19.747	4.30	91	1		
H26-98	46	68	0.01497	3.05	0.05827	1.47	18.185	7.78	365	5		
H26-99	362	885	0.01853	3.83	0.06593	1.00	17.479	2.21	412	4		
H26-100	288	92	0.00396	4.76	0.01765	1.25	16.730	7.56	113	1		
07KS05-1	71	39	0.02420	2.99	0.02364	2.31	19.193	7.99	151	3		
07KS05-2	95	73	0.01382	2.81	0.02331	1.23	19.295	7.37	149	2		
07KS05-3	117	104	0.01308	4.23	0.02578	3.48	19.590	6.28	164	6		
07KS05-4	1291	810	0.00756	1.72	0.03138	1.00	19.768	1.48	199	2		
07KS05-5	3	11	0.00502	27.4	0.02551	####	#####	#####	162	35		
07KS05-6	268	153	0.01100	4.3	0.02304	1.32	19.495	5.93	147	2		
07KS05-7	85	54	0.01895	3.51	0.02242	1.49	18.906	8.85	143	2		
07KS05-8	115	106	0.01106	2.88	0.02582	1.74	18.811	8.64	164	3		
07KS05-9	75	72	0.01550	4.02	0.02176	1.60	18.795	9.67	139	2		
07KS05-10	101	93	0.01048	6.06	0.02323	2.39	18.154	14.22	148	3		
07KS05-11	554	281	0.00826	5.27	0.02541	1.87	19.704	5.06	162	3		

07KS05-12	1522	1180	0.00667	1.02	0.02971	1.04	20.115	1.48	189	2	
07KS05-13	76	46	0.02701	5.36	0.02329	2.15	18.268	12.02	148	3	
07KS05-14	102	89	0.01412	2.88	0.02345	1.24	20.022	4.64	149	2	
07KS05-15	85	66	0.01618	6.91	0.02181	5.36	19.319	8.95	139	7	
07KS05-16	123	110	0.01287	2.2	0.02165	2.46	19.341	8.50	138	3	
07KS05-17	66	48	0.02473	2.1	0.02282	2.26	18.571	11.31	145	3	
07KS05-18	145	115	0.01330	5.26	0.02229	1.00	19.115	8.15	142	1	
07KS05-19	52	33	0.02896	4	0.02357	4.25	18.962	9.23	150	6	
07KS05-20	118	70	0.01914	2.15	0.02265	2.11	19.612	4.96	144	3	
07KS05-21	109	41	0.02575	3.54	0.02920	1.70	19.179	6.65	186	3	
07KS05-22	94	76	0.01352	6.04	0.02394	5.01	19.289	6.92	153	8	
07KS05-23	163	96	0.01183	2.9	0.02251	1.00	18.266	12.90	143	1	
07KS05-24	107	84	0.01413	2.1	0.02266	3.28	18.994	8.78	144	5	
07KS05-25	250	186	0.00942	4.47	0.02347	1.97	19.768	3.43	150	3	
07KS05-26	142	107	0.01316	1.39	0.02988	2.10	19.364	4.75	190	4	
07KS05-27	96	57	0.01815	1.51	0.02192	5.13	19.663	6.17	140	7	
07KS05-28	95	73	0.01402	6.83	0.02237	2.58	19.551	6.96	143	4	
07KS05-30	139	57	0.02196	3.24	0.02925	1.29	19.196	4.64	186	2	
07KS05-31	78	52	0.01917	6.13	0.02309	4.67	19.512	6.87	147	7	
07KS05-32	125	41	0.02981	1.3	0.03091	1.97	19.477	3.93	196	4	
07KS05-33	135	121	0.01087	1.62	0.02324	1.73	19.546	6.16	148	3	
07KS05-34	250	173	0.00940	2.76	0.02232	1.54	19.950	4.92	142	2	
07KS05-35	101	82	0.01422	7.61	0.02350	3.32	19.087	8.70	150	5	
07KS05-36	78	65	0.01901	2.29	0.02260	3.40	19.022	8.30	144	5	
07KS05-37	97	64	0.01817	8.74	0.02243	4.69	19.324	6.27	143	7	
07KS05-38	142	114	0.01194	1.34	0.02602	1.00	19.410	5.09	166	2	
07KS05-39	157	106	0.01437	5.9	0.02243	1.70	19.258	7.19	143	2	
07KS05-40	150	140	0.01163	1.73	0.02248	1.75	19.583	5.10	143	2	
07KS05-41	206	185	0.01024	2.76	0.02275	1.02	19.296	5.85	145	1	
07KS05-42	203	146	0.01099	1.74	0.02155	3.34	15.724	28.00	137	5	
07KS05-43	151	120	0.01414	2.57	0.02291	1.43	19.491	5.71	146	2	
07KS05-44	131	90	0.01923	1.13	0.03007	1.91	19.471	3.75	191	4	
07KS05-45	141	133	0.01289	1.6	0.02324	3.12	19.800	4.79	148	5	
07KS05-46	215	154	0.01015	2.55	0.02627	1.00	19.839	4.85	167	2	
07KS05-47	170	81	0.01919	2.02	0.02980	1.68	19.247	5.17	189	3	
07KS05-48	167	141	0.01188	2.22	0.02251	2.38	19.613	5.07	143	3	
07KS05-49	178	76	0.01857	5.3	0.02627	1.32	19.869	4.51	167	2	
07KS05-50	178	172	0.00962	2.76	0.02333	1.00	18.832	8.71	149	1	
07KS05-51	490	87	0.02167	3.23	0.02101	####	17.012	19.73	134	16	
07KS05-52	572	455	0.00712	3.53	0.02282	1.86	18.944	10.09	145	3	
07KS05-53	87	60	0.01863	11.6	0.02353	1.42	18.808	8.72	150	2	
07KS05-54	95	91	0.01613	2.84	0.02361	1.72	19.559	7.02	150	3	
07KS05-55	96	82	0.01766	2.4	0.02315	1.82	19.644	6.38	148	3	

07KS05-56	43	24	0.04625	1.9	0.02613	1.68	18.639	10.53	166	3	
07KS05-57	97	80	0.01321	11.3	0.02546	2.65	18.165	4.31	162	4	
07KS05-58	108	105	0.01345	3.79	0.02646	2.46	19.040	9.43	168	4	
07KS05-59	117	74	0.02005	2.02	0.02570	1.60	19.106	6.46	164	3	
07KS05-60	118	70	0.01839	6.07	0.02162	1.52	19.295	6.52	138	2	
07KS05-61	42	23	0.05185	4.92	0.02264	3.49	17.506	18.64	144	5	
07KS05-62	341	378	0.00668	2.01	0.02365	2.22	19.581	5.58	151	3	
07KS05-63	65	45	0.02804	2.24	0.02334	1.33	18.737	9.58	149	2	
07KS05-64	86	51	0.02345	8.67	0.02421	1.73	18.018	13.57	154	3	
07KS05-65	85	52	0.02445	2.46	0.02533	2.70	17.683	16.74	161	4	
07KS05-66	157	144	0.01065	1.21	0.02339	1.26	19.590	4.81	149	2	
07KS05-67	83	71	0.01386	4.03	0.02558	2.31	18.652	9.00	163	4	
07KS05-68	110	78	0.01687	2.11	0.02300	2.62	18.955	7.84	147	4	
07KS05-69	990	668	0.00690	1.04	0.02855	1.78	19.910	1.24	181	3	
07KS05-70	240	117	0.01418	1.36	0.02322	1.64	19.850	3.40	148	2	
07KS05-71	80	60	0.02022	1.54	0.02336	1.55	18.551	11.19	149	2	
07KS05-72	136	82	0.01712	1.84	0.02309	2.97	19.400	7.27	147	4	
07KS05-73	142	90	0.01457	9.36	0.02302	3.94	19.426	6.01	147	6	
07KS05-74	363	207	0.00638	39.8	0.02862	4.25	18.602	9.68	182	8	
07KS05-75	164	84	0.01749	3.79	0.03047	1.10	19.675	3.43	193	2	
07KS05-76	62	49	0.02592	3.26	0.02383	5.99	18.563	9.55	152	9	
07KS05-77	191	178	0.00984	3.83	0.02332	3.55	19.778	4.67	149	5	
07KS05-78	64	37	0.03306	2.86	0.02290	5.75	19.051	9.08	146	8	
07KS05-79	258	127	0.01414	4.9	0.02373	1.44	19.754	4.51	151	2	
07KS05-80	153	112	0.01224	3.43	0.02279	1.00	19.442	7.28	145	1	
07KS05-81	104	71	0.01853	1.96	0.02334	3.29	19.600	5.80	149	5	
07KS05-82	346	266	0.00957	2.12	0.02999	1.76	19.676	2.72	190	3	
07KS05-83	249	200	0.00886	1.87	0.02196	1.73	19.791	4.78	140	2	
07KS05-85	215	102	0.01867	2.13	0.03078	1.46	19.424	3.10	195	3	
07KS05-84	170	151	0.01092	2.82	0.02234	2.47	19.796	5.38	142	3	
07KS05-86	147	122	0.00734	40.1	0.02248	1.70	17.700	16.75	143	2	
07KS05-87	49	29	0.04204	3.86	0.02196	2.65	18.305	14.48	140	4	
07KS05-88	103	64	0.01896	2.62	0.02248	1.60	18.380	10.88	143	2	
07KS05-89	273	240	0.00883	1.29	0.02246	2.71	19.443	5.40	143	4	
07KS05-90	263	153	0.01192	5.48	0.02125	5.25	18.977	8.29	136	7	
07KS05-91	120	94	0.01481	2.57	0.02535	1.64	18.936	8.01	161	3	
07KS05-92	258	222	0.00851	2.55	0.02260	1.95	19.949	3.34	144	3	
07KS05-93	395	253	0.01050	1.06	0.03020	1.98	19.922	2.58	192	4	
07KS05-94	77	28	0.04358	1.93	0.03000	2.27	18.930	8.32	191	4	
07KS05-95	115	85	0.01575	2.02	0.02298	2.25	19.500	5.95	146	3	
07KS05-96	218	136	0.01271	1.27	0.02360	1.00	19.007	7.86	150	1	
07KS05-97	257	205	0.00931	1.04	0.02238	2.82	20.225	2.09	143	4	
07KS05-98	117	84	0.01551	2.9	0.02237	1.32	19.125	7.35	143	2	

07KS05-99	132	122	0.01226	1.8	0.02274	1.01	19.467	7.31	145	1	
07KS05-100	126	113	0.01378	2.91	0.02350	1.13	19.237	6.14	150	2	
07KS05-101	140	86	0.01688	4.31	0.02242	2.45	18.829	10.30	143	3	
07KS05-102	119	99	0.01437	1.42	0.02251	2.41	19.531	6.63	144	3	
07KS05-103	307	49	0.02666	5.89	0.02274	3.00	19.822	4.50	145	4	
07KS05-104	394	299	0.00899	1.34	0.02189	2.06	20.025	2.78	140	3	
07KS05-105	485	265	0.01011	1.26	0.02879	1.67	19.996	1.51	183	3	
07KS06-1	379	199	0.00983	3.56	0.02597	1.14	19.680	2.94	165	2	
07KS06-2	253	134	0.00631	36.8	0.02535	1.28	19.510	5.19	161	2	
07KS06-3	696	490	0.00640	12.6	0.02547	1.42	19.873	3.57	162	2	
07KS06-4	816	710	0.00575	6.98	0.02520	1.29	20.051	2.52	160	2	
07KS06-5	231	111	0.01171	10.4	0.02663	1.00	19.644	3.28	169	2	
07KS06-6	432	261	0.00958	1.62	0.02579	1.00	19.830	2.33	164	2	
07KS06-7	396	321	0.00692	6.6	0.02303	1.35	18.843	8.61	147	2	
07KS06-8	228	110	0.01494	3.71	0.02635	1.00	19.273	5.96	168	2	
07KS06-9	352	318	0.00808	1.78	0.02574	1.06	18.908	8.25	164	2	
07KS06-10	91	54	0.02674	2.77	0.02337	2.75	19.344	6.14	149	4	
07KS06-11	282	146	0.01198	3.09	0.02328	1.00	20.021	3.45	148	1	
07KS06-12	195	94	0.01532	3.04	0.02359	2.18	19.293	5.74	150	3	
07KS06-13	480	350	0.00771	5.96	0.02703	1.14	19.895	2.58	172	2	
07KS06-14	1117	952	0.00520	6.22	0.02497	1.00	19.968	4.80	159	2	
07KS06-15	392	322	0.00829	2.05	0.02572	1.00	20.032	2.94	164	2	
07KS06-16	848	772	0.00625	1.94	0.02504	1.13	19.635	3.41	159	2	
07KS06-17	241	19	0.04409	1.63	0.02551	1.01	19.575	4.51	162	2	
07KS06-18	360	155	0.00993	4.87	0.02547	1.06	20.146	1.68	162	2	
07KS06-19	463	362	0.00848	1.8	0.02612	1.95	18.328	10.60	166	3	
07KS06-20	778	806	0.00335	14.9	0.02111	4.33	18.312	14.36	135	6	
07KS06-21	461	344	0.00705	14.1	0.02612	1.00	19.903	3.17	166	2	
07KS06-22	154	90	0.01444	5.82	0.02293	2.53	18.550	12.52	146	4	
07KS06-23	397	247	0.00749	16.2	0.02704	1.00	19.851	3.94	172	2	
07KS06-24	222	88	0.01562	1.62	0.02941	1.01	19.433	4.25	187	2	
07KS06-25	465	287	0.00804	10.2	0.02609	1.00	20.038	2.57	166	2	
07KS06-26	227	123	0.01073	7.89	0.02397	1.00	19.602	5.04	153	2	
07KS06-27	266	186	0.00915	3.9	0.02356	1.00	18.412	10.70	150	1	
07KS06-28	497	362	0.00738	3.04	0.02581	1.00	19.087	7.71	164	2	
07KS06-29	1016	788	0.00509	2.2	0.02165	3.33	22.401	5.20	138	5	
07KS06-30	592	677	0.00400	3.22	0.02111	1.60	19.250	6.63	135	2	
07KS06-31	70	22	0.02734	3.89	0.02937	1.00	19.113	7.19	187	2	
07KS06-32	376	455	0.00778	6.2	0.02475	1.00	20.173	2.30	158	2	
07KS06-33	233	191	0.00882	3.39	0.02487	2.07	19.274	5.69	158	3	
07KS06-34	390	162	0.00948	1.56	0.02468	1.00	20.170	2.14	157	2	
07KS06-35	115	47	0.01333	4.42	0.02501	2.42	19.295	7.10	159	4	
07KS06-36	239	98	0.01101	2.56	0.02459	2.37	19.769	5.14	157	4	

07KS06-37	228	139	0.00940	7.11	0.02530	2.09	19.637	4.33	161	3
07KS06-38	238	103	0.01165	1.75	0.02291	1.21	19.483	4.56	146	2
07KS06-39	436	267	0.00693	9.68	0.02501	1.00	20.120	3.11	159	2
07KS06-40	500	565	0.00581	3.45	0.02463	1.06	20.033	3.08	157	2
07KS06-41	513	508	0.00472	18.3	0.02163	1.00	19.678	5.94	138	1
07KS06-42	243	142	0.00984	7.79	0.02287	1.63	19.766	5.55	146	2
07KS06-43	1068	948	0.00502	2.7	0.02423	2.17	19.695	3.83	154	3
07KS06-44	491	362	0.00676	4.92	0.02559	1.00	20.124	2.98	163	2
07KS06-45	520	350	0.00676	4.13	0.02611	1.00	18.729	8.88	166	2
07KS06-46	706	532	0.00608	1.84	0.02519	1.00	19.822	2.43	160	2
07KS06-47	916	720	0.00475	2.2	0.02276	2.26	20.439	2.85	145	3
07KS06-48	634	382	0.00636	17.4	0.02694	1.13	18.916	6.81	171	2
07KS06-49	222	111	0.00990	6.01	0.02555	2.54	18.229	12.05	163	4
07KS06-50	287	140	0.00866	1.92	0.02550	2.97	19.628	5.10	162	5
07KS06-51	150	59	0.01345	3.94	0.02294	1.25	19.371	7.81	146	2
07KS06-52	82	35	0.01573	20.9	0.02283	2.59	17.938	13.28	145	4
07KS06-53	306	205	0.00788	3.67	0.02546	1.00	19.814	4.01	162	2
07KS06-54	406	172	0.00848	4.05	0.02639	1.17	19.553	3.57	168	2
07KS06-55	1469	623	-0.00350	471	0.01413	4.71	#####	87.81	90	4
07KS06-56	429	298	0.00677	3.17	0.02584	1.00	19.934	5.80	164	2
07KS06-57	181	85	0.01238	3.55	0.02580	1.16	19.097	6.44	164	2
07KS06-58	189	82	0.01408	2.61	0.02656	1.18	19.115	7.14	169	2
07KS06-59	251	166	0.00858	6.16	0.02561	1.00	19.768	3.56	163	2
07KS06-60	392	330	0.00748	8.68	0.02495	1.00	19.773	3.59	159	2
07KS06-61	280	173	0.00935	2.66	0.02331	1.00	19.716	4.85	149	1
07KS06-62	331	185	0.00849	3.15	0.02501	1.00	19.697	4.60	159	2
07KS06-63	511	402	0.00670	3.09	0.02467	1.44	19.695	5.18	157	2
07KS06-64	361	277	0.00755	1.78	0.02536	2.04	17.699	16.30	161	3
07KS06-65	322	235	0.00853	1.15	0.02515	1.27	20.009	2.12	160	2
07KS06-66	277	199	0.00937	1.27	0.02286	1.11	19.648	6.13	146	2
07KS06-67	160	85	0.01545	2.51	0.02290	2.95	19.464	6.53	146	4
07KS06-68	210	148	0.00718	36.4	0.02312	1.51	18.952	8.16	147	2
07KS06-69	474	318	0.00730	4.73	0.02432	3.50	19.708	3.35	155	5
07KS06-70	182	97	0.01180	6.12	0.02410	1.00	20.213	2.29	154	2
07KS06-71	262	121	0.01119	4.51	0.02593	1.08	19.852	2.27	165	2
07KS06-72	576	479	0.00644	13.9	0.02443	1.00	20.146	2.71	156	2
07KS06-73	141	96	0.01269	3.83	0.02317	1.09	19.512	5.01	148	2
07KS06-74	325	321	0.00686	7.32	0.02636	1.00	19.617	3.22	168	2
07KS06-75	560	478	0.00724	3.56	0.02460	1.00	19.330	6.98	157	2
07KS06-76	417	251	0.00846	4.65	0.02597	1.00	19.406	5.38	165	2
07KS06-77	398	296	0.00604	17.9	0.02185	5.79	17.092	19.97	139	8
07KS06-78	321	197	0.00955	3.17	0.02287	5.67	20.136	2.62	146	8
07KS06-79	233	454	0.00605	1.69	0.02514	1.26	19.429	4.79	160	2

07KS06-80	202	111	0.01199	6.72	0.02358	1.34	18.901	8.95	150	2		
07KS06-81	146	90	0.01210	10.9	0.02343	1.18	19.224	7.79	149	2		
07KS06-82	219	109	0.01158	1.48	0.02333	1.03	19.374	5.98	149	2		
07KS06-83	248	142	0.00732	16.9	0.02174	4.20	19.483	5.89	139	6		
07KS06-84	98	74	0.01385	2.68	0.02133	1.00	19.408	7.72	136	1		
07KS06-85	540	369	0.00737	2.75	0.02483	1.90	19.828	4.07	158	3		
07KS06-86	227	116	0.01065	15.4	0.02314	1.99	18.721	9.70	147	3		
07KS06-87	514	528	0.00511	4.38	0.02558	1.00	19.843	2.37	163	2		
07KS06-88	540	459	0.00611	7.54	0.02471	1.64	19.808	3.91	157	3		
07KS06-89	528	340	0.00736	1.3	0.02504	1.00	20.045	2.10	159	2		
07KS06-90	112	74	0.01264	8.49	0.02316	1.11	18.801	8.34	148	2		
07KS06-91	359	203	0.00910	1.67	0.02539	1.29	19.968	2.51	162	2		
07KS06-92	128	70	0.01502	23.1	0.02300	1.93	18.077	13.35	147	3		
07KS06-93	479	385	0.00706	5.65	0.02254	1.27	20.086	3.14	144	2		
07KS06-94	548	495	0.00674	1.23	0.02543	1.29	20.078	2.29	162	2		
07KS06-95	220	144	0.00982	3.03	0.02440	1.00	20.120	2.96	155	2		
K11-1	275	163	0.01182	3.88	0.04883	1.42	19.525	3.54	307	4		
K11-2	399	290	0.00365	3.42	0.01396	2.05	19.949	7.98	89	2		
K11-3	658	642	0.00455	5.23	0.01641	1.20	20.861	3.43	105	1		
K11-4	121	91	0.00545	5.44	0.02472	1.00	21.002	9.17	157	2		
K11-5	355	228	0.00374	3	0.01454	1.00	21.934	5.02	93	1		
K11-6	131	76	0.00496	2.9	0.02224	1.00	21.750	8.05	142	1		
K11-7	605	551	0.00442	3.06	0.01515	1.00	21.395	4.39	97	1		
K11-8	603	307	0.00744	4.25	0.02587	2.32	19.781	5.10	165	4		
K11-9	651	246	0.00356	10.5	0.01531	1.00	20.642	2.33	98	1		
K11-10	93	47	0.00172	19.3	0.01447	1.34	25.169	18.74	93	1		
K11-11	101	64	0.00265	9.37	0.01355	1.64	21.267	15.57	87	1		
K11-12	101	51	0.00566	5.64	0.02332	2.18	16.802	13.74	149	3		
K11-13	178	99	0.00514	5.89	0.02080	1.75	22.297	9.38	133	2		
K11-14	661	301	0.00383	3.13	0.01459	1.00	21.300	4.44	93	1		
K11-15	125	97	0.00496	3.43	0.02198	1.13	21.415	9.72	140	2		
K11-16	1140	45	0.00467	10.3	0.02485	1.00	20.108	2.10	158	2		
K11-17	776	359	0.00380	4.47	0.01417	3.12	19.903	4.96	91	3		
K11-18	951	1461	0.00469	1.62	0.01540	2.44	19.857	3.12	99	2		
K11-19	1626	587	0.00428	2.68	0.01504	1.01	21.076	2.27	96	1		
K11-20	956	518	0.00464	3.1	0.01579	1.89	21.118	3.28	101	2		
K11-21	574	153	0.00861	3.07	0.02987	1.58	20.196	2.94	190	3		
K11-23	946	1063	0.00671	10.6	0.02854	1.59	20.352	3.64	181	3		
K11-24	238	122	0.00594	4.87	0.02571	1.00	20.844	3.19	164	2		
K11-22	155	80	0.00622	7.66	0.02574	1.00	20.445	6.44	164	2		
K11-25	919	972	0.00353	7.7	0.01367	1.46	19.979	3.50	88	1		
K11-26	378	411	0.00374	3.87	0.01400	1.00	21.798	5.09	90	1		
K11-27	432	278	0.00501	3.03	0.01329	1.00	13.039	4.51	85	1	1113	90

K11-28	78	42	0.00761	5.81	0.03020	1.77	21.637	19.80	192	3		
K11-29	821	953	0.00791	5.64	0.03274	1.70	19.594	1.78	208	3		
K11-30	107	52	0.00331	10.5	0.01765	1.77	21.752	20.39	113	2		
K11-31	493	313	0.00646	2.91	0.02439	1.44	20.087	4.27	155	2		
K11-32	414	145	0.05267	2.65	0.20715	2.68	6.269	2.36	1214	30	2451	40
K11-33	37	24	0.00064	65	0.01915	####	11.521	20.43	122	14	1356	398
K11-34	139	62	0.00648	4.14	0.02324	2.40	21.457	9.21	148	4		
K11-35	108	42	0.00353	11.4	0.02506	2.23	21.109	10.84	160	4		
K11-36	692	373	0.00317	4.69	0.01364	1.99	20.847	4.87	87	2		
K11-37	177	106	0.00589	2.18	0.02484	2.56	20.771	6.90	158	4		
K11-38	86	28	0.00324	26	0.02434	1.48	20.221	14.01	155	2		
K11-39	59	23	0.00227	18.4	0.01797	1.62	20.363	27.57	115	2		
K11-40	209	255	0.00479	11.2	0.02321	2.82	21.157	5.51	148	4		
K11-41	743	592	0.00316	7.94	0.01337	3.66	18.614	10.93	86	3		
K11-42	801	396	0.00307	3.99	0.01404	1.00	22.012	5.11	90	1		
K11-43	644	432	0.00322	3.38	0.01415	1.60	20.868	4.99	91	1		
K11-44	320	125	0.00284	6.65	0.01482	3.18	20.777	5.03	95	3		
K11-45	412	252	0.00358	8.22	0.01384	1.08	22.196	6.29	89	1		
K11-46	239	169	0.00591	4.5	0.02565	1.00	20.566	5.62	163	2		
K11-49	54	21	0.00250	27.5	0.01763	1.20	28.002	28.54	113	1		
K11-47	214	240	0.00371	4.08	0.01569	1.13	20.921	12.14	100	1		
K11-48	67	36	0.00228	17.6	0.01579	2.10	17.626	21.02	101	2		
K11-50	454	172	0.00315	5.22	0.01385	1.20	21.193	3.99	89	1		
K11-51	36	19	0.00311	20.9	0.02603	2.41	25.523	31.88	166	4		
K11-52	259	111	0.00354	6.5	0.01483	1.00	19.536	8.85	95	1		
K11-53	400	111	0.00606	4.2	0.02106	1.00	21.098	3.48	134	1		
K11-54	59	24	0.00485	7.95	0.02250	1.10	22.956	19.29	143	2		
K11-55	462	211	0.00331	4.84	0.01395	2.20	22.175	6.98	89	2		
K11-56	1305	76	0.00338	9.29	0.01582	1.00	20.326	4.39	101	1		
K11-57	36	15	0.00564	6.93	0.03623	1.69	22.481	13.46	229	4		
K11-58	626	295	0.00318	2.8	0.01406	1.00	21.056	2.62	90	1		
K11-59	70	27	0.00266	18.6	0.01823	3.44	22.345	17.42	116	4		
K11-60	1254	219	0.06400	3.89	0.23924	1.00	11.332	1.50	1383	12	1388	29
K11-61	108	85	0.00539	5.61	0.02404	2.25	21.889	7.51	153	3		
K11-62	46	13	0.00094	96	0.01841	1.04	21.601	31.41	118	1		
K11-63	176	109	0.00365	6.58	0.01759	1.10	19.800	10.28	112	1		
K11-64	131	62	0.00611	9.3	0.02720	2.78	20.103	6.36	173	5		
K11-65	126	75	0.00502	8.21	0.02278	1.00	20.594	8.03	145	1		
K11-66	148	97	0.00386	5.98	0.01707	1.75	20.618	10.23	109	2		
K11-67	607	40	0.00232	9.63	0.01406	1.65	21.229	5.53	90	1		
K11-68	66	58	0.00360	6.1	0.01298	5.99	30.032	62.88	83	5		
K11-69	258	88	0.00300	7.37	0.01382	1.79	20.270	9.98	88	2		
K11-70	437	163	0.00337	5.73	0.01449	1.84	21.013	6.75	93	2		

K11-71	77	28	0.00325	14.9	0.02228	2.47	20.521	20.01	142	3		
K11-73	237	119	0.06874	3.16	0.24993	1.92	10.976	2.09	1438	25	1449	40
K11-72	751	364	0.00437	3.33	0.01407	1.21	21.084	5.47	90	1		
K11-74	102	41	0.00791	6.4	0.02575	3.43	21.928	12.25	164	6		
K11-75	52	24	0.00265	26.3	0.01322	4.13	29.832	#####	85	3		
K11-76	54	15	0.00637	16.5	0.02969	1.28	18.701	15.83	189	2		
K11-77	58	16	0.01121	8.46	0.04382	1.00	18.870	12.38	276	3		
K11-78	467	189	0.00433	5.28	0.01459	1.44	21.987	5.68	93	1		
K11-79	2707	936	0.00446	5.92	0.01538	1.24	20.489	1.96	98	1		
K11-80	182	67	0.00373	7.43	0.01532	1.00	20.329	11.27	98	1		
K11-81	103	58	0.00219	13.2	0.01728	1.36	21.362	14.44	110	1		
K11-83	183	128	0.00484	5.98	0.02467	1.22	21.024	3.52	157	2		
K11-84	256	186	0.00597	3.85	0.02366	1.96	20.841	4.69	151	3		
K11-82	95	59	0.00325	8.35	0.01621	3.03	24.737	19.81	104	3		
K11-85	271	188	0.00548	7.5	0.02570	1.40	19.968	4.26	164	2		
K11-86	187	75	0.00267	6.2	0.01443	2.05	23.252	14.93	92	2		
K11-87	683	689	0.00595	10.3	0.02634	1.70	20.191	2.46	168	3		
~~xx~~	~~168~~	~~525~~	~~0.00663~~	~~5.02~~	~~0.02674~~	~~2.39~~	~~12.347~~	~~2.91~~	~~170~~	~~4~~	~~1221~~	~~57~~
K11-89	1250	29	0.00081	38.2	0.01713	1.37	20.577	1.97	109	1		
K11-90	343	208	0.00600	4.31	0.02640	1.06	20.383	4.17	168	2		
K11-91	639	286	0.00392	3.52	0.01463	2.49	21.196	3.71	94	2		
K11-93	88	17	0.00203	27.6	0.01494	1.39	24.296	17.39	96	1		
K11-92	118	69	0.00625	5.06	0.02428	1.00	21.817	10.51	155	2		
K11-95	105	44	0.00401	9.93	0.02244	1.13	22.676	13.24	143	2		
K11-94	54	27	0.00302	17.9	0.02425	1.19	22.078	24.17	154	2		
K11-96	97	29	0.00877	10.2	0.02511	1.72	19.468	10.36	160	3		
K11-97	182	218	0.00836	3.1	0.02501	1.45	14.089	3.68	159	2		
K11-98	325	31	0.00760	7.95	0.02622	1.29	19.522	4.40	167	2		
K11-99	357	91	0.00638	4.82	0.01660	2.14	20.792	3.69	106	2		
K11-100	1058	990	0.00854	4.46	0.02465	1.00	20.188	3.08	157	2		